Magnetic core/gold shell nanoparticle immunoassay for rapid detection of biomolecules using Raman spectroscopy

A thesis submitted to the faculty of science and engineering of Queensland University of Technology in fulfilment of the requirements for the degree of Master of Applied Science

Author:	Roland Agoston r.agoston@qut.edu.au
Primary Supervisor:	Dr. Emad Kiriakous e.kiriakous@qut.edu.au
Associate Supervisors:	Dr. Bill Lott b.lott@qut.edu.au
	Prof. Godwin Ayoko g.ayoko@qut.edu.au
	Prof. Martin Sillence martin.sillence@qut.edu.au

Faculty of Science and Engineering
Queensland University of Technology

2016

Abstract

Separation, identification, and quantitation of biomolecules within complex matrices can be costly and laborious. The gold-coated iron oxide nanoparticles functionalised with antibodies selectively developed here recovered the target protein, erythropoietin (EPO), from a complex biological matrix. Equine blood serum was spiked with EPO and then monitored indirectly and detected directly. Surface-enhanced Raman spectroscopy (SERS) was used to monitor the antibody-antigen binding event by comparing the spectra before and after protein capture using the extractor nanoparticles. As antibody-antigen binding is target-specific, this allowed for pre-screening to indirectly detect the protein. Monitoring this antibody-antigen binding event can be also be used as a rapid presumptive test for EPO. The captured EPO molecules were then released from the extractor nanoparticles, deposited on nanostructured gold substrates, and detected directly by SERS on nanostructure gold substrates using a handheld Raman spectrometer. The Raman fingerprint identification of the protein was cross-validated using independent ELISA analysis. The first model described above established a linear response to the log of analyte concentration across the range of 50 nM to 5 pM, with a calculated LOD of 1 pM. The second model, utilising aptamers immobilised on a developed SERS-active surface, showed a similar relationship between 10 nM to 10 pM analyte concentrations measured, with a consistent Raman signal RSD of 4.92% across the surface. The SERS detection modes used in this method provided label-free rapid and direct spectroscopic identification of the purified analyte from biological fluids. Thus, this project combines SERS nanosensors with a handheld Raman spectrometer as a proof of concept for the rapid, selective, and sensitive analysis of proteins in biological matrices. The developed methodology can be applied in real-world applications to screen proteins at points of care, analytical service laboratories, toxicology laboratories, and doping control agencies.

Statement of original authorship

The work contained in this thesis has not been previously submitted to meet requirements for an award at this or any other higher education institution. To the best of my knowledge and belief, the thesis contains no material previously published or written by another person except where due reference is made.

QUT Verified Signature

Roland Agoston

July 2016

Acknowledgements

I would first like to express sincere thanks to my supervisor, Dr. Emad Kiriakous. I always felt like your doors were open to me when I needed guidance; you pushed me when I needed it, and were supportive when nothing seemed to be working.

To my associate supervisor, Dr. Bill Lott, thank you for your help with the editing of my thesis and letting me pick your brain on all things biology. Your sincerity and willingness to help were always appreciated, and I will look back on our long chats in your office fondly.

To my dear colleague, Dr. Sivanesan Arumugam, my deepest thanks for all of your help with this project, thesis, and in the lab. Your love of science and enthusiasm are infectious, and you have been a great source of support and inspiration during this time.

I would like to express appreciation to the other academics of our research group, Prof. Godwin Ayoko and Adj. Prof. Peter Fredericks for their helpful comments and suggestions during our group meetings.

I am also grateful for the assistance of all of the QUT technical and support staff, whose work I feel is often underappreciated. Thank you for keeping us research grunts safe and making sure the machines go 'ping!'

Dr. Llew Rintoul, for lending your expertise, training, and use of your vibrational spectroscopy instruments, particularly the Raman.

Dr. Jamie Riches, for training and sample advice with the electron microscopes.

To the QUT Chemistry (E-block) technical staff, Leonora Newby, Dr. Lorraine Caldwell, Dr. Lauren Butler, and Karl Jaques, thank you for the loans of materials or temporary lab space for experiments. A special thanks to Dr. Chris Carvalho, for lifting my spirits with terrible jokes, and for taking a vested interest in accommodating the students' needs with the instruments.

Additional thanks to Dr. Wayde Martens, for use of laboratory space and help with early experimental work, and for being so easy-going and approachable when I needed advice.

To the QUT CARF staff, Dr. Tony Raftery, Tri Nguyen, and Dr. Henry Spratt, for assistance with the collection and interpretation of XRD data.

I would also like to express thanks to Dr. Rohan Steel of the Biological Research Unit, Racing Analytical Services Ltd, for his assistance in the analysis of all protein samples.

To Mitchell Bailey, thanks for the weekends of hanging out, talking, and general distraction from university life. It helped a lot to relax and definitely kept me sane.

I would like to give my heartfelt thanks to Sarah Fletcher, for always lending an ear when I needed someone to talk to, and especially for being the best sport and laughing at my jokes.

I'd like to thank Pabhon Poonpatana for sharing in the highs and lows of research life at QUT with me. Thanks for all the laughs and lunches together talking nonsense.

Thanks to Madeleine Brown, for all of our chats in the office - for hearing out my stories and being supportive, your warmth and kindness know no bounds.

Thank you to Ayden Staff, for helping to put me on the path to university, and for sharing a passion for gaming and all things nerdy.

To Jonathan Lillis, thank you for being a friend to me for all these years, for the things you have taught me and for all of the great conversation.

Lastly, I would like to acknowledge my parents. Thank you for all you have done for me; for migrating to this country and facing such hardships so your son could know a better life than you had. I could not have dreamed of a better life and family, and I am eternally grateful. This thesis is dedicated to you both.

List of publications

R. Agoston, E. L. Izake, A. Sivanesan, W. B. Lott, M. Sillence and R. Steel. Rapid isolation and detection of erythropoietin in blood plasma by magnetic core gold nanoparticles and portable Raman spectroscopy. *Nanomedicine: Nanotechnology, Biology and Medicine*. (Accepted 2015, I.F. = 6.155)

A. Sivanesan, E. Izake, R. Agoston, G. Ayoko and M. Sillence. Reproducible and label-free biosensor for the selective extraction and rapid detection of proteins in biological fluids. *Journal of Nanobiotechnology* **2015**, *13*, 43. (I.F. = 4.12)

A. K. M. Jamil, E. L. Izake, A. Sivanesan, R. Agoston and G. A. Ayoko. A homogeneous surface-enhanced Raman scattering platform for ultra-trace detection of trinitrotoluene in the environment. *Analytical Methods* **2015**, *7*, 3863-3868. (I.F. = 1.821)

Keywords

surface-enhanced Raman spectroscopy; SERS; portable analysis; in-field; nanosensors; trace analysis; ultra-trace analysis; selective protein extraction; immunoassay; erythropoietin; EPO; blood plasma; nanoparticles; magnetic nanoparticles; gold nanoparticles; iron oxide nanoparticles; hybrid nanoparticles; composite nanoparticles; core-shell nanoparticles; coated nanoparticles; functionalized nanoparticles; nanostructured surfaces; nanomedicine; nanotechnology.

Glossary of terms

NP	Nanoparticle
AuNP	Gold nanoparticle
AgNP	Silver nanoparticle
MNP	Magnetic nanoparticle
AuMNP	Gold-coated magnetic nanoparticle
AuNS	Gold nanostructure
pAu/AuNS	Gold nanostructures over a gold substrate
EPO	Erythropoietin
ESA	Erythropoietin-stimulating agent
rHuEPO	Recombinant human erythropoietin
SERS	Surface-enhanced Raman spectroscopy/scattering
EM	Electromagnetic
LSPR	Localised surface plasmon resonance
HR-TEM	High resolution transmission electron microscopy
LOD	Limit of detection
LOQ	Limit of quantitation
NIR	Near-infrared (spectroscopy)
DNA	Deoxyribonucleic acid
RNA	Ribonucleic acid
SAM	Self-assembled monolayer
cfu (units)	Colony forming units
aptasensor	Aptamer-functionalised biosensor
WAI	Wide area illumination
2-QT	2-quinolinethiol
SDS-PAGE	Sodium dodecyl sulfate polyacrylamide gel electrophoresis

Thesis structure

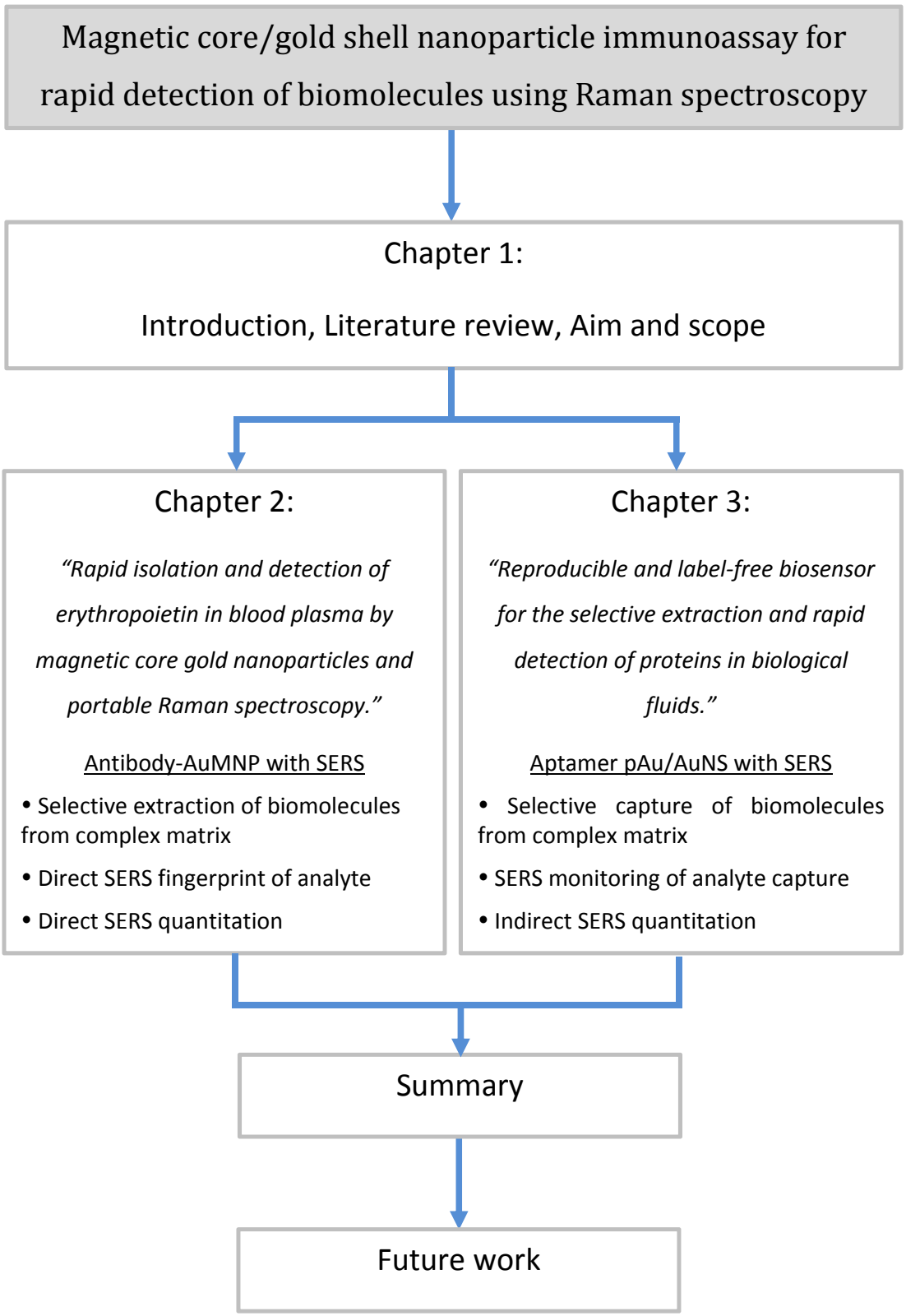

Table of contents

List of figures

List of tables

Chapter 1

[1.1] Significance of study

Biomarkers within biological fluids, such as blood or urine, are usually present in trace or ultra-trace quantities making them difficult to detect. Ultra-trace biomarker detection is currently carried out using LC-MS, GC-MS-MS, electrophoresis, electrophoresis, blotting, and immunodetection methods (e.g. ELISA). However, protein analysis using these techniques is challenging due to costly instrumentation, requirement for highly trained labour, cross-reactivity,[1] insufficient limits of detection (LOD), or matrix effects.[2] Developing sensitive, rapid, and cost-effective detection tools for biomarkers and illicit substances would have both life-saving and ethical implications, leading to improvements in the quality of clinical diagnosis services and assisting anti-doping law enforcement agencies with their duties. Beyond the laboratory, portable methods of detection for biomolecules of interest from a background of confounding species can be broadly applied to a range of fields. Illicit substance abuse can affect the health and safety of individuals in a workplace, or provide an unjust advantage in a competitive sporting environment if left unchecked.[3] On-site spot testing of individuals for such substances may prevent incident and act as a deterrent for future offenders. The in-field detection of pollutants at trace levels can be used to monitor ecological systems before reaching critical concentrations and causing damage.[4] Such events can cause long-lasting agricultural, environmental, and economical ramifications to which prevention may be the only cure. The quality control of foods involves routine testing for toxins and pathogens to prevent foodborne illness, and is vital to ensure consumer health. Improved analytical platforms in this area would be highly valuable to the global multi-billion dollar food industry.[5] Novel biomolecule detection methods therefore have a myriad of prospective applications, with the potential for environmental, financial, and health impacts on a global scale.

When coupled with recognition molecules for the selective identification of analytes, nanotechnologies have led to the development of improved biomolecular detection techniques.[6] Many materials exhibit unique optical, magnetic, and electronic properties at the nanoscale (1-100 nm) not observed in the bulk form. The modification of a nanomaterial surface with a selective molecule, such as an antibody, peptide, aptamer, or other

recognition ligands, allows for the selective capture of target species onto the surface, thereby providing a versatile platform for biomolecule detection.[7] Recognition modifications can also enable guided therapies by selectively delivering materials to specific cell types for drug delivery,[8] theranostics,[9] and tissue and cell imaging.[10] Once bound, the analyte is usually detected through interactions with a recognition molecule, the presence of a high response reporter molecule, or changes in the surface properties of the nanomaterial.[11] These modes of detection rely on indirect evidence to confirm the presence of the target analyte, which may reflect changes in systems affected by the analyte rather than the identifying characteristics of the analyte itself. This approach, however, may lead to lower selectivity and misleading results when the reporter is detected under unintended circumstances.[12] Our strategy employed a highly efficient and specific extractor nanoparticle to selectively capture a trace biomolecule of interest from a complex biological matrix. The capture event itself was monitored to indirectly detect the presence of the target analyte. Once captured, the nanoparticle-analyte complex was then easily separated from the matrix, the analyte was released from the nanoparticle, and direct spectroscopic identification of the analyte carried out by SERS.

The development of emerging technologies is often application-driven, and is evaluated relative to the currently available technologies. Factors such as cross-reactivity, sensitivity, portability, and cost-effectiveness are the major considerations. Many field applications such as forensic analyses, environmental monitoring, and testing for doping agents in sports can be unsuitable for laboratory-based analyses; sample transport, handling, and processing times add costs and delays, thus limiting the timely availability of critical data. The development of our method considered efficiency and portability as essential. Robust low-volume sample handling techniques coupled with a portable handheld Raman spectrometer allowed all analyte capture, monitoring and SERS measurements to be performed rapidly in the field. The developed technique can be easily adapted to any target biomolecule, provided a suitable recognition molecule is available. Thus, our methodology can be adapted with tuneable designs or for multiplex analyte measurements.

Our combined separation and detection method aimed to have the following features: (i) simple analysis requiring little or no sample pre-treatment; (ii) highly specific

capture and separation of a target analyte from a complex matrix with SERS-based monitoring; (iii) release of purified target analyte for direct SERS-based analysis and/or other cross-validation methods; (iv) semi-quantitation using SERS fingerprint signal intensity; (v) portability for the screening of biomolecules in the field and; (vi) customisable synthetic method that can be adapted for a wide variety of analytes.

[1.2] Introduction

[1.2.1] The significance of biomolecules

As human understanding expands to unravel the mysteries of biology, the need to detect biomolecules of interest becomes paramount for a broad range of applications.[13-16] The presence, absence, or quantity of biomarkers such as proteins can be used to monitor and assess the health state of biological systems to assist patient care and is also important for anti-doping and forensic practices.[17, 18]

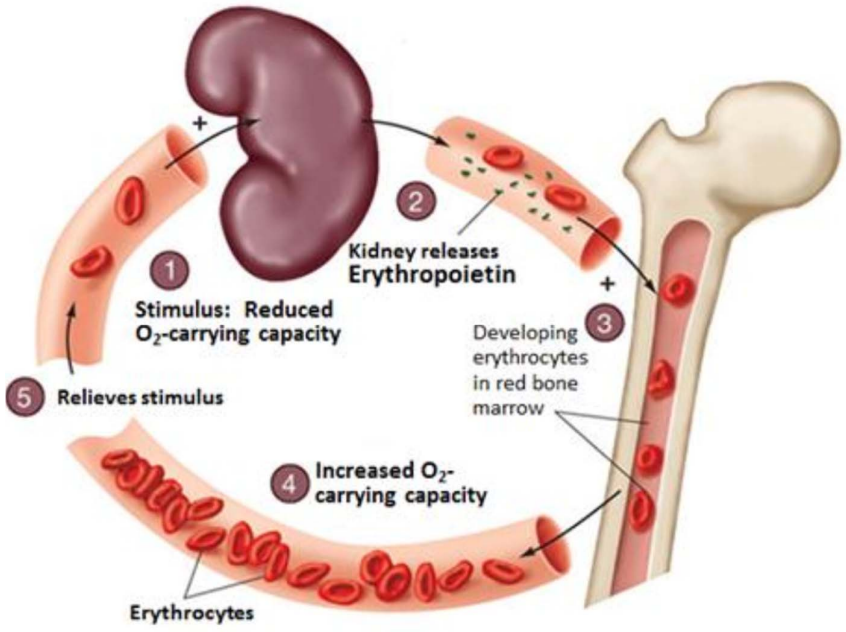

Figure 1 - Erythropoiesis cycle (red blood cell production).

The significance of biomolecules cannot be overstated; they control almost every aspect of biological life, and any unrectified imbalance can lead to deleterious health effects or death of the parent organism. In humans, there are many well-known biomolecules such as insulin, thyroid hormones, and erythropoietin (EPO) which can have drastic health impacts on humans. For example, if the body is unable to properly utilise or produce insulin to break down sugars due to diabetes, blood sugar levels may rise beyond manageable levels (hyperglycemia) which can lead to kidney damage, cardiovascular disease, and nerve damage.[19] The natural EPO hormone is used for the control of red blood cell production (Figure 1), and recombinant EPO can be used for treatment of several types of anemias.

Thyroid hormones are used to regulate metabolism in the body, and their production is in turn controlled by a biomolecule known as thyroid stimulating hormone. Thus, to be able to treat any kind of imbalance of biomolecules and combat resulting diseases, first the quantities of the biomolecule(s) of interest must be known. Therefore, the separation and detection of biomolecules is crucial for the understanding and treatment of biological states and disease.

Many substances can have powerful effects on the human body, able to alter behaviours, perceptions, and even physical traits, making their regulation necessary for the safety of the general population. A diverse range of recreational drugs with varying physiological effects exist, and can be broadly grouped into hallucinogens, depressants, or stimulants. Due to their ability to impair normal function, the production and sale of many of these is illegal.[20, 21] Detecting and correctly identifying these substances, as well as their metabolites produced by the body, is therefore vital for forensic science and law enforcement. Substances that occur naturally within the body, along with their analogues, can also be used to gain a competitive advantage. Recombinant EPO is one such example which can be abused by athletes, as doping can lead to increased oxygen carrying capacity and superior athletic performance. Insulin has also been banned by the International Olympic Committee for non-diabetic athletes, as doping can inhibit protein breakdown leading to reduced muscle degradation.[22] As such, anti-doping practices must improve to properly detect such abuses in order to maintain sporting integrity.

[1.2.2] Biomolecule separation and detection techniques

There are a wide range of techniques currently available for biomolecule detection, each with their own associated advantages and limitations. Discussed herein are several common techniques used for the analysis of proteins and other biological species.

Microscopy is among the earliest techniques used to investigate the world beyond the perceptions of the human eye. Single cells, and sometimes even their organelles, are often visible through the use of a light microscope, and can be analysed visually.[23] Investigation into the molecular composition of these cells *in situ* requires techniques to allow microscopic visualisation, such as chemical staining or the more advanced immunostaining. The latter utilises antibodies coupled with fluorescent tags, radiolabels, or more commonly enzymatic colour producing reactions to visualise and detect target

molecules or sites.[24] Preparation for immunostaining may involve first immobilising cells in a process called fixation, which can affect the structure of cells and tissues and can be destructive to some antigens. Immunostaining agents can also bind non-specifically to cells and tissues, which can cause background issues. To compensate for non-specific binding, optimisation of several factors may be required, including binding time, blocking agents, and washing procedures.[25] Flow cytometry can overcome some of these limitations, as immunostaining of biomolecules, typically on the cell surface, is carried out in a mobile solution. Multiple analytes can be differentiated using several different fluorescently labelled antibodies. The different types of biomolecules are screened, identified, sorted, and quantified by conductivity or optical excitation.[26] However, flow cytometers are expensive and the technique is limited to suspended cells only. Furthermore, distinct cell populations with similar surface markers are difficult to differentiate, and cells must be permeabilised to detect internal contents.

Purification of biomolecules commonly involves the use of chromatography, the separation of mixtures according to their physical properties. For proteins in particular, chromatography separates molecules on the basis of size, charge, hydrophobicity, and binding affinity (Table 1).[27] After separation of a mixture using chromatography, appropriate detection methods such can be chosen depending on the analytes. The main drawback is that many column chromatography methods require bulky and expensive equipment, operator expertise, and method optimisation to sufficiently resolve similar species.

Table 1 - Comparison of common chromatography techniques used for biomolecule separation.

CHROMATOGRAPHY TECHNIQUE	SEPARATION PARAMETER	ADVANTAGES	DISADVANTAGES
SIZE-EXCLUSION	Size	Simple, fast, cheap, mild conditions	Poor resolution of similarly sized species, difficult to fine-tune
ION EXCHANGE	Charge	High flow rate may recover active protein, high yield	Pretreatment required, needs low salt buffers, resin and equipment expensive, pH conditions may cause denaturation
HYDROPHOBIC INTERACTION	Hydrophobicity	Mild conditions allows for high recovery of natively folded protein	Column and equipment costs, buffer MP must be suitable for analytes to retain activity

REVERSE PHASE	Hydrophobicity	Readily available, simple optimisation	Column and equipment costs, larger proteins are rapidly denatured by harsh solvent conditions

Size-exclusion chromatography is perhaps the simplest of these. Columns are typically packed with a tuneable porous medium, which retards the flow of smaller particles able to travel through the packing material. Larger molecules are excluded from entering the packing material, allowing them to flow through the column relatively unimpeded.[28] This allows for rapid separation of large species from small, however it is not effective for the separation of multiple species of comparable size.

In ion exchange chromatography, mixtures to be purified are carried across an ion doped resin stationary phase (SP) using a pH controlled mobile phase (MP), and the analytes are separated according to their surface charges.[29] Molecules with charges opposite to the SP displace adsorbed MP ions as they are carried through the column, thereby interacting with the SP more frequently and being retained for a longer time. The important parameters of this technique are column selection and pH control, which must combine to create an environment in which there is a significant charge difference between the target and the contaminants. The pH may vary by up to 1 unit from that of the MP at the SP interface depending on the resin used. This restricts the pH to within the tolerance of the desired target and may denature proteins.

Hydrophobic interaction chromatography is a specific form of reverse phase liquid chromatography, useful for protein analysis.[30] It involves the passing of proteins across a hydrophobic SP using a buffer MP. Due to the presence of hydrophobic amino acid residues, the surface of protein analytes can have regions of high hydrophobicity leading to attraction toward other hydrophobic surfaces, in this case the SP, in a salt-rich aqueous environment. The extent of analyte hydrophobicity determines the degree of interaction with the SP, which affects the retention time of the analyte on the separation column. Due to the milder conditions, this method allows for high recovery of natively folded proteins.

Reverse phase (RP) chromatography for proteins involves similar principles to hydrophobic interaction chromatography, where a polar MP is passed over a non-polar SP to elute hydrophilic species before hydrophobic ones. However, analytes must be

considerably more hydrophobic in RP chromatography, so much so that adsorption onto the SP may occur in pure water. These interactions can be so strong that desorption and elution away from the SP requires the use of gradient elution with increasingly non-polar MP mixtures. This allows for the sequential elution of increasingly non-polar compounds to be separated, which can then be individually detected. The use of non-polar eluents may have a denaturing effect on proteins, affecting downstream characterisation.

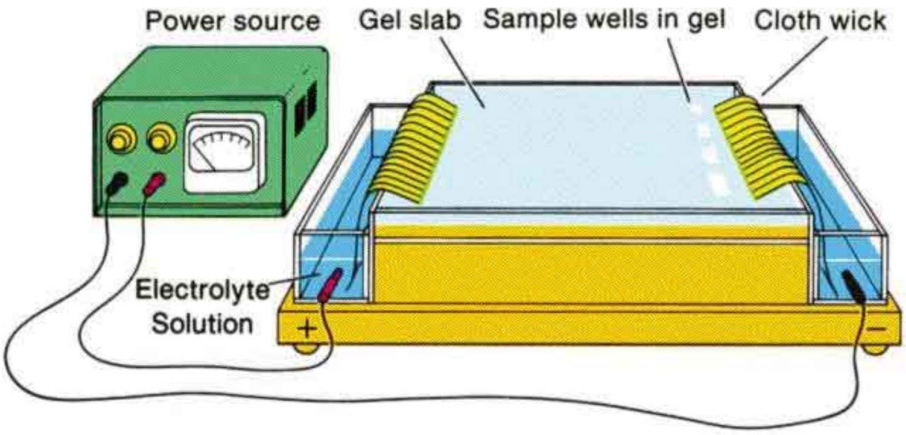

Figure 2 - A typical gel electrophoresis setup.

In addition to size exclusion chromatography, size-based separation of macromolecules such as proteins can also be achieved using gel electrophoresis. This technique uses a permeable gel to separate a mixture based on a combination of electrostatic and friction forces (Figure 2). Gels are commonly made of agarose or polyacrylamide, and mixtures loaded into sample wells at one end. A potential is then applied across the gel, causing the components to migrate according to charge sign and strength. Migration rates are determined primarily by a combination of the forward electrostatic force applied by the electric field and the retarding force of friction caused by the gel viscosity. Proteins can be separated based on either their native folded structures or the molecular weight of the denatured polypeptides, which are then visualised by transferral to a membrane for immunostaining before detection. A similar form of gel electrophoresis, sodium dodecyl sulfate polyacrylamide gel electrophoresis (SDS-PAGE), utilises sodium dodecyl sulfate (SDS) to denature proteins. These then migrate and separate from other macromolecules by polyacrylamide gel electrophoresis according to a

combination of charge, length, and conformation. SDS-PAGE is typically sensitive to picogram levels of analyte, but does not provide information about the folded protein and can be subject to cross-contamination or species conversion effects.[31] After completion, additional visualisation or detection techniques are used to observe the separated species. Though the technique is relatively straight forward, care must be taken not to overload the gel lanes and cause smears or streaking (Figure 3). Electrophoresis is a simple and powerful analytical technique, especially when combined with other techniques[32].

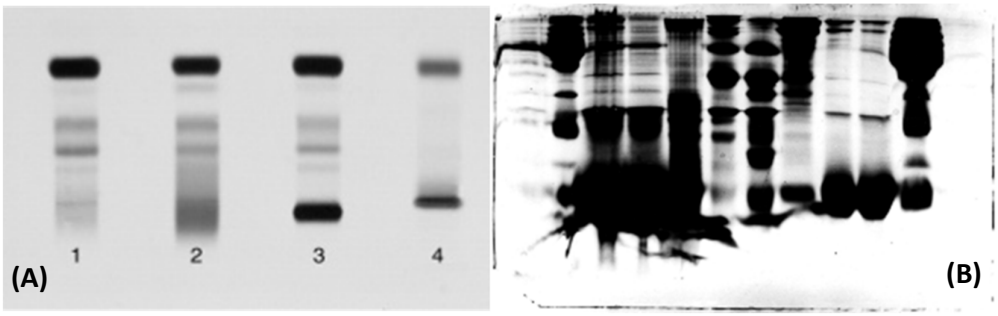

Figure 3 - Examples of (A) good and (B) poor SDS-PAGE electrophoresis plate results after visualisation.

The most diverse range of immunoseparation methods, broadly referred to as immunoassays, takes advantage of the antibody-antigen interaction to separate the target protein from a complex matrix. Immunoseparation methods use a label molecule coupled with either antibody or antigen immobilised to indirectly detect and/or quantify the antigen after antibody-antigen binding. In immunoassays, a ligand binding event can cause changes to the conformation, charge, or optical properties of the recognition molecule. These often minute changes can be detected using spectroscopic, amperometric, or potentiometric techniques.[33] By immobilising target-specific antibodies onto a suitable substrate, a desired ligand can be exclusively captured and extracted from a background of potentially interfering species or directed to a target location. These methods can work on competitive or non-competitive principles, in single antibody or two-site 'sandwich' format (Figure 4). Enzyme-linked immunosorbent assay (ELISA) is a popular technique that utilises a combination of a specific antibody-antigen interaction along with an enzyme-substrate reaction for colorimetric detection. These types of detection utilise label molecules, often fluorescent species, to rapidly detect the analyte of interest. This is an important distinction, in that it is the labelling molecule being detected to indirectly indicate the presence of the

analyte, rather than detecting the analyte directly. The limit of detection for immunoseparation techniques depends on a wide variety of factors, and is especially contingent on the antibody-antigen binding affinity which can vary by up to 7 orders of magnitude.[34] Immunoassay-based technologies are attractive for in-field applications, as they can be effectively miniaturised.

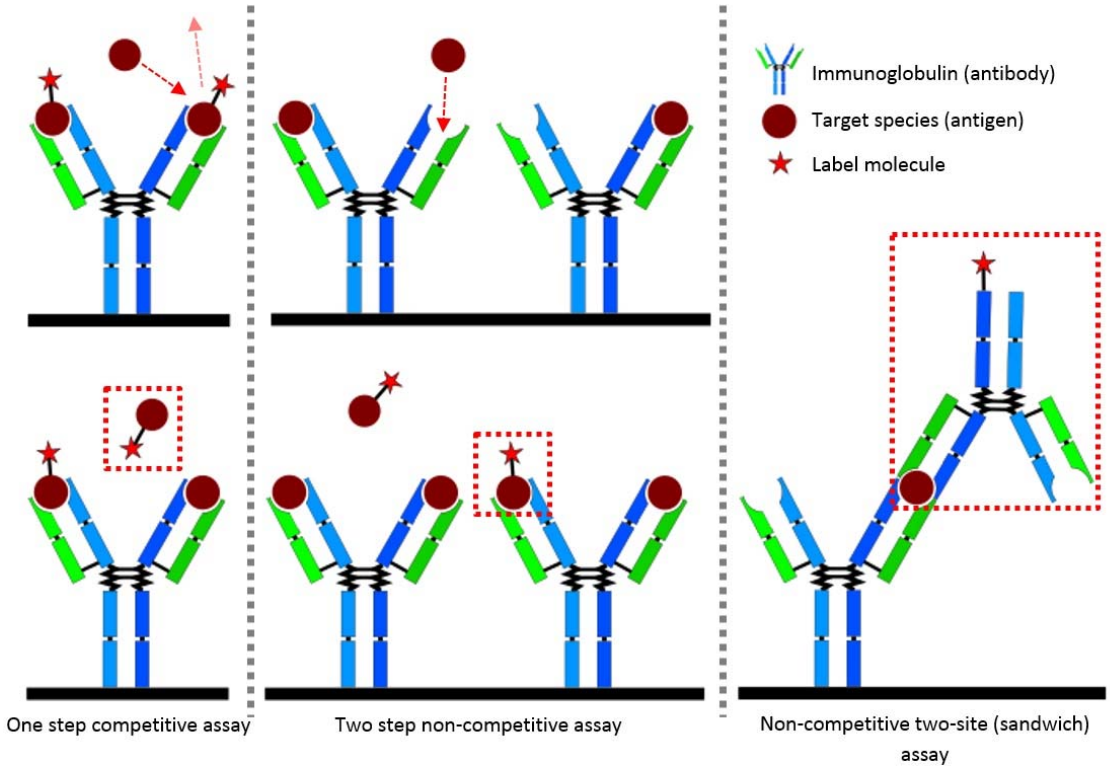

Figure 4 – Several types of immunoassay for the detection of biomolecules. In the one step competitive assay, labelled analytes held by the antibody are replaced by non-labelled analyte (left-top). The two step non-competitive assay, open antibody sites are filled with analyte (middle-top), then remaining sites are occupied by labelled analyte (middle-bottom). Non-competitive two-site assays uses an immobilised primary antibody to capture the analyte, onto which a labelled secondary antibody then binds (right). Detected species are shown in red boxes; in each case, detection is indirect, relying on the presence of a labelled species.

Mass spectrometry (MS) is a powerful technique that provides qualitative and quantitative information about the target analyte. This detector is traditionally coupled in-line with HPLC for the separation and detection of proteins in biological fluids, environmental samples as well as pharmaceutical preparations. In MS, the separated analytes are first vaporised and ionised. The generated analyte ions and fragments are then uniformly accelerated under vacuum and passed through a bent path where they are then

deflected by electromagnets before detection (Figure 5). The mass and charge of the ion determine the degree of deflection, and is expressed as a mass-to-charge ratio (m/z). This provides information on the masses of molecular ions, the intact molecule sans electron, and their fragments.[35] MS is especially valuable for protein analysis as fragmentation patterns can provide structural information, and can be used to identify a particular protein.

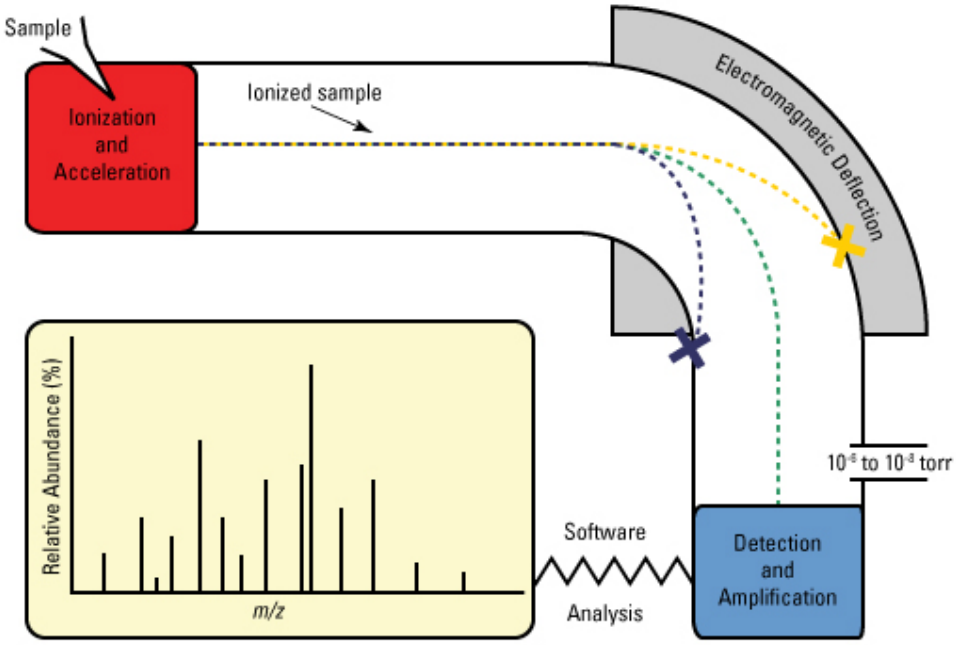

Figure 5 - Schematic diagram of typical mass spectrometry system along with example output spectrum [Image courtesy of Thermo Fisher Scientific].

Matrix-assisted laser desorption/ionisation-coupled time of flight mass spectrometry (MALDI-TOF MS) is a variation of MS that is often used for protein analysis to detect the intact molecular ion. Aqueous analyte is mixed with the matrix solution consisting of an organic solvent, proton source, and a polar molecule capable of strongly absorbing within the UV or IR range. The mixture solvent is then allowed to evaporate on a MALDI plate, leaving behind the recrystallised matrix with embedded analyte ready for measurement. The co-crystallised matrix is then typically pulsed with a nitrogen laser (377 nm) to desorb and ionise the sample. This leads to the formation of deprotonated species, cation radicals and, in the presence of a proton source, protonated species.[36] A time-of-flight mass spectrometer then uses a strong electric field to accelerate the ions under vacuum through a void space. The time taken to reach the detector through the void space is then used to

determine the m/z along with the molecular mass of the intact molecular ion. The running costs of MALDI-TOF MS are relatively inexpensive, but initial instrument purchase is costly. As MALDI is a soft ionisation process, with little residual energy imparted to the analyte, fragmentation is less likely. Therefore, protein identification can only be achieved crudely by comparing the molecular ion, rather than fingerprint-like comparisons using characteristic fragmentation patterns.

Exciting new technologies that combine nanomaterials with existing analytical methods are now emerging, such as nanoelectromechanical systems resonator based mass spectrometry (NEMS-based MS). This technology potentially provides for real-time acquisition of spectra, molecule-by-molecule. It can detect high molecular weight molecules such as proteins (>500 kDa), including neutral species, with very high mass resolution down to a few Daltons.[37] Nanomaterial-based technologies such as this show promise to grow and help shape the future of the sciences.

[1.2.3] Raman spectroscopy for biomolecule detection

Raman spectroscopy can be used to investigate molecular vibrational modes, similar and complementary to infrared spectroscopy. This technique utilises monochromatic light to excite the sample from the ground state to a short-lived virtual excited state, and then measures the resulting scattering of inelastic photons using a CCD detector (Figure 6). The number of scattered photons is directly proportional to the concentration of analyte, and can therefore be used to quantify samples. These inelastically scattered photons are either of a lower or higher energy than the incident radiation, known as Stokes and Anti-Stokes shifts respectively (Figure 7). The difference in wavelength between the incident and scattered radiation is used to generate peaks, which provide information about the present chemical bonds.[38] These inelastic scattering events describe specific vibrational and rotational modes, which can yield a uniquely characteristic, fingerprint-like spectrum. This is particularly useful when analysing unknown samples, where peak positions and their relative intensities can be compared to a reference spectrum for rapid qualitative identification.

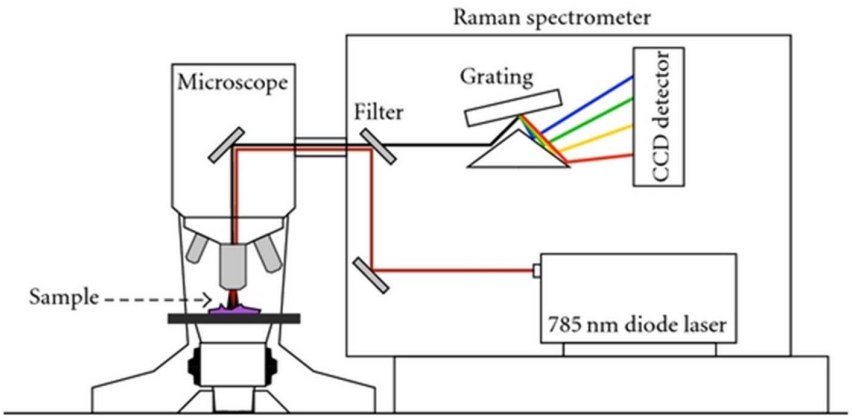

Figure 6 - Schematic diagram of a Raman spectrometer setup with NIR laser and microscope attached.[39]

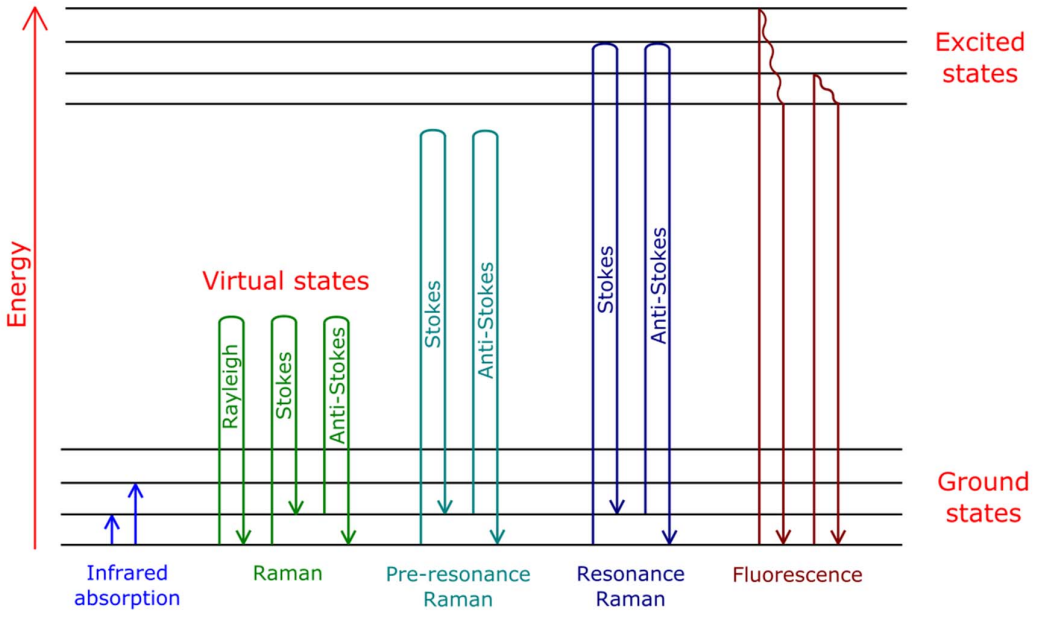

Figure 7 – Simplified diagram comparing energy transitions monitored by infrared, Raman, and fluorescence spectroscopies.

These scattering photons are both infrequent and of lower intensity, approximately 10^{-10} fewer than the excitation photons. Due to the infrequency of these scattering events, Raman measurements can be limited by sample concentration or require significant input energy to acquire sufficient detector counts. As a result, exposing sensitive samples at the required power to obtain a Raman signal can induce photo-damage during excitation, which

renders this mode of detection undesirable for sensitive analysis. However, phenomena capable of significantly enhancing Raman signals are available that allows low power Raman spectroscopy analysis for precious samples.

[1.2.3.1] Surface-enhanced Raman spectroscopy (SERS)

Surface-enhanced Raman spectroscopy (SERS) is an enhancement technique that can improve the Raman intensity of analytes in the proximity of a roughened noble metal surface by several orders of magnitude.[40, 41] This ability to address the sensitivity limitations of the parent Raman technique, whilst also providing spectroscopic information for the potential identification of the analyte, was a promising detection technique for this project.

The ability to significantly amplify weak Raman signals by several orders of magnitude when close to a nanostructured noble metallic surface makes SERS a valuable tool for the identification and quantification of ultra-trace amounts of Raman-active compounds.[42] Enhancement is distance dependent, with an inverse relationship between signal strength and metal proximity, however, steady enhancements have been observed as far as 30 nm from the surface.[43] The exact mechanism of the SERS enhancement is still debated in the literature, but the two main mechanisms proposed for the enhancement phenomenon are the electromagnetic (EM) effect and the chemical effect, with major contribution from the EM effect.[44] The chemical effect is comprised of contributions from metal-adsorbate bonding, charge transfer, image dipole enhancements, effective polarizability, and surface resonance. The EM effect includes contributions from the image field effect (IFE), the lightning rod effect, and the surface plasmon resonance (SPR) effect. SPR arises when surface plasmons in a SERS-active substrate are excited by incident light. This is most effective when the wavelength of the excitation radiation matches with, or is close to, that of the surface plasmon resonance of the metal.[45] The most commonly used SERS-active metals are silver and gold, as their excitation wavelengths are in or near the visible range, although copper, palladium, or platinum can also be used.[46] The magnitude of the SPR effect is influenced strongly by size, surface structure, shape, and proximity to other SERS-active surfaces. In the case of noble metal nanoparticles, multiple particles in close quarters can cause coupling effects between the surface plasmons at the interfaces of adjacent particles, thereby drastically increasing the localised SPR field (LSPR) within

interstices of clustered nanoparticles.[47] This type of interaction produces regions of incredible signal enhancement referred to as “hot spots”, potentially capable of single molecule detection (Figure 8).[48, 49] LSPR is observed when the wavelength of the excitation light exceeds the nanoparticle size, with increasing field intensity nearer to the particle surface. However, enhancement may not be uniform across all regions of the spectrum, even between replicate measurements, and some form of spectral averaging is often required to obtain reliable spectra. Furthermore, SERS enhancement of interfering species may complicate spectral interpretation or convolute diagnostic peaks. The non-homogenous distribution of such hot spots on the SERS substrate surface can contribute to variations in signal intensity between sample measurement sites.[50] When working with ultra-low analyte concentrations or molecules with poor Raman cross-sections, significant variations in the SERS signal intensity, known as SERS blinking, may arise. These blinking effects can affect SERS-based quantification using point-and-measure techniques, and there are many contributing factors that are still poorly understood.[51] To alleviate inconsistencies in the SERS signal intensity, labelling or reporter molecules such as Raman-active dyes or other strong Raman scatterers can be used to produce an intense Raman response that facilitates extrinsic detection.[52] However, the high signal intensity of the Raman reporter often precludes the direct detection of the target analyte Raman fingerprint. By using indirect detection, the user is forced to assume that the detection of the labelling molecule correlates to the presence of the target analyte, which may be quantitatively misleading or create a false positive result.

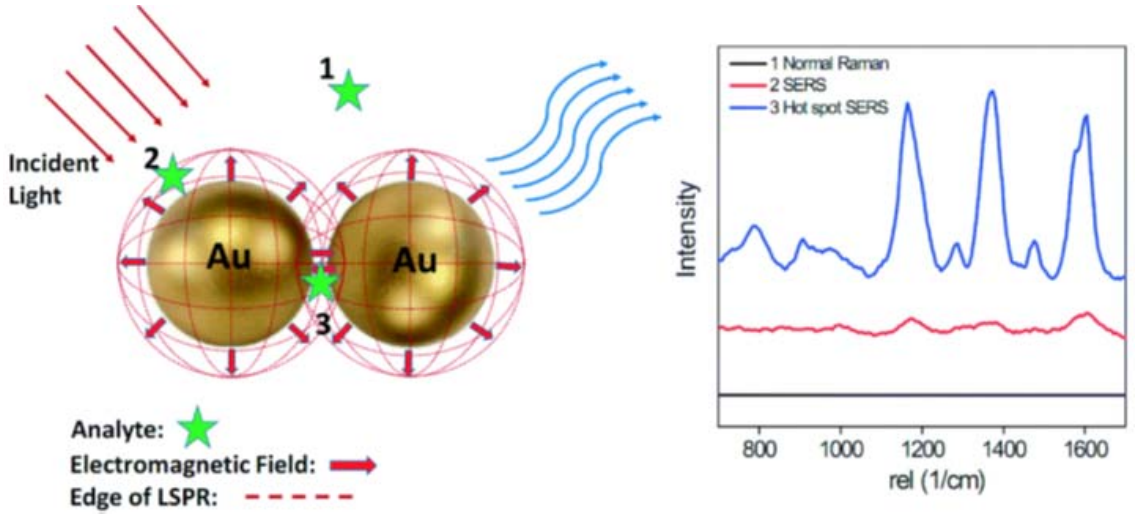

Figure 8 - Electromagnetic amplification of Raman signals via LSPR and resulting 'hot spot' SERS enhancements.

The main attraction of the Raman signal enhancement provided by SERS is undermined by the lack of selectivity when a bare substrate is used for the measurement. This lack of selectivity causes impure samples to produce complex SERS spectra that are nearly impossible to deconvolute. As such, SERS measurement is usually preceded by significant sample preparation and pre-treatment procedures in order to obtain reliable data from the target analyte. These purification procedures can be simplified or eliminated by developing an analyte-specific recognition layer directly onto the nanostructured surface in order to produce simple and effective analyte-specific SERS-based tools that are tailored to each application.

[1.2.4] Recognition molecules for selective SERS

To selectively capture an analyte of interest, a suitable high affinity recognition molecule is required. Natural recognition molecules such as antibodies and aptamers exhibit a high degree of specificity towards their associated ligands.

[1.2.4.1] Antibodies and their fragments

Naturally occurring antibodies are large bidentate binding proteins that are able to bind to specific target molecules (antigens), and are used by the immune system to recognise potentially harmful pathogens. Also known as immunoglobulin (Ig), antibodies are

a class of proteins with a high degree of selectivity. The structure (Figure 9) and binding mechanisms of antibodies have been extensively studied.[53]

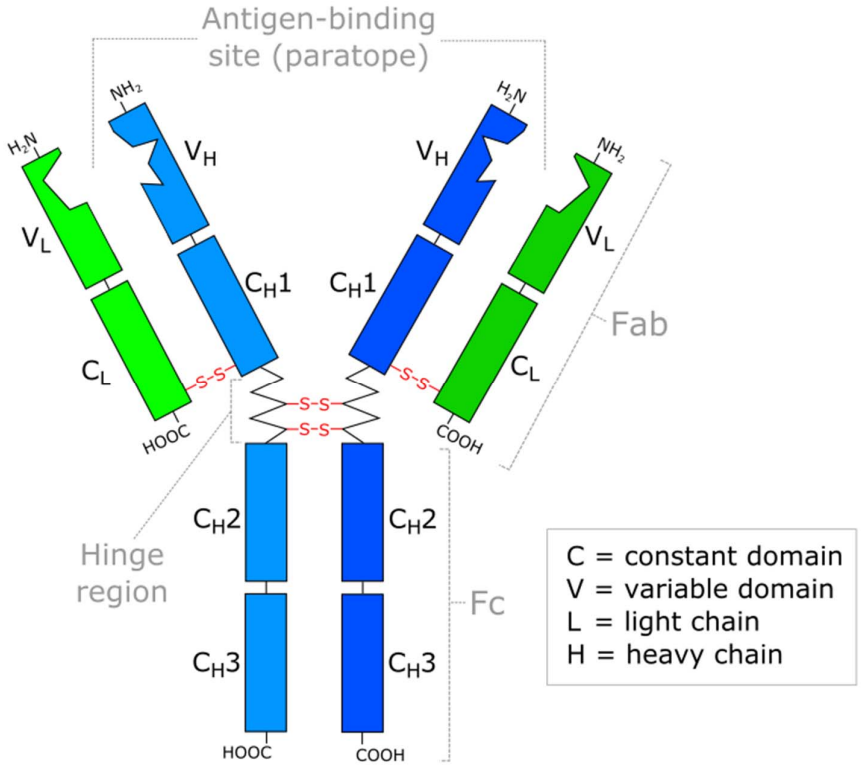

Figure 9 - General structure of an antibody.

The heterotetramer structure is similar across all Ig antibodies, with each region consisting of conjoined chains subdivided into a combination of constant domains (C) and variable domains (V) for both the large heavy chain (H) and small light chain (L). The heavy chain consists of four regions; one upper V_H domain which makes up half of the antigen binding site, linked to the C_H1 domain, which is then bound via a flexible hinge region to the lower C_H2 and C_H3 domains. The light chain contributes the other half of the binding region from its V_L domain, followed by a C_L domain. The upper half of the antibody (V_H, C_H1, V_L, C_L) is known as the fragment antigen-binding (Fab) region. The lower half of the antibody (C_H2, C_H3) is the fragment crystallisable (Fc) region, which interacts with surface receptors and is responsible for immunogenicity of the antibody. The light and heavy chains are held together by disulfide bridges between the C_H1 and C_L domains for each prong, and the two prongs are linked via similar disulfide bridges between the two hinge regions. This gives the

antibody its characteristic Y-shaped structure, with either antibody binding site (paratope) able to independently bind its antigen via its complementary recognition site (epitope). Although the antibody-antigen binding interaction is analogous to a lock-and-key mechanism, the true nature of binding is somewhat more nuanced. As both the V_H and V_L domains contribute to the effectiveness of the complementarity-determining regions (CDRs) of the paratope, it is a combination of both that is responsible for the antigen specificity, known as combinatorial diversity.[54] Each antibody can therefore bind to one or two antigens, via one or both binding sites, depending on the present CDRs. In the case of smaller molecules or peptides, the antigen may be captured by internalisation into a cavity within the binding region, leading to detectable conformational changes in the antibody structure.[55, 56] Large antigens that are too bulky to fit within the confines of the antigen binding site, must bind over a larger area via their CDRs. Antibody-antigen binding involves weak forces such as hydrogen bonding, electrostatic forces, Van Der Waals forces, and hydrophobic forces. These are reversible noncovalent interactions and can be easily disrupted by pH extremes, salt concentration, detergents, and even the presence of excess epitope.[57]

In order to reduce complexity and decrease the size requirements of antibodies while retaining function, smaller antibody fragments have been developed. These include cleaved antibodies, antigen-binding fragments (Fab), single chain variable fragments (scFv), and 3rd generation (3G) technologies such as single domain molecules.[58] Cleaved antibodies are bifurcated by reducing the disulfide bonds holding the two heavy chains together. Thusly reduced antibody may be attractive for noble metal surface applications due to the availability of free thiol linkages. Antigen-binding fragments consist of individual cleaved Fab regions of the antibody. Compared to intact antibody, Fab fragments have the additional advantage of reducing the chance of triggering an undesirable immune response in the absence of the Fc region. Single chain variable fragments consist of the V_H and V_L antigen-binding domains. However, scFvs are not produced by cleavage from the neighbouring constant domains on their respective chains, but rather by protein fusion of the variable domains using a short peptide chain. As the name implies, single domain molecules consist of one variable domain, able to bind to a target with a lower degree of specificity due to the effective halving of the paratope. While these antibody fragments show potential for

recognition applications, the impact on their binding efficiencies and how the reduced size affects conformational changes are not yet well understood.

[1.2.4.2] Aptamers

Aptamers are short single stranded chains of DNA, RNA, or peptides able to recognise and bind to a target molecule with a high degree of specificity. Aptamers bind to their antigen targets by forming complementary secondary and tertiary structures.[59] DNA and RNA aptamers are small in size, typically between 20-60 nucleotides and bind completely, whilst peptide aptamers are larger and bind only using a small portion of variable sequence, analogous to antibodies. To form the binding aptamer complex, complementary bases form secondary structures such as loops or helices which further fold into tertiary structures. These are then able to recognise and bind to the antigen through weak noncovalent interactions such as electrostatic and hydrophobic interactions.[60] As the aptamer binding site is largely random, the function of the ligand can be blocked upon aptamer binding.[61] Specific aptamers are raised against a target *in vitro* using a process called systematic evolution of ligands by exponential enrichments (SELEX), and can be easily amplified or synthesised at a fraction of the cost relative to antibodies. When compared to the 3-6 month shelf-life of antibodies, aptamers are far more stable, and can be stored dry at ambient temperatures or kept frozen in a suitable buffer solution at -20˚C indefinitely.[62]

Biological systems often contain nuclease enzymes, capable of cleaving the phosphodiester bonds between the nucleotides of aptamers, which is problematic when working in biological mediums. This renders stock aptamers ineffective, however there are several modifications that can impart resistance against nuclease degradation, such as chemical modification of the nucleobases or reverse-polarity capping of the termini.

[1.2.5] Nanomaterials for biological separation

There is a wide array of types and sizes of nanomaterials, such as nanorods, nanoparticles, nanostructured surfaces, nanofibers, quantum dots, and nanofilms. Each of these nanomaterials possesses varying properties which can be tuned to fit a specific requirement. These are materials with nanoscale dimensions (1-100 nm) of their superstructure or textured surface, and exhibit properties not observed in the bulk material. When considering liquid biological separation using nanomaterials, applications can be

broadly classified into two categories, surface-immobilised capture or dispersion capture, each with their own merits.

[1.2.5.1] Surface-immobilised separation methods

Surface-immobilised methods of separation involving selective retention of target analytes, where mobile samples are passed across a stationary nanostructured surface to be captured and detected. These nanostructured surfaces include nanocoated surfaces, nanocomposite surfaces, and nanostructured surfaces. Such nanomaterials are desirable due to their on-line measurement capabilities and ease of use. Nanocoated surfaces are those which have a nanometre scale coating on the surface to impart desirable properties, such as the popularised superhydrophobic coatings, or functionalised magnetic beads for bioseparation. Nanocomposites are made up of multiple distinct nanomaterials, imparting a mixture properties that are unavailable in traditional composites.[63] Nanostructured surfaces are often covered in jagged structures such as pillars, spikes, or cones, which confer a far greater overall surface area than featureless surfaces. Noble metal materials with sharp angled surfaces are capable of amplifying Raman signals. These tips are areas of localised surface plasmon field enhancement which are the basis of specialised techniques such as tip-enhanced Raman spectroscopy (TERS) for nanometre scale spatial resolution.[64, 65]

Nanomaterial surfaces can be prepared using a variety of techniques, including electrochemical deposition,[66] lithography,[67] and colloid deposition.[68, 69] These surfaces can be functionalised by forming self-assembled monolayers (SAM), an immobilised and uniform sheet of packed molecules over the metal which provides an ideal mechanism for tuning the surface properties. By depositing molecules over a surface of known area, the loading capacity of the surface can be easily calculated. By creating a SAM composed of recognition molecules over gold or other noble metal surfaces, chemical and physical events occurring on the surface (e.g. binding event between an antibody and antigen) can be monitored. This can be observed through changes in optical properties,[70] electrochemical properties,[71] or changes in LSPR oscillations,[72] and is the basis for many types of biosensor. Although immobilised separation methods allow for simpler sample measurement, they are often not suitable for *in-vivo* or *ex-vivo* measurement due to size constraints and potential cytotoxicity of the platform material.

[1.2.5.2] Dispersion separation methods

Nanomaterials able to stay freely suspended within their medium boast several advantages over immobilised surfaces related to their mobility, as well as possessing a high surface area to volume ratio. Nanomaterials, including nanoparticles, nanorods, nanoflowers, and quantum dots, exhibit a wide range of properties that can be tuned similarly to nanosurfaces through the use of composite materials or the addition of SAMs. Functionalisation using recognition molecules can allow dispersed nanomaterials to act as either platforms for analyte capture, or as mobile vectors for specific regions or tissues. Depending on their size, the surface area of these materials can accommodate a high loading capacity of recognition molecules on their surface. Due to the increased freedom of movement, collection of these materials after dispersion can be more difficult. Common concentration and collection techniques involve centrifugation, targeted accumulation, or magnetic extraction for compatible materials.

[1.2.5.3] Gold nanoparticles as versatile targeting platforms

Gold nanoparticles (AuNPs) have been popularised due to a variety of attractive properties such as potential biocompatibility,[73-75] photothermal therapy and imaging capabilities,[76] plasmonic properties,[77] optical properties, and ease of functionalisation.[78] Although gold NPs are often considered biologically inert at low concentration,[75] the exact nature of their cytotoxicity is still a matter of debate.[73, 74] The ability to form strong covalent bonds between gold and thiolated compounds (e.g. thiolated aptamer, reduced antibody, and antibody fragments), makes it an ideal metallic surface for functionalisation. Amine- and carboxy-terminated species can also bind to gold via their lone pairs of electrons, although these bonds are weaker than the Au-S bond.[79] In addition, this type of bonding is non-specific and can lead to cross-linking aggregation of nanoparticles.[70]

Noble metal surfaces utilising coupled recognition elements are often used to capture a target analyte onto the parent substrate, but can also be used to direct free-moving nanomaterials to a target location. Localised concentration of such materials can therefore be used to enhance the SERS signal of the bound target site, enabling SERS characterisation of relatively large species, such as cells.

[1.2.5.4] Hybrid nanomaterials as customisable platforms

The development of nanocomposites materials consisting of a magnetic material and noble metal coating allows retention of desirable properties along with rapid magnetic separation with minimal physical stress. Due to their potential cytotoxicity, magnetic nanoparticles such as iron oxides are often coated with a protective shell prior to functionalisation to impart biocompatibility and tune the NPs properties for a wide variety of applications.[80] Coating may consist of a noble metal, polymers, or silicates. The ability to easily functionalise noble metal surfaces, selectivity of the particles towards particular cell types, concentration of analyte prior to detection, and biocompatibility makes them ideal for biomedical applications. Core/shell configurations comprised of iron oxide nanoparticles coated in noble metals are popular due to their size-tuneable plasmonic properties and potential for biomedical applications.[81] Furthermore, the array of available detection modes such as visual detection and colourimetry,[82] UV-Vis spectroscopy, MRI, X-ray computed tomography (CT),[83] and SERS makes these magnetic nanomaterial hybrids a diverse multi-modal detection platform.

[1.2.6] Erythropoietin

Although a sparse array of biomarkers are available, Erythropoietin was chosen as a model protein for this study due to its significance in clinical diagnosis, sports doping, and the treatment of anaemia. Erythropoietin is a glycoprotein hormone produced predominantly in the kidneys used to stimulate red blood cell production (erythropoiesis) in the bone marrow, and is an effective treatment for many forms of anemia including those related to cancer therapy. EPO is a highly glycosylated protein of approx. 30 kDa size, with naturally produced (endogenous) and synthetic recombinant (exogenous) types, which can be differentiated by variations in their glycosylation patterns (Figure 10). Recombinant human erythropoietin (rHuEPO) can be produced by inserting DNA coding for the protein into the genomes of bacterial or eukaryotic systems, although additional post-translational modifications may be required.[84] Such modifications by non-native organisms can produce variations in the mature protein that can be used to differentiate the exogenous and endogenous isoforms.[85]

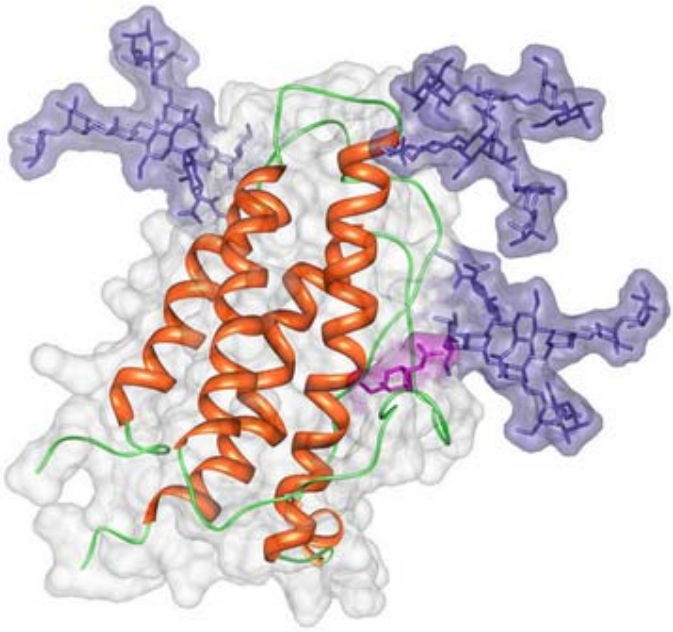

Figure 10 - Predicted structure of glycosylated human erythropoietin with three N-linked glycans (purple) and one O-linked glycan (pink).[86]

The structure of EPO consists of 165 amino acids and four carbohydrate groups with a circular polypeptide chain. EPO contains two disulfide bridges, the first of which completes the circular structure between cysteines 7 and 161, and the second between cysteines 29 and 33. The former bridge is particularly crucial as it is responsible for holding the molecule in the correct shape for binding to the erythropoietin receptor.[87]

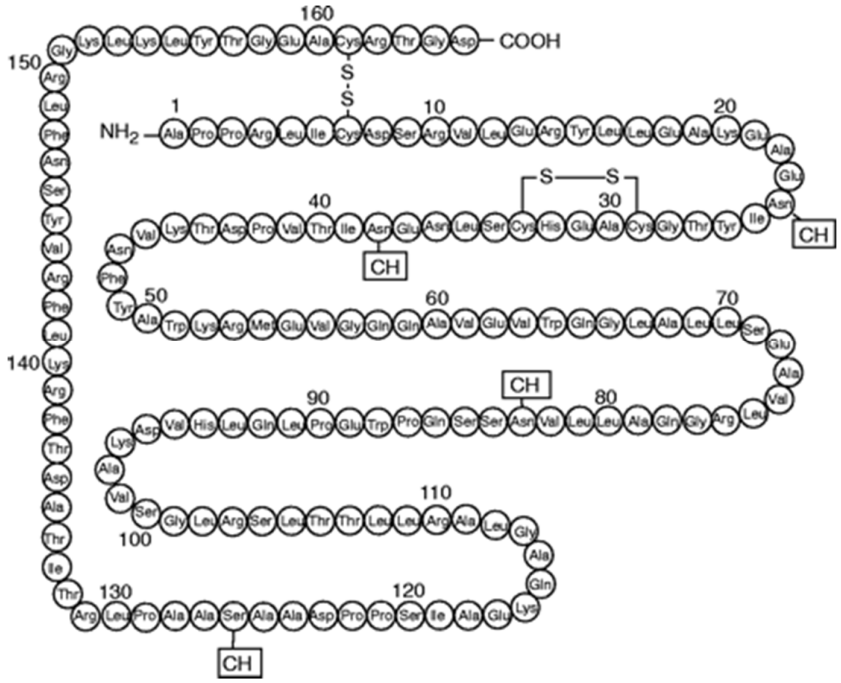

Figure 11 - Primary structure of erythropoietin, with disulfide bridges (S-S) and carbohydrate groups (CH).[87]

Doping of EPO or erythropoietin-stimulating agents (ESA) can lead to increased oxygen uptake due to an increase in red blood cell proportions in blood (haematocrit). This increase in haematocrit can improve respiration of muscles through improved oxygen uptake and delivery, translating to improved endurance and athletic performance. For these reasons, doping with EPO and ESAs has been banned by the World Anti-Doping Agency (WADA) since the early 1990s. However, reliable tests for EPO weren't available until the year 2000, where they were introduced to the Summer Olympic Games in Sydney.[88] Blood doping of EPO and ESAs in sports such as horse racing, greyhound racing, cycling, boxing, rowing, and other endurance events continues to fuel the evolution of new forms of these substances. As a result, analysis methods must constantly improve in order to keep up with these changes.

[1.3] Literature review

The presence of absence of biomolecules such as proteins can be indicative of the health state of a biological system and is a fascinating area of study. Erythropoietin in particular is a protein of interest due to its use as a blood doping agent in sports, as well as its overexpression in certain types of cancers. The detection of proteins at clinically relevant levels is often expensive and laborious. As such, the development of new methods able to both qualitatively identify and quantitate biomarkers quickly and easily can have widespread applications. Raman spectroscopy, specifically SERS, was identified as a technique with great potential in this regard, as it is capable of providing information on both the chemical bonds and quantity of analyte at ultra-trace concentrations under controlled conditions. Therefore, this review will follow the development and applications of SERS-based methods of biomolecule detection, and any relevant literature regarding detection of the EPO protein.

[1.3.1] Biomolecule detection within pure samples

[1.3.1.1] AgNPs and SERS for biomolecule detection

The most common metals used for SERS enhancement are silver and gold, as both provide enhancement when stimulated by radiation of visible or NIR wavelengths. Silver is typically less expensive than gold. Despite the fact that Ag can deliver higher SERS enhancement, it is very liable to oxidise and consequently loses its SERS activity. Therefore, gold nanoparticles are more suitable candidates to applications in the biomedical area due to their very high stability in biological environments. In addition, Ag nanoparticles can cause damage to biological systems. To prevent this, silver nanoparticles were encased in a passivating iodide layer and direct interaction with the metal surface was prevented, imparting biocompatibility toward tested proteins.[89] The iodide protected silver nanoparticles were able to provide SERS spectra of lysozyme with comparable profiles to normal Raman, and outperformed similarly modified and tested gold nanoparticles, whilst keeping tested proteins intact.

[1.3.1.2] Bare AuNPs and SERS for biomolecule detection

The close proximity of an analyte to a noble metal NPs surface can lead to SERS signal enhancement, and can be enormously amplified through particle aggregation. A previous 2004 study showed that particular species, in this case rhodamine 6G (R6G), normally difficult to detect on gold substrates, yielded SERS enhancement of 10^7 – 10^9,

which was attributed to the surface properties and strong NIR absorption of the aggregates used.[90] The use of enhancing noble metal nanoparticle aggregates has since become more widespread, with more advanced methodologies employed to generate these NP clusters. Microfluidic devices direct liquids to active sites through small channels, with potential for low volume and high throughput processing, multiplexing capabilities, and automation. By using a polydimethylsiloxane chip and constricting a downstream microvalve, researchers were able to dam the flow of AuNPs in a microfluidic device and cause reversible aggregation to create hot-spots for the on-line measurement of bovine serum albumin (BSA) by Raman.[91] The microfluidic chip was able to attain a detection limit for BSA at picomolar levels, on par with mass spectrometry. This method of detection is limited by sample purity, as unwanted species may affect the SERS measurement in the presence of the enhancing AuNP aggregates.

[1.3.1.3] Immuno-AuNPs for biomolecule detection

The optical absorption of AuNPs within the visible region can be exploited to prepare simple yet elegant visual tests. A lateral-flow immunoassay dipstick for aflatoxin B_2 (AFB_2) detection was developed using iron oxide cores decorated with AuNPs and functionalised with anti-AFB_2 antibodies, which allowed the rapid and simple visual detection.[92]

Although many methods of specific biomolecule separation utilise nanomaterials with anchored separation entities, surface functionalisation may also occur using weaker interactions such as adsorption. In the case of AuNPs, increasing the ratio of nanoparticles or peptides in solution has been shown to induce or reverse aggregation, respectively.[93] This method of aggregation control is attractive, as UV-Vis spectroscopy showed the effect to be reversible without having to manipulate the pH, temperature, or salt concentration of the medium. These aggregated clusters of gold nanoparticles can produce hot spots leading to high SERS enhancements, increasing detection sensitivity. Within this study, separation methods were also demonstrated using single biotinylated AuNPs to extract streptavidin from a protein mixture. This method is susceptible to competitive surface interactions such as compounds containing thiol groups, which would displace the relatively weakly bound adsorbed species onto the gold surface.

Competitive binding interactions can be exploited to detect species with differing binding affinities toward a surface. By utilising an adsorbed SAM of Raman reporter

molecules on a noble metal surface, compounds containing thiol groups can be detected when they displace the reporter due to their stronger binding affinity, thereby producing a decrease in reporter signal.[94] This reverse reporting method was investigated using three different Raman reporters, R6G, crystal violet, and 5,5'-dichloro-3,3'-disulfopropyl thiacyanine, which were deposited onto a silver nanoparticle surface to detect glutathione. A decrease in reporter signal intensity was observed in the presence of glutathione. This decrease was attributed in part to the displacement of the Raman reporter by the more strongly binding glutathione and the aggregation of the silver colloid. The reasoning for displacement is sound, as the proximity of the reporter to the SERS-active surface will affect whether its signal will be enhanced by the silver. However, the justification for reduced signal intensity due to aggregation is somewhat unclear, as cross-linking and aggregation of noble metal nanoparticles often serves to increase SERS signals through LSPR enhancement. This detection mechanism is simple, can be used to selectively separate thiol-terminated molecules, and has a rapid 20 minute analysis time. However, it does not allow for high sensitivity, with a detection limit of *ca.* 1 µM. The poor sensitivity may be due to the high signal intensity produced by the Raman reporters, whereby displacement of a few reporter molecules by small quantities of thiol analytes would not produce a sufficiently significant signal reduction for reliable detection by SERS. This detection range is not suitable for many clinical applications.

[1.3.2] Hybrid nanomaterials for combined separation and detection of biomolecules

[1.3.2.1] Functionalised AuMNPs

A recent study utilised AuMNPs functionalised with a mixed SAM of 3-mercaptophenylboronic acid and 1-decanethiol to bind to the glucoside moieties expressed on the surface of *Escherichia coli* cells, which were then concentrated using a magnetic field prior to SERS measurement.[95] The mixed monolayer system was found to specifically bind to the target cells, as demonstrated by comparable SERS spectra between NPs bound to both pure *E. coli* and *E.coli* extracted from a bacterial growth solution. By functionalising the surface to direct localisation towards specific sites, the magnetic properties of such nanocomposites can also be harnessed *in-vivo* as magnetic resonance imaging (MRI) contrasting agents. Polyethylene glycol functionalised AuMNPs have been used as negative

MRI contrasts to demonstrate specific accumulation within tumor masses of colon cancer in mice, and pancreatic adenocarcinoma cells in humans, through the enhanced permeability and retention (EPR) effect.[96] These papers demonstrate the flexibility of mobile noble metal surfaces such as composite nanoparticles to act as either selective capturing sites or targeting vehicles, streamlines separation procedures using magnetic concentration, and enables identification using SERS.

AuMNPs have also been used to mechanically concentrate bacteria by applying an external point magnetic field, attracting added AuMNPs to gather bacteria and particles in tightly condensed clusters, reminiscent of a sweeping action.[97] This led to subtle SERS spectral differences between three bacterial strains, with strains clearly separated by principle component analysis (PCA). The method also detected 4-mercaptopyrine down to 0.1 ppb. The closeness of individual particles in these clusters led to the formation of hot spots, thereby increasing SERS enhancement of present analytes. Such enhancing regions can be created in a more permanently way, by creating nanomaterials with closely packed nanoparticles or other irregular surface structures. One such method uses a magnetite core coated in silica, small AuNP seeds are adsorbed and then fastened with more silica by filling inter-particle gaps, and finally the exposed AuNP faces are plated in gold to form a closely-packed arrangement of bulbous gold, with the overall surface structure arrangement reminiscent of raspberries.[98] This allowed for sensitive detection of femtomolar levels of Raman-active test analyte, R6G, due to the magnetic concentration of the iron core and surface-adsorbed species in a magnetic field, along with the controllable size and reproducibility of the high performance SERS-enhancing surface.

Sandwich immunoassays are a popular approach to detecting target analytes,[99-102] and work by capturing a target species between two non-competitive antibodies which allows for extreme specificity and sensitivity. Typically, one antibody is immobilised onto a surface or NP, and a secondary antibody that identifies a different binding region can be coupled with a labelling molecule. The analyte then becomes ‘sandwiched’ between the two antibodies and detected indirectly through the labelling molecule. A study aimed at developing a SERS detection method for bovine leukemia virus antigen gp51 utilised AuMNPs with either randomly oriented anti-gp51 antibody or its half-antibody fragment in a fixed orientation as one half of the sandwich, and gold nanorods with a mixed layer of anti-

gp51 antibody and a Raman-active label, 5-thionitrobenzoic acid (TNB), as the other half.[103] The method demonstrated antibody fragments to be more advantageous, and LOD and LOQ were found to be 0.95 μg mL^{-1} and 3.14 μg mL^{-1}, respectively. The method was also able to detect gp51 in milk. A similar approach using sequential antibody-based AuMNP extraction followed by SERS detection, where reporters consisting of gold nanorods bearing antibodies and TNB to quantify *E.coli* with LOD and LOQ of 8 and 24 cfu mL^{-1}, respectively.[104] A similar study to detect Staphylococcal enterotoxin B (SEB) evaluated two sandwich assay types. The first type was a heterogeneous assay that utilised gold-coated glass slides functionalised with commercial SEB-specific aptamer. The second system used a homogenous assay comprised of magnetic core gold nanorods functionalised with SEB-specific aptamer. For SERS detection, both assays used gold nanorods modified with a mixed layer of TNB and SEB-specific aptamer as the second component.[105] The homogeneous nanorod assay was found to be more sensitive than its immobile heterogeneous counterpart, which was attributed to the superior capturing efficiency due to the comparatively higher surface area. Detection of SEB was achieved at attomolar concentrations, and allowed quantification within complex matrices such as milk, blood, and urine. A recent study demonstrated the use of mixed aptamer SAMs in a magnetic sandwich assay to simultaneously capture and detect two common foodborne pathogens, *Salmonella typhimurium* and *Staphylococcus aureus*, using SERS detection.[106] In this work, a capture probe consisting of AuMNPs adorned with both *S. aureus* and *S. typhimurium* aptamers was used in conjunction with two different signal probes. The first probe was AuNPs decorated with *S. aureus* aptamer and TNB. The second probe was AuNPs coated with *S. typhimurium* aptamers and mercaptobenzoic acid (MBA). Once captured, the sandwiched target bacteria were magnetically separated and detected by SERS, with detection limits of 35 cfu mL^{-1} and 15 cfu mL^{-1} for *S. aureus* and *S. typhimurium*, respectively. The use of a heterogeneous recognition SAM has been demonstrated to accommodate the simultaneous detection of analytes without complicating the extraction procedure. These studies illustrate the potential for aptamer-mediated binding as an alternative to antibodies, with a trade-off of binding efficiency for lower costs, less complexity, and superior long-term stability. An investigation into the development of immunoassays with higher binding efficiencies utilised a combination of antibody-functionalised AuMNPs for separation and antibody-functionalised AuNPs coated with Raman-active labels for SERS-based detection.[107] A mixture of human

and mouse IgGs were separated using goat anti-human IgG functionalised AuMNPs and remaining IgGs monitored over time using the labelled AuMNP-surface sandwich immunoassay. The results showed that the immuno-AuMNPs reduced the concentration of human IgG in the mixture whilst leaving the mouse IgG relatively unchanged. This design assumes that removal of the target analyte is by specific means only, which is undermined by an observed reduction in mouse IgG signal over time. The aforementioned literature demonstrates the efficacy of magnetic nanomaterial-based immunoassay methods for selective capture and SERS-based detection. Although the inclusion of a Raman reporter allows for far greater sensitivity, detection of the target analyte was carried out by indirect means and assumes that the reporter presence is a result of specific binding to the target analyte. Due to the requirement of sandwich assays to use multiple NP or surface types for separation and detection, additional complexity is imparted to the system. The requirement of these assays to utilise two non-competitively binding recognition molecules significantly adds to the cost of these assays, and can be restrictive if suitable antibody or aptamer sets are not accessible.

[1.3.2.2] Functionalised MNPs, AuNPs, or AuMNPs used in combination

Sets of SERS probes aimed at the detection of the foodborne pathogens *Salmonella enterica* serovar Typhimurium and *Staphylococcus aureus* within a food matrix were developed using tailored sets of magnetic separator particles and SERS probes.[108] Iron oxide nanoparticle clusters were group-coated in an APTMS polymer coat with pathogen-specific antibody used for immunoseparation from a mixture. Additional SERS probes consisting of AuNPs decorated with an assigned Raman reporter and antibody for each pathogen were then conjoined with the clusters. Using this scheme, 10^3 cfu mL^{-1} of the target pathogens were detected in spinach. A blind test in peanut butter confirmed the detection limit and the specificity of the test. Although the reported sensitivity was fairly low, the use of more suitable Raman reporters and SERS substrates than those trialled would possibly improve the sensitivity of this method down to the single pathogen level.

Uncoated magnetic nanoparticles have been used to separate thrombin (TB) using aptamer functionalised TBA_{15}-MNPs, and subsequently detected with SERS through aptamer-reporter co-functionalised gold nanoparticles, TBA_{29}-AuNP-XRITC.[109] The lower limit of the SERS detection was determined to be 0.27 pM. This shows the potential for

immuno-functionalised AuNP/MNP systems toward detection of biomolecules at clinically relevant concentrations.

[1.3.2.3] Immuno-AuMNPs for selective and label-free SERS

The use of labels such as Raman-active molecules often allows for greater sensitivity, due to their enhanced Raman cross-section, however one must assume that the detection of the label corresponds to the presence of the analyte. Furthermore, quantification using labelling assumes a correlation between label and target analyte concentrations. Methods that utilise label-free SERS detection allow for the presence of the analyte to be measured directly. By attaching AuMNPs to a graphene surface and functionalising the gold surface with antibodies specific for Alzheimer biomarkers, tau protein and β-amyloid, a rapid separation-detection technique was devised with femtogram-level sensitivity.[110] The high sensitivity was attributed to the plasmon-coupling of neighbouring AuMNPs to form hot spots. However, the HR-TEM images of freshly prepared AuMNP-graphene oxide surfaces showed a heterogeneous particle distribution, often with large inter-particle distances. Therefore the efficiency and reproducibility of this method with respect to SERS signal enhancement may be limited by the random loading distribution of the AuMNPs. Popcorn-shaped AuMNPs functionalised with antibodies have been demonstrated for targeted magnetic separation and enrichment, and label-free SERS detection of the multi-drug-resistant *Salmonella* DT104.[111] The detection was carried out by monitoring the changes in UV-Vis and SERS profiles of the functionalized NPs before and after binding to the targeted bacteria. The spectra of the separated bacteria showed sequential decreases in SERS intensity that coincide with reduced concentrations, opening the door for SERS-based quantitation. The AuMNPs were also used in conjunction with a NIR laser to induce photothermal damage to target cells, and monitored by SERS. The selectivity of the system and requirement for gold proximity to cause photothermal damage was shown by using the *Salmonella* DT104-specific AuMNPs in a solution of concentrated *E. coli* bacteria, with 97% of the *E. coli* surviving a laser dose shown to kill 100% of the target species. This study demonstrates the versatility of AuMNPs for both separation and detection applications, as well as the potential for theranostics. The design of this system is quite elegant, with all components serving one or more purposes.

[1.3.2.4] Immuno-AuNPs for label-free SERS separation and detection of EPO

As stated earlier, SERS can been used to monitor the binding event between selective recognition elements and their ligands. In a recent study, anti-EPO antibodies were anchored to silica-coated AuNPs and used for label-free SERS detection of the protein in a biological matrix.[112] The silica shell was used to prevent non-selective binding to the AuNP surface without impairing the signal enhancement. The SERS quantification of EPO using this nanosensor was $3.5x10^{-13}$ M. This nanosensor demonstrated the suitability of specific recognition-coupled nanoparticles as a combined selective extraction and label-free SERS detection platforms when coupled with SERS, for proteins at biologically relevant levels. However, this study did not provide any direct detection of the analyte. Instead, the method monitored the SERS variations attributed to conformational changes within the antibody recognition layer upon interaction with EPO. Such spectral variations can be so minor that it may be difficult to attribute differences conclusively to antibody-antigen binding events rather than other external influences. Furthermore, this mode of monitoring does not allow for quantitation of the analyte.

[1.4] Aim and scope

To the best of our knowledge, there have been no reports of a rapid methodology for the combined selective separation and label-free direct SERS detection of biomolecules in complex biological fluids. Research on SERS-based methods for the direct detection of erythropoietin is lacking, with no reported Raman spectrum of an extracted EPO protein found in the literature. Thus, our research was aimed at the development and testing of a selective extraction system, able to separate biomolecules from complex biological samples, coupled with label-free SERS detection and quantitation capabilities. Though the detection and quantitation of EPO from complex samples is achievable using existing methods, our goals were to improve upon these methods in several areas, as outlined below.

1. Develop a system able to (a) selectively capture, (b) detect, and (c) quantify biomolecules from complex biological matrices using SERS.
2. Complement current methods for biomolecule detection by considering: (a) cost-effectiveness; (b) analysis time; (c) ease of use; (d) detection limits and; (e) portability.

After reviewing the broad array of literature on nanomaterials for biomolecule analysis (Chapter 1), the initial approach develops and tests antibody-functionalised hybrid nanoparticles to selectively extract EPO, and uses label-free direct SERS to monitor, identify, and quantify (Chapter 2). The initial methodology was then modified and adapted to aptamer-functionalised nanostructured surfaces for the same model protein, for label-free indirect monitoring and quantitation of EPO using SERS (Chapter 3).

Chapter 2

Preface

In the previous chapter (Chapter 1), the lack of literature on cost-effective and rapid selective isolation methods for the label-free SERS detection of biomolecules from complex biological matrices was established. Furthermore, existing research into SERS-based detection of EPO in complex biological samples is lacking, with no reported Raman spectrum of post-separation EPO found in the literature. As a result, the first step was to establish a method of selectively extracting EPO from a relevant biological mixture.

This chapter will focus firstly on the development of hybrid material nanoparticles functionalised with antibodies. The use of hybridised materials allows for the combination of multiple desirable material properties, whilst antibodies allow for selective capture of a target species. Secondly, the chapter will evaluate the use of these developed nanoparticles for extraction of erythropoietin from a blood matrix. The medical and anti-doping relevance of EPO is well-known, and as EPO is an endocrine hormone, blood is the logical choice of test matrix. This will be carried out using label-free SERS as a detection and quantification method. The advantages of this are two-fold, with SERS able to provide a spectroscopic fingerprint of the EPO analyte, rather than indirect evidence of its presence using a labelling molecule, as well as being a highly sensitive detection method.

This chapter details the synthesis and testing of hybrid nanoparticles, consisting of an iron oxide core and gold shell, functionalised with thiol-bound antibody for the specific and rapid separation of a target protein, EPO. Label-free SERS methods were used to monitor the antibody-antigen binding, followed by release of EPO for direct spectroscopic fingerprinting of the purified analyte, and direct spectroscopic quantitation. Our primary focus was the successful development and testing of the aforementioned process using EPO as a model protein, along with appropriate validation techniques. The overarching design goal was to devise a system suitable for point-of-care testing and in-field protein screening. The approach methodology is justified briefly below.

(i) **Hybrid iron oxide/gold coated nanoparticles:** provides benefits of gold surface for SERS and ease of functionalisation using thiol chemistry whilst retaining magnetic properties for rapid separation.

(ii) **Selective extraction**: by functionalising the gold surface with target-specific antibody and backfilling with a small thiol, biomolecules can be selectively captured from a complex matrix.

(iii) **Screening**: spectroscopic monitoring of antibody-antigen binding using SERS.

(iv) **Direct detection and quantitation**: releasing captured protein from antibody-antigen complex to obtain purified protein extract, then measure its direct SERS fingerprint. This can then be used for label-free quantitation.

(v) **Portability**: developed system to be paired with a handheld Raman spectrometer to analyse the extracted biomolecules and test the system for in-field use.

Statement of Contribution of Co-Authors for Thesis by Published Paper

The following is the suggested format for the required declaration provided at the start of any thesis chapter which includes a co-authored publication.

The authors listed below have certified* that:

1. they meet the criteria for authorship in that they have participated in the conception, execution, or interpretation, of at least that part of the publication in their field of expertise;
2. they take public responsibility for their part of the publication, except for the responsible author who accepts overall responsibility for the publication;
3. there are no other authors of the publication according to these criteria;
4. potential conflicts of interest have been disclosed to (a) granting bodies, (b) the editor or publisher of journals or other publications, and (c) the head of the responsible academic unit, and
5. they agree to the use of the publication in the student's thesis and its publication on the Australasian Research Online database consistent with any limitations set by publisher requirements.

In the case of this chapter: R. Agoston, E. L. Izake, A. Sivanesan, W. B. Lott, M. Sillence and R. Steel. Rapid isolation and detection of erythropoietin in blood plasma by magnetic core gold nanoparticles and portable Raman spectroscopy. *Nanomedicine: Nanotechnology, Biology and Medicine.*

Publication title and date of publication or status:

Contributor	Statement of Contribution*
Roland Agoston QUT Verified Signature Date: 15/03/2016	Conducted experiments, data analysis, and primary manuscript authorship and editing.
Emad L. Izake	Supervision and editing.
Sivanesan Arumugam	Contributed to experimental work, research discussions, and editing.
William B. Lott	Contributed to research discussions and editing.
Martin Sillence	Contributed to research discussions and editing.
Rohan Steel	Contributed to experimental data, and research discussions.

Principal Supervisor Confirmation
I have sighted email or other correspondence from all Co-authors confirming their certifying authorship.

Emad Kiriakous	QUT Verified Signature	15/03/2016
Name	Signature	Date

Rapid isolation and detection of erythropoietin in blood plasma by magnetic core gold nanoparticles and portable Raman spectroscopy

Roland Agoston[a], Emad L Izake[a*], Arumugam Sivanesan[a*], William B. Lott[a], Martin Sillence[a], Rohan Steel[b]

[a] Nanotechnology and Molecular Sciences Discipline, Faculty of Science and Engineering, Queensland University of Technology, 2 George St., Brisbane, QLD 4001, Australia

[b] Biological Research Unit, Racing Analytical Services Ltd, 400 Epsom Road, Melbourne 3031, VIC, Australia

*Corresponding author:

E-mail address: e.kiriakous@qut.edu.au (E. L. Izake) Tel.: +61 7 3138 2501; Fax: +61 7 3138 2501

E-mail address: sivanesan.arumugam@qut.edu.au; asnesan@gmail.com (A. Sivanesan) Tel: +61 07 3138 0607

[2.1] Abstract

Isolating, purifying, and identifying proteins in complex biological matrices is often difficult, time consuming, and unreliable. Herein we describe a rapid screening technique for proteins in biological matrices that combines selective protein isolation with direct surface enhanced Raman spectroscopy (SERS) detection. Magnetic core gold nanoparticles were synthesised, characterised, and subsequently functionalized with recombinant human erythropoietin (rHuEPO)-specific antibody. The functionalized nanoparticles were used to capture rHuEPO from horse blood plasma within 15 minutes. The selective binding between the protein and the functionalized nanoparticles was monitored by SERS. The purified protein was then released from the nanoparticles' surface and directly spectroscopically identified on a commercial nanopillar SERS substrate. ELISA independently confirmed the SERS identification and quantified the released rHuEPO. Finally, the direct SERS detection of the extracted protein was successfully demonstrated for in-field screening by a handheld Raman spectrometer within 1 minute sample measurement time.

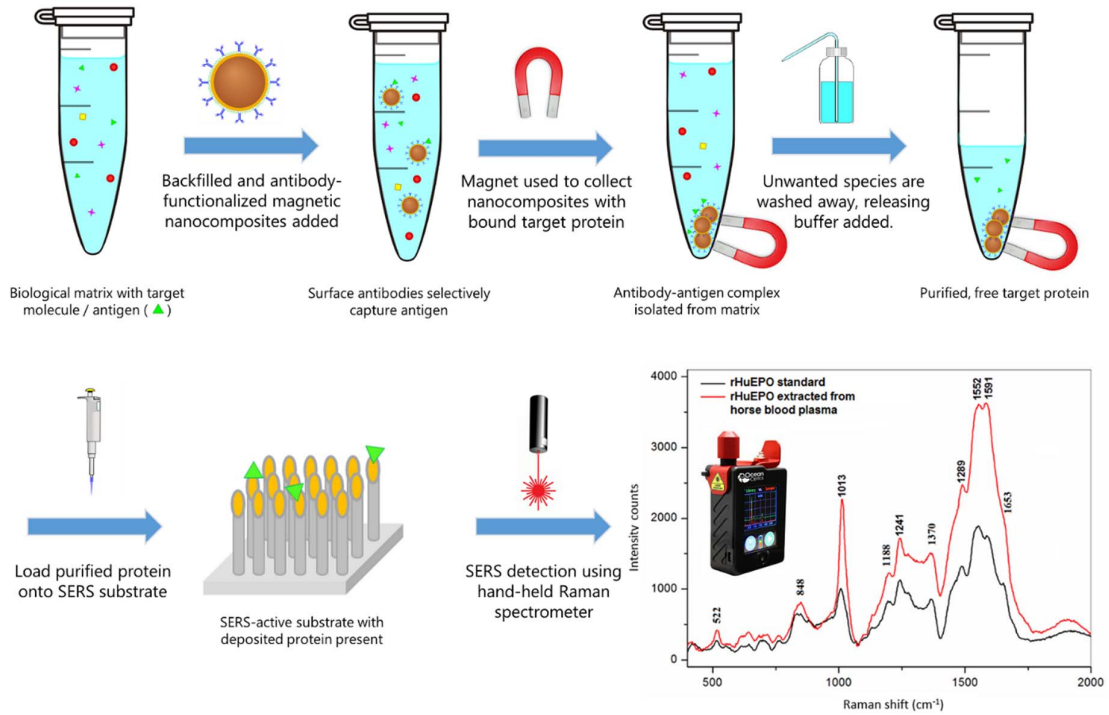

Scheme 1 - Extraction of target analyte using developed specific extractor nanocomposites and SERS detection using handheld Raman.

[2.2] Keywords

Selective isolation, Label-free SERS, Magnetic core gold nanoparticles, Erythropoietin, In-field screening, Proteins in biological fluids

[2.3] Background

The efficient and accurate analysis of biomolecules found in complex biological matrices like blood or urine is essential for many applications, including protein characterization, clinical diagnostics, and drug dosing protein analysis, but current methods are usually expensive and time consuming.[113-116] Simultaneous methods for sample separation and detection must exhibit sufficiently high resolution, high sensitivity and wide dynamic range to detect low concentrations of proteins.[34, 117, 118] Ideally, these methods should also be easy to perform, rapid, non-toxic, environment-friendly, and cost-effective. No current protein detection technique meets all these demands.[34, 117, 118] Although mass spectrometry (MS) is sensitive and accurate for the analysis of proteins,[119, 120] it is relatively expensive, requires specialised skills, and cannot be field adapted.

Enzyme-linked immunosorbent assay (ELISA) is a widely used technique in protein analysis. ELISA methods fall in two categories, direct and indirect. The direct methods use only one primary antibody while the indirect methods use primary and secondary antibodies. Direct ELISA methods have significant disadvantages such as: 1) the antibody's immune-reactivity is adversely affected by labelling with enzymes or tags; 2) labelling the used antibody is time-consuming and expensive; 3) there is only a limited choice of antibody labels that can be used from one experiment to another; 4) the signal amplification is modest. Indirect ELISA methods suffer from other disadvantages such as the long analysis time, due to the introduction of extra incubation steps in the procedure, and cross-reactivity with the secondary antibody, which result in nonspecific signals.[121]

Surface-enhanced Raman spectroscopy (SERS), which characterises molecules by their vibrational fingerprint, is a rapidly emerging technique for the detection of biomolecules.[122, 123] In SERS, the surface plasmon resonance (SPR) of a nanostructured noble metal surface enhances the oscillating electric field of incident light.[124] This near-field enhancement increases the Raman signal of analyte molecules that are in close proximity to the metal surface by factors as high as 10^6–10^8 relative to the unenhanced Raman signal,[124-126] making it useful for ultra-trace detection and potentially allowing for single-molecule detection.[42, 127]

SERS strategies may be employed to either directly or indirectly detect biomolecules. In the direct method, a biological sample is loaded onto a noble metal substrate and directly

analysed by SERS to acquire the Raman signature of the biomolecule.[89, 128, 129] SERS provides direct structural information about the bound target molecule and identifies qualitative differences between similar samples. However, this approach lacks specificity and the Raman spectroscopic features other molecules present in a complex biological matrix can obscure the Raman characteristics of the target analyte. For this reason, extensive isolation and clean-up procedures are required prior to direct SERS detection.[112] By comparison, SERS may indirectly detect biomolecules by attaching a Raman-active dye to the metal SERS substrate.[128, 130] The substrate's surface carrying the Raman dye is then pacified with a protective layer (e.g. silica shell) to prevent the non-specific binding of potentially interfering biomolecules in a complex biological matrix. Analyte-specific recognition molecules, such as antibodies or aptamers, are attached to the SERS substrate to provide target specificity.[128] However, indirect SERS detection does not detect the target biomolecule itself, but only detects the SERS spectrum of the Raman dye.[112] Specific recognition of the target analyte by the antibody or aptamer must be assumed to occur without significant cross reactivity.

We recently demonstrated a hybrid approach for label-free indirect SERS detection of proteins, in which a SERS substrate was functionalized with a protein-specific antibody or aptamer for target specificity, but no Raman dye was attached to the SERS substrate.[112, 130] Instead, the SERS spectra of surface-bound antibody or aptamer were compared before and after the binding of the target protein. Differences in features between the spectra were used to identify the target protein in aqueous and biological samples.

Erythropoietin (EPO) is a glycoprotein hormone used in the regulation of erythropoiesis and is involved as a signalling protein in the production of red blood cells in bone marrow.[131] Sports doping with exogenous rHuEPO increases oxygen capacity and leads to enhanced aerobic performance by athletes. The short biological half-life of rHuEPO makes it only detectable in urine for 3–7 days.[132-134] Recent doping regimens, in which micro-doses of rHuEPO (approximately 20–25 IU/kg) are administered to avoid random detection by anti-doping authorities, have reduced the rHuEPO detection window to only 12–18 hours.[135] The standard protocol currently used to detect rHuEPO doping in competitive sports, isoelectric focusing and double blotting,[136] takes several days to perform in a laboratory-based environment and requires skilled technicians, complex

procedures, and expensive equipment. To detect rHuEPO doping in sports environment, a reliable rHuEPO screening technique is required that is both rapid and field adaptable. In order to identify rHuEPO in urine and blood, the existing reference techniques attempt direct detection of the substance and/or its metabolite in its original biological matrix.[117, 137] This requires extensive clean-up procedures to isolate the protein from the biological matrix of origin prior to the measurement.

Here we introduce a modified approach for simplified selective isolation and label-free direct SERS detection of rHuEPO to demonstrate the utility of this technique for detecting biomolecules in complex biological matrices (Scheme 1). We first developed magnetic core gold nanoparticles and functionalized their surfaces with rHuEPO-specific antibodies to create a rHuEPO-specific recognition layer. The remaining bare gold surface on the nanoparticles surface was pacified by backfilling with an alkane thiol to block non-specific binding of potentially interfering molecules. The functionalized nanoparticles selectively captured rHuEPO from spiked horse plasma. The binding event between rHuEPO and the functionalized nanoparticles was monitored by SERS.[138] To confirm the selective capture of rHuEPO, as well as to directly detect the its Raman fingerprint, the bound rHuEPO molecules were released from the extractor nanoparticles, loaded onto a gold-coated silicon nanopillar substrate and characterised by SERS. To cross-validate our methodology, rHuEPO that had been captured by our functionalized nanoparticles was screened by an independent laboratory using rHuEPO-specific ELISA. Finally, to demonstrate applicability of this new method for the in-field rapid screening of rHuEPO, we directly acquired the SERS spectrum of the captured and released rHuEPO using a handheld Raman device and compared it to a standard rHuEPO SERS spectrum.

The significant advantages of the protein analysis methodology that we describe here include: 1) the rapid and selective isolation of the target proteins directly from a complex biological matrix; 2) the ability to monitor the selective antibody-antigen binding event by SERS; 3) the ability to directly detect the native protein's Raman fingerprint by SERS; and 4) the applicability of this technique to the rapid detection of proteins in the field.

[2.4] Experimental details

[2.4.1] Chemicals and materials

Recombinant human erythropoietin international standard (rHuEPO IS, 3rd International Reference Preparation) was sourced from the National Institute for Biological Standards and Control, UK. 7D3 mouse monoclonal anti-human erythropoietin antibody was purchased from MAIIA Diagnostics, Uppsala, Sweden. Gold (III) chloride ($HAuCl_4$), phosphate buffered saline, bovine serum albumin, sodium borohydride ($NaBH_4$, 99%), trisodium citrate ($Na_3C_6H_5O_7 \cdot 2H_2O$), ferrous chloride ($FeCl_2 . 4H_2O$), ferric chloride ($FeCl_3 . 6H_2O$), nitric acid and sodium hydroxide were of analytical grade and purchased from Sigma-Aldrich (USA). Gravity flow size-exclusion columns (illustra NAP-5) were obtained from GE Healthcare Life Sciences (AU). Deionized water (ultrapure Millipore filtered, 18.2 MΩ.cm@25˚C) was used in all preparations. All glassware was cleaned with aqua regia and thoroughly rinsed with deionized water prior to use. Quantikine IVD human erythropoietin ELISA kit from R&D Systems (USA, catalogue No DEP00) was used for the detection of rHuEPO in horse plasma.

[2.4.2] Instrumentation

The iron oxide nanoparticles and the magnetic core gold nanoparticles were characterised by transmission electron microscopy (TEM) [JEOLJEM-1400 (JEOL, USA)] and UV–visible spectroscopy [Cary 100 spectrophotometer (Agilent Technologies, USA)]. For the determination of the iron oxide phase, samples were dried and prepared as a thin film, then the X-Ray diffraction patterns were collected using a Philips X'pert wide angle X-Ray diffractometer operating in step scan mode, with Co Kα radiation (1.7903 Å). Patterns were collected in the range 10 to 80° 2θ with a step size of 0.02° and a rate of 30s per step. The XRD patterns were matched with ICSD reference patterns using the software package HighScore Plus.

Raman spectra were collected on the Renishaw inVia Raman Microscope using an excitation wavelength of 785 nm and 0.5% of maximum (450mW) laser power. Spectra were collected by a 50x objective lens over a wavelength range from 300 cm^{-1} to 1800 cm^{-1} using 10 accumulations (1 second exposure time per accumulation). At least 30 spots, on various locations of the SERS substrate, were screened per each submitted sample.

For SERS measurement using the handheld IDRaman Mini, the sample was screened in the Raster Orbital Scanning (ROS) mode using 785 nm excitation wavelength and 40 accumulations per minute per sample.[139]

[2.4.3] Synthesis of iron oxide nanoparticles

To develop the magnetic iron oxide cores, Fe_3O_4 nanoparticles were first prepared by precipitation, and then chemically oxidized to γ-Fe_2O_3.[107, 140] Briefly, $FeCl_3.6H_2O$ (10 mmol) and $FeCl_2.4H_2O$ (5 mmol) were dissolved in dilute hydrochloric acid solution (12.5 mL, 0.36 M) with magnetic stirring. The developed clear yellow solution was then added dropwise to NaOH solution (125 mL, 1.5 M) with vigorous stirring where a black precipitate was immediately formed. The resulting mixture was stirred for 10 minutes after complete addition. The formed precipitate was then collected using strong permanent magnet. To neutralize the pH of the precipitate, it was rinsed with dilute hydrochloric acid solution (250 mL total, 0.01 M). Finally, the precipitate was washed several times with deionized water. The washed precipitate was then re-suspended in dilute nitric acid solution (125 mL, 0.01 M), boiled to reflux for one hour, then cooled to room temperature. The resulting iron oxide nanoparticles were collected using a magnet and rinsed several times with deionized water to neutralize the medium. The clean brown-coloured product was resuspended in 50 mL of deionized water, and the concentration was determined gravimetrically to be 0.177 M.

[2.4.4] Development of magnetic core gold nanoparticles

To develop a gold shell onto the iron oxide nanoparticle surface, a method described by Tamer et. al[141] was adopted with modifications. 0.6 mL of the iron oxide nanoparticle colloid (0.177 M) was transferred into a 100 mL volumetric flask and diluted with deionized water. 19 mL of the resulting solution was transferred to another round-bottomed flask. $HAuCl_4$ (0.5 mL, 1%) was then added and the resulting mixture diluted to 100 mL with deionized water. To reduce gold atoms onto the iron oxide nanoparticles' surface, freshly prepared $NaBH_4$ solution (0.2 mL, 0.05 M) was added to the mixture, followed by 5 successive additions of 0.1 mL $NaBH_4$ (0.05 M). The mixture was vigorously swirled for 10 minutes after each addition. The mixture was then heated to boil and 3 mL of sodium citrate solution (0.1 M) was added dropwise to produce a pink coloured colloid. The formed magnetic core gold nanoparticles were removed from the reaction mixture using a magnet.

The nanoparticles were then washed several times with DI water and finally resuspended in 4 mL of DI water.

[2.4.5] Development of antibody-functionalized magnetic core gold nanoparticles

To attach the 7D3 anti rHuEPO antibodies to the gold surface of the magnetic core gold nanoparticles, cysteamine was used as a linker. The amine group of cysteamine was utilized to form amide bond with the C-terminus of the antibody structure.[142] For this purpose, 1-ethyl-3-(3-dimethylaminopropyl) carbodiimide solution (EDAC, 0.2 M) and N-hydroxysuccinimide solution (NHS, 0.1 M) were prepared in PBS (pH 7.4) and used to activate the -COOH groups of the 7D3 anti-rHuEPO antibody.[142] 50 µL of both EDAC and NHS solutions were added to a LoBind vial and vortexed for 15 minutes. 100 µL of aqueous cysteamine ($3x10^{-5}$ M) was then added to the vial and mixed for another 15 minutes. 50 µL of the 7D3 anti-rHuEPO antibody ($2x10^{-5}$ M in PBS, pH 7.4) was then added to the mixture in ten equal volumes with 2 minutes vortex between additions. After complete mixing, the solution was allowed to stand for 5 hours under dark conditions at 4˚C. After this time, the reaction mixture was purified using a gravity flow size-exclusion column to obtain the cysteamine-bound 7D3 antibody.

To attach the cysteamine-bound 7D3 antibody to the magnetic core gold nanoparticles, 100 µL of the nanoparticles were mixed with 50 µL of the antibody in a LoBind Eppendorf vial and left to form Au-S bonds between the thiol (-SH) group of cysteamine-bound antibodies and the gold surface of the nanoparticles overnight at 4˚C. To prevent non-specific binding of interfering analytes and enhance the selectivity of the functionalized nanoparticles towards the target protein, any remaining bare sites (i.e. gold surface areas that were not occupied by the antibodies) were backfilled by adding 15 µL of 1-butanethiol ($1x10^{-6}$ M in PBS, pH 7.4) and allowing the mixture to stand for at 1 hour.[143, 144] The backfilled functionalized magnetic core gold nanoparticles were then separated using a magnet, resuspended in 100 µL PBS (pH 7.4), and stored in a refrigerator at 4˚C.

[2.4.6] Selective isolation and SERS monitoring of rHuEPO binding to functionalized nanoparticles

The backfilled functionalized nanoparticles were used to selectively capture rHuEPO from aqueous solution. An aqueous standard of rHuEPO ($1.1 x10^{-8}$ M in PBS buffer, pH 7.4)

was added to the functionalized nanoparticle colloid in the ratio of 1:10 v/v. The mixture was left to stand for 15 minutes to complete binding between the antibody and rHuEPO. The protein-bearing functionalized nanoparticles were then collected using a magnet and washed several times with PBS buffer (pH 7.4) to remove unbound protein. The protein-bearing functionalized nanoparticles were then screened using SERS and the acquired spectrum compared to that of the functionalized nanoparticles prior to their interaction with the rHuEPO.

For the isolation of rHuEPO from a biological matrix, rHuEPO spiked horse plasma was mixed with the backfilled functionalized nanoparticles and PBS buffer (pH 7.4) in the ratio of 1: 5: 50 respectively, to a total volume of 100 µL. The final concentration of rHuEPO in the mixture was 1 nM. The mixture was then left to stand for 15 minutes to the complete binding between the nanoparticles and rHuEPO. The nanoparticles were then magnetically removed from the matrix and rinsed several times with PBS buffer (pH 7.4) to remove any unbound proteins.

Blank horse plasma samples were donated by Biological Research Unit, Racing Analytical Services Ltd, Melbourne. The samples were collected under the Melbourne lab protocols and ethical clearances, arrangements and protocols are all maintained by this lab. The samples were also shipped under their lab protocols for shipping biological specimens. The samples were received at QUT and used as a matrix for Raman testing.

[2.4.7] Direct SERS detection and ELISA assay of extracted rHuEPO from horse plasma

For the direct SERS detection of rHuEPO from spiked horse plasma, the protein-bearing functionalized nanoparticles were reconstituted in 100 µL of N-acetyl glucosamine buffer to release the captured protein.[145] The released protein solution was then loaded onto a preconditioned gravity flow size exclusion column for 5 minutes to remove the buffer. The protein was eluted off the column using 500 µL of deionized water. 10 µL of the clean rHuEPO solution was then loaded onto gold-coated silicon nanopillars SERS substrate[146, 147] and directly screened by SERS for 1 minute using the Renishaw inVia Raman Microscope as well as a handheld Raman spectrometer (ID Raman, ocean optics, USA).

For cross validation of the SERS measurements, aliquots of the extracted rHuEPO were submitted to independent screening by Solid Phase Sandwich ELISA[148] at the research unit, Racing Analytical Services Ltd, Melbourne, Australia.

[2.5] Results

[2.5.1] Synthesis and characterization of magnetic core gold nanoparticles

The attraction towards magnetic core gold nanoparticle synthesis is due to their novel properties and potential applications in various fields such as cellular hyperthermia,[149] magnetic resonance imaging,[150] drug and gene delivery,[78] as well as biotechnology.[151] In these applications, the iron oxide core performs as a giant paramagnetic atom with a fast response to the applied magnetic field especially when the size of the core is between 5 and 20 nm.[152] Gold is chemically stable, biocompatible, and has excellent plasmonic properties for SERS.[153] Due to the surface chemistry of gold, the development of gold shells onto the iron oxide nanoparticles surface facilitates the functionalization of the nanoparticles with EPO-specific antibody[149] as well as enhances the stability of the magnetic core of the nanoparticles.[107, 140]

In this work, γ-Fe_2O_3 nanoparticles were synthesised for the deposition of a gold shell.[154, 155] The synthesized nanoparticles were spherical in shape with a mean size distribution of 10±2 nm as characterized by TEM (Figure 12a). The phase of the γ-Fe_2O_3 nanoparticles was confirmed by X-ray diffraction (Figure 13). Both the magnetite and maghemite phases have the same spinel structure as well as very similar lattice parameters. The peaks at diffraction angles (2θ) of 35.3°, 41.7°, 50.8,° 67.7°, and 74.9° degrees indicate that the pattern could be indexed to a cubic structure of either magnetite or maghemite. The peaks at 24.7° and 21.3° also suggest the presence of both magnetite and maghemite phases of the iron oxide. However, the high intensity of the peak at 41.7 indicates that the iron oxide nanoparticles exist predominantly in the maghemite phase.[152]

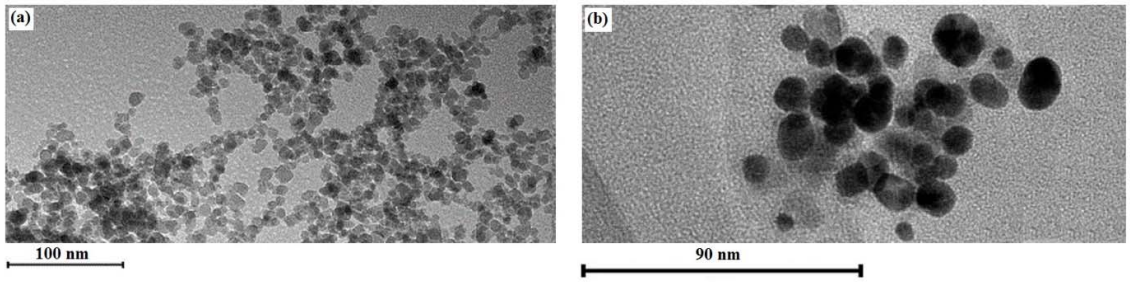

Figure 12 - TEM micrograph of (a) iron oxide nanoparticles and (b) iron core gold coated nanoparticles.

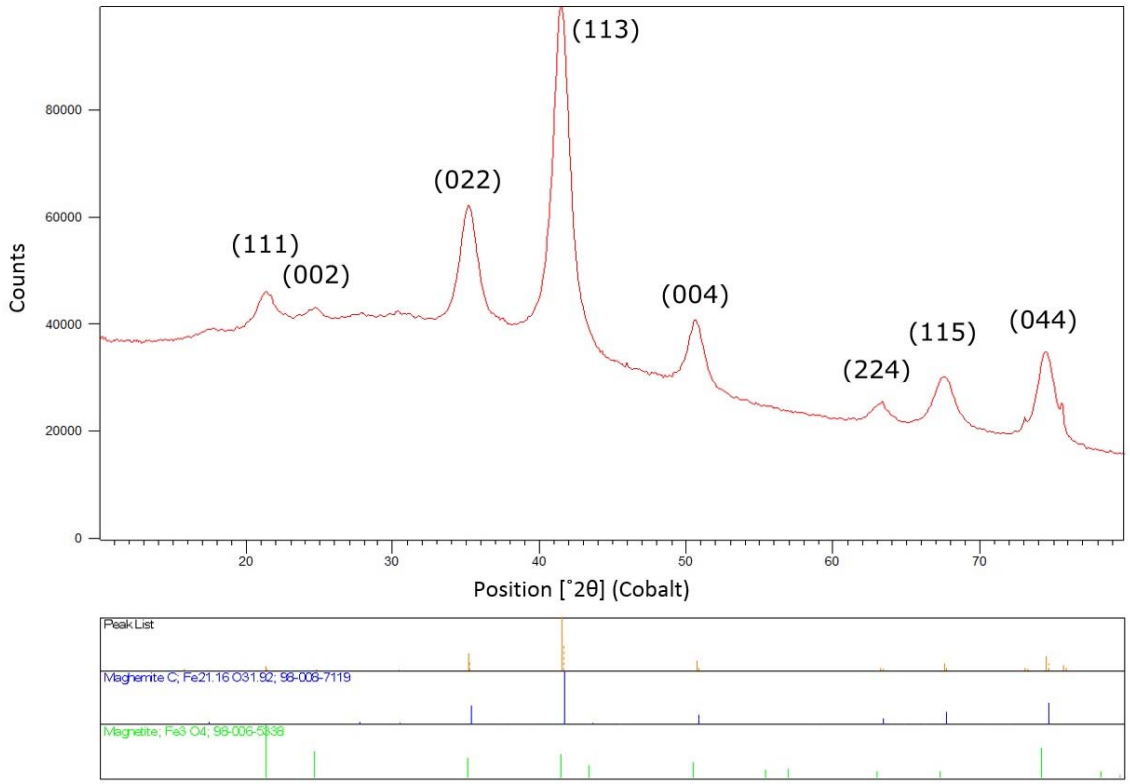

Figure 13 - XRD pattern of iron oxide nanoparticles.

To develop a gold shell onto the surface of the magnetic nanoparticles, iterative reduction of $HAuCl_4$ was carried out using sodium borohydride to initially nucleate gold onto the iron oxide nanoparticles surface. Subsequent sodium citrate reduction of Au^{3+} ions to Au expanded the nucleated gold into a shell around the magnetic core. The resulting magnetic core gold nanoparticles were spherical with an average size of 15±6 nm as indicated by TEM (Figure 12b). The plasmonic properties of the magnetic core gold nanoparticles were

confirmed by a characteristic plasmon band at 530 nm observed by UV–visible spectroscopy (Figure 14).

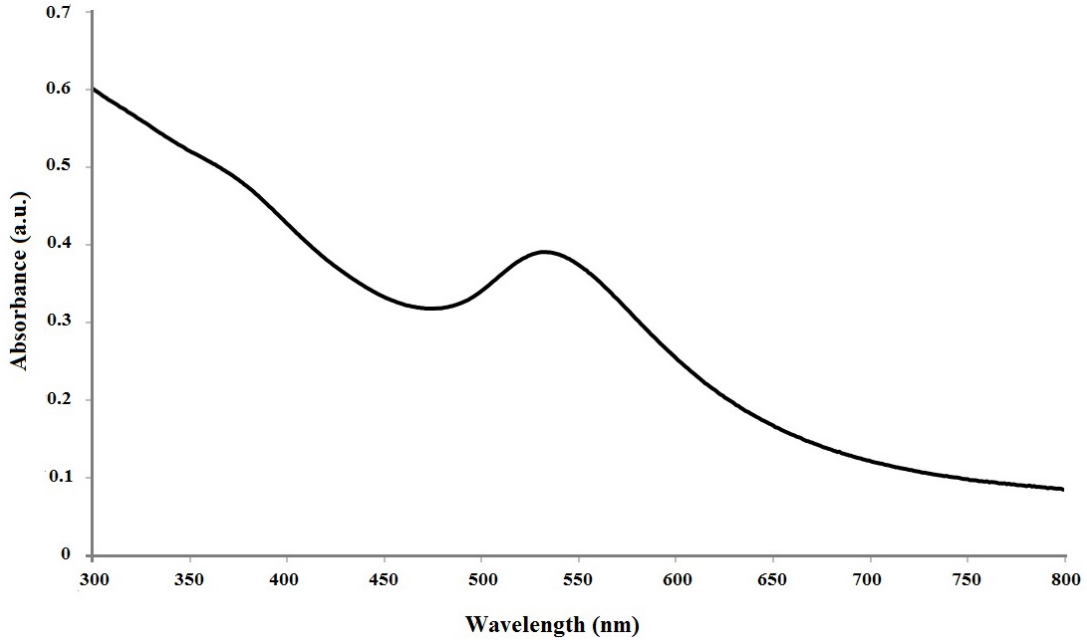

Figure 14 - UV-Vis spectrum of magnetic core gold nanoparticles.

[2.5.2] Selective isolation and SERS monitoring of rHuEPO binding to AuMNPs

The magnetic core gold nanoparticles were then functionalized with 7D3 anti-rHuEPO antibodies and used for the selective isolation of rHuEPO. Functionalizing a gold nanoparticle surface with antibodies has been previously described,[142] where cysteamine was used to link an active carboxylic acid terminus, of Aflatoxin B1 antibody (via an amide bond) to the gold surface. Unfortunately, cysteamine on a gold surface may adopt a gauche configuration in which the cysteamine molecule binds to the gold nanoparticles from both its thiol and amine ends.[156] In this conformation, the amine group of cysteamine would not be available to bind the antibody.[66] To maximize the number of antibody molecules bound to the surface of gold nanoparticles and enhance the capacity of the nanoparticles to bind the target protein, the amide bond between cysteamine and the active 7D3 antibody carboxylate groups was formed in solution. Next, the cysteamine-bound antibody was attached to the gold surface of the magnetic core nanoparticles via an Au-S bond. The unfunctionalized areas of the nanoparticles' surface were backfilled with 1-butanethiol to

prevent non-specific binding of interfering analytes and ensure the selectivity of the nanoparticles towards rHuEPO.

[2.6] Discussion

[2.6.1] Surface-enhanced Raman spectra

Once functionalized and blocked, the magnetic core gold nanoparticles were then used to isolate rHuEPO from an aqueous solution. The binding of rHuEPO to the functionalized nanoparticles was directly monitored by comparing the SERS spectra of the nanoparticles before and after interaction with the protein. The SERS spectrum of the functionalized nanoparticles before interaction with the protein is depicted in Figure 15a. The Raman bands at 565 cm^{-1}, 752 cm^{-1} and 1549 cm^{-1} are characteristic of the antibody tryptophan residues.[154, 155, 157-159] The 960 cm^{-1} band represents a C-C stretching vibrational mode[154, 158] and the 1062 cm^{-1} band may be attributed to a C–N stretching vibrational mode.[154, 157, 160] The characteristic band at 1203cm^{-1} arose from the phenylalanine and tyrosine residues in the antibody.[154, 157, 160] The 1425 cm^{-1} band may be attributed to the tyrosine residues and the CH vibrations of tryptophan indole rings within the antibody skeleton.[154, 158] Finally the band at 1584 cm^{-1} may be attributed to Tryptophan, Tyrosine, Phenylalanine residues[157, 159, 161] while the band at 1611 cm^{-1} is due to Phenylalanine and amide I (α helix) vibration modes.[154, 155, 162]

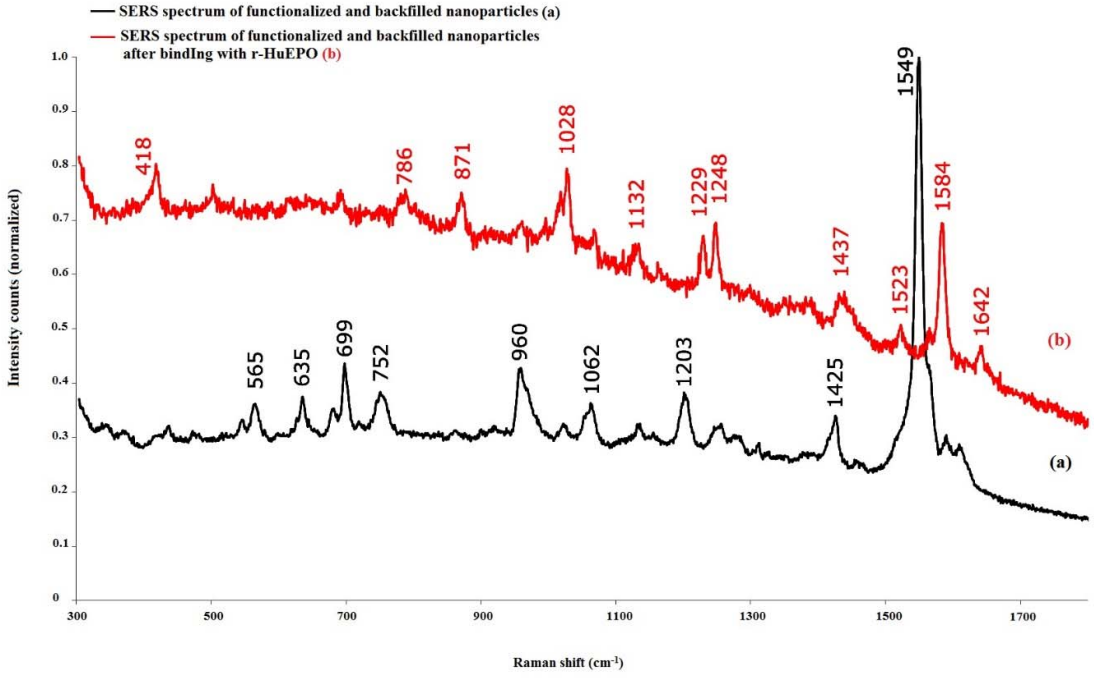

Figure 15 - SERS spectrum of antibody-functionalized gold nanoparticles a) before and b) after binding with rHuEPO.

The SERS spectrum of the functionalized nanoparticles after interaction with rHuEPO (Figure 15b) showed significant changes in spectral features that may be attributed to the binding event between the 7D3 antibody and the target protein.[161] The characteristic tryptophan Raman bands now appear at 786 cm^{-1}, 871 cm^{-1} and 1584 cm^{-1}.[154] The band at 1437 cm^{-1} may be attributed to CH_2 scissoring vibration mode.[154, 158, 159, 162] The band at 1028 cm^{-1} may be attributed to the in-plane ring CH deformation of the phenylalanine residues of the protein.[154] The low intensity of this band suggests that the phenyl ring approaches the gold surface of the nanoparticles but is not directly adsorbed onto the surface. Thus, the phenyl ring–nanoparticles interaction is weak.[154] The absence of the phenyl ring breathing vibration at 1002 cm^{-1} also suggests that the protein is not directly adsorbed onto the gold nanoparticles and the rHuEPO phenylalanine residues reside at a distance from the substrate's gold surface.[154]

The asymmetric vibrations (Cα CN and NH_3^+ deformation) of the CNH_2 groups within the protein structure are expressed by the band at 1132 cm^{-1}.[154, 157, 159, 160] The amide III vibrations of the complex formed between the antibody and rHuEPO are indicated by two Raman bands at 1225 cm^{-1} and 1248 cm^{-1}.[154, 155, 159, 162] The weak band at 1523 cm^{-1} can be attributed to the amide II vibration of antibody-rHuEPO complex.[154, 157] Despite the fact that the amide II band of proteins is Raman inactive, it may become enhanced when the protein structure is immobilized in a close proximity to the surface of a noble metal.[154] Finally, the amide I vibration of the antibody-EPO complex now appears at 1642 cm^{-1}.[154, 155, 157-159, 162] The spectral differences between the free functionalized nanoparticles and the rHuEPO-bound nanoparticles were used to monitor the binding event between the protein and the functionalized nanoparticles and, in effect, the selective isolation of the target protein from the sample matrix. This process is simple and does not require complex pretreatment and preconcentration procedures as in the case of other techniques, such as HPLC-MS.

[2.6.2] Direct SERS detection of rHuEPO

To confirm the selective isolation of rHuEPO and to demonstrate the direct detection of the extracted protein by SERS, we used the functionalized nanoparticles to extract the protein from spiked horse plasma. The captured protein was then released from the nanoparticles' surface using a releasing buffer.[163] The purified protein extract was then

directly screened by SERS. The SERS spectra of the extracted protein and rHuEPO standard are depicted in Figure 16 and show significant correlation. The SERS spectrum of the extracted rHuEPO (Figure 16b) shows the characteristic Raman bands of a protein (Table 2).

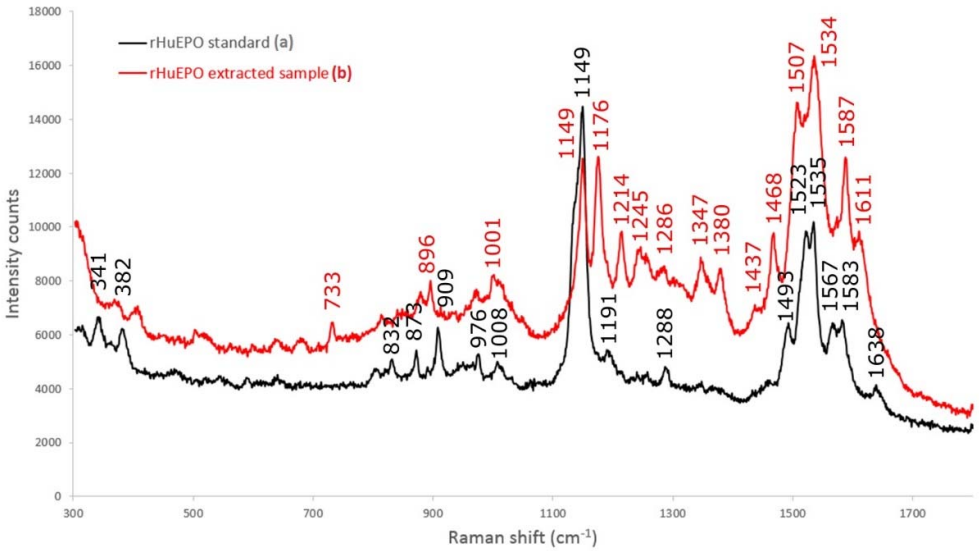

Figure 16 - SERS spectrum of (a) rHuEPO standard and (b) rHuEPO extracted from horse plasma. Measurements were carried out on gold-coated silicon nanopillars SERS substrate and using the inVia Renishaw Raman spectrometer.

Table 2 - Assignments of Raman bands in the SERS Spectra (Figure 16b) of rHuEPO extracted from spiked horse plasma.

RAMAN SHIFT (CM^{-1})	BAND ASSIGNMENT	REFERENCE
1001	Benzene ring breathing of phenylalanine	[155]
1149	ring stretch/$\nu_{as}(C_{\alpha}CN)$	[157, 162]
1176	Phenylalanine, Tyrosine	[154, 159, 160]
1214	Phenylalanine	[154, 161]
1245	Amide III	[154, 162]
1286	Amide III	[154]
1347	Tryptophan	[154]
1380	$\nu_{as}(COO^{-})$	[154, 157]
1468	CH_2 (scissoring)	[155, 157, 162]
1507	Phenylalanine, Histidine, Tryptophan	[154, 159]
1534	Amide II	[157]
1587	Tryptophan, Tyrosine, Phenylalanine	[157, 160, 161]
1611	Amide I (α helix), Phenylalanine	[154, 155, 162]

For cross-validation purposes, an aliquot of the post-extraction product was also screened by independent analytical services laboratory using ELISA. The ELISA screening

confirmed that rHuEPO was present in this protein extract at concentration of 72 mIU/mL (553.7 pg/mL).

[2.6.3] Direct SERS detection of rHuEPO by handheld Raman spectrometer

In order to demonstrate our methodology for the in-field screening of rHuEPO in biological matrices, we loaded the protein extract (from horse plasma) onto a commercial SERS substrate and used a handheld Raman spectrometer for the direct SERS detection of rHuEPO. The SERS spectra of the extracted protein and rHuEPO standard are depicted in Figure 17. The match between the two spectra is obvious. The measurements were carried out in the Raster Orbital Scanning (ROS) mode and took only one minute per sample to acquire the SERS spectrum. This sample scanning mode allows for scanning of a large area of the sample with a tightly focused laser beam. The ability to screen a large area of the sample increases the number of Raman-active molecules being probed by the excitation laser beam and, therefore, provides higher sensitivity data. The quality and the notable match in the SERS spectra (Figure 17) may be attributed to the ability of the ROS screening mode to acquire an average SERS spectrum from the entire sample load on the SERS substrate.[150, 164]

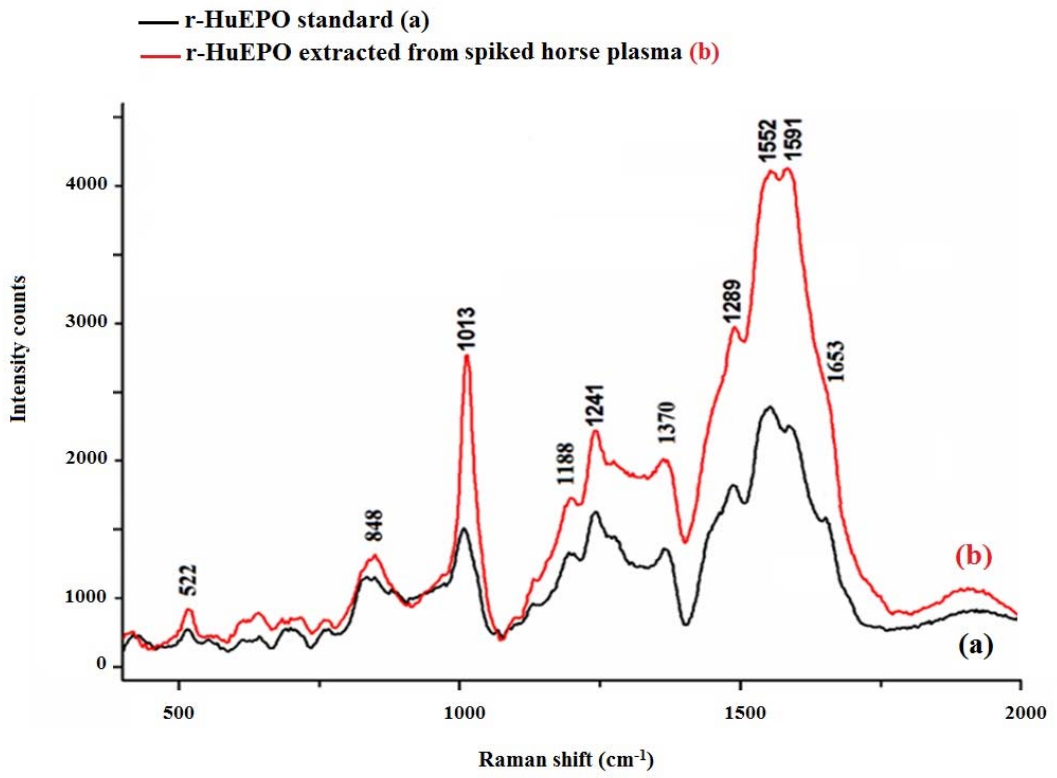

Figure 17 - SERS spectrum of a) rHuEPO standard and b) rHuEPO extracted from horse plasma. Measurements were carried out on using handheld Raman spectrometer (1 minute measurement time per sample). Spectra were collected using 785 nm excitation wavelength and a single 40 second accumulation in Raster Orbital Scanning (ROS) mode.

In order to demonstrate the capacity of our protein analysis method, towards SERS quantification of rHuEPO, various concentrations of in the range of 50nM – 5 pM aqueous rHuEPO were employed. To each concentration of rHuEPO, a fresh substrate was used for the SERS quantification by the handheld Raman spectrometer. The laser power at the sample was 50 mW and a 5 second accumulation was carried out for each concentration. The band at 1551 cm^{-1} was used a as a reference band for rHuEPO quantification. The SERS signals were found to decrease with decreasing concentration as indicated by Figure 18a. A linear relationship was obtained between the SERS signal intensity at 1551 cm^{-1} and the corresponding rHuEPO log concentration plot is depicted in Figure 18b. As indicated by Figure 7b, close correlation (r^2 = 0.995) was found over the concentration range of 50 nM to 5 pM rHuEPO. The minimum limit of detection was estimated mathematically using the regression equation in Figure 18b and found to be 1 pM.

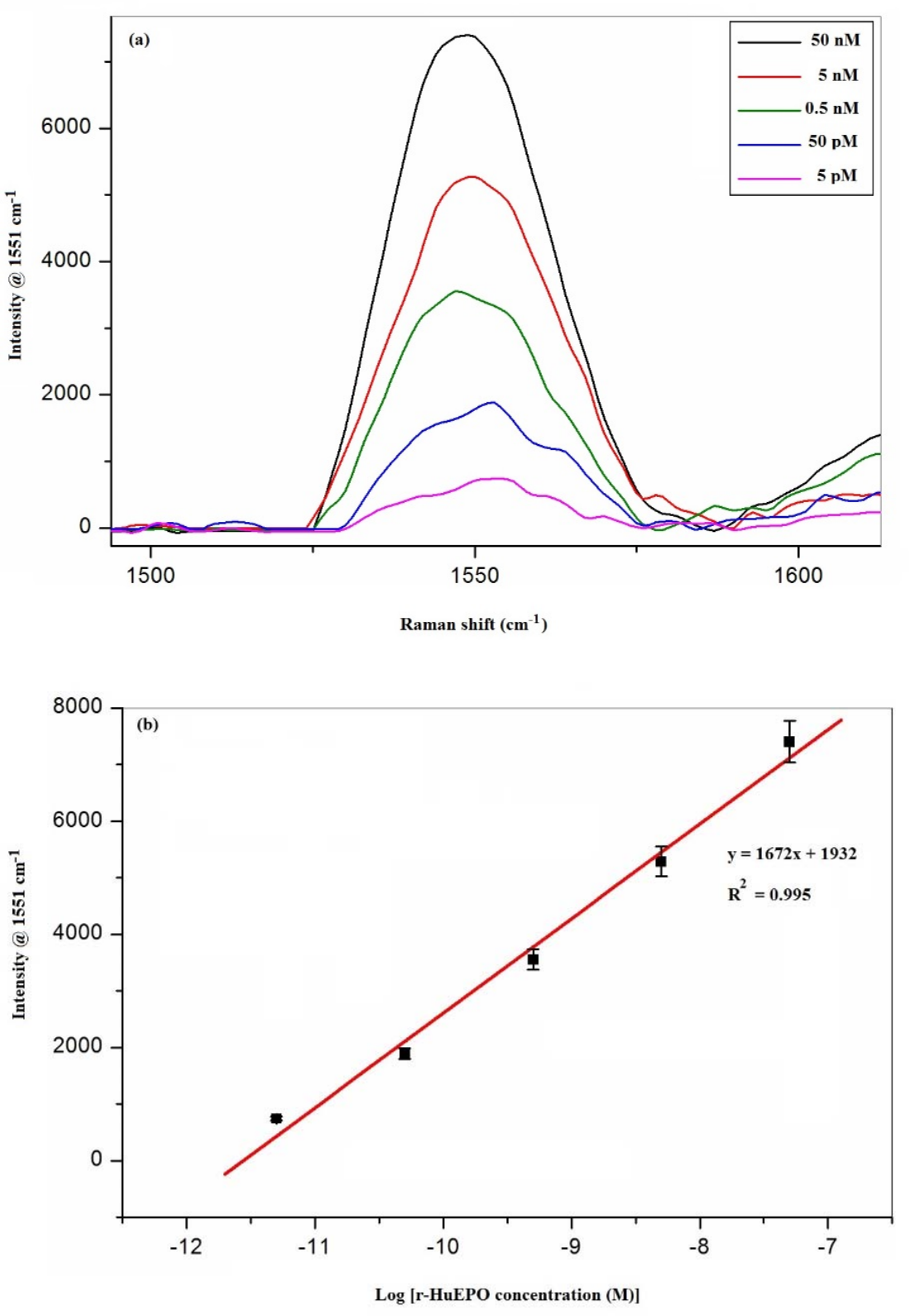

Figure 18 – (a) SERS spectra, at 1551 cm^{-1}, of rHuEPO in the concentration range 50 nM to 5 pM and (b) Plot demonstrating the linear relationship between log concentration of rHuEPO and SERS intensity at 1551 cm^{-1}.

[2.7] Conclusion

In conclusion, we demonstrated the selective isolation and direct SERS detection of rHuEPO using antibody-functionalized nanoparticles and SERS. The changes in the SERS spectrum of the antibody-functionalized nanoparticles after their binding to a protein allow for monitoring the binding event by SERS. The direct SERS detection of extracted rHuEPO from a biological matrix is demonstrated for the first time. The SERS detection of the protein was supported by ELISA, which confirmed and quantified the rHuEPO in the protein extract. The iron core of the gold-coated nanoparticle plays a key role in the magnetically induced separation of rHuEPO from the matrix. However it does not play any operational role in the detection process of rHuEPO. The burden of detection rests entirely on the plasmonic response of the Au shell and thus the detection mechanism is independent of whether the core is magnetic or not. Finally, the methodology was successfully utilized for the rapid in-field screening of rHuEPO within a biological matrix using a commercial SERS substrate and handheld Raman device. This study demonstrates a proof of concept for the combined selective isolation and in-field direct SERS detection of proteins in complex matrices. Our future work is directed towards reproducible direct SERS quantification of ultra-trace amounts of proteins in biological matrices using the demonstrated methodology and handheld spectrometer.

Chapter 3

Preface

In the previous chapter (Chapter 2), iron/gold core/shell hybrid nanoparticles functionalised with anti-EPO antibodies were demonstrated to be capable of rapid and selective capture and direct spectroscopic identification rHuEPO from a blood matrix. Furthermore, the SERS spectrum could be used to quantify rHuEPO at nanomolar to picomolar concentrations.

Areas of the previous work were investigated for potential improvement. Firstly, the nature of nanoparticle-based SERS screening, where high enhancement regions known as "hot spots" are dependent on the distribution of the nanoparticles could be better controlled for improved screening signal homogeneity. Secondly, the use of aptamers as alternatives to antibodies for selective capturing was investigated to try to reduce production costs and improve shelf-life.

This chapter details the development of aptamer-functionalised nanostructured surfaces for the selective extraction of EPO, followed by SERS identification and quantitation. The issue of nanoparticle distribution was addressed by electrochemically reducing gold to form spherical gold nanoparticles (AuNS) over a polished gold substrate (pAu). This method was selected to deposit densely packed nanospheres across the surface in a highly controlled fashion. The pAu/AuNS surface could then be functionalised with aptamers to selectively capture a target species, rHuEPO, prior to SERS analysis. This method analyses species captured on the surface rather than the pure (captured and released) analyte. The explored methodology is similar to that of the previous chapter (Chapter 2 Preface), with appropriate modifications shown below.

(i) **pAu/AuNS synthesis**: electrochemical deposition of gold nanospheres allows for controlled distribution, as well as enabling SERS capabilities and ease of surface functionalisation using thiol chemistry.

(ii) **Reproducibility of SERS spectra**: analyse AuNS distribution and packing density across pAu to assess SERS enhancement and signal homogeneity.

(iii) **Selective extraction**: by functionalising the gold surface with target-specific aptamer and backfilling with a small thiol molecule, target biomolecules can be selectively and rapidly captured onto the surface from a complex matrix.

(iv) **Screening and quantitation**: monitoring of aptamer-antigen binding using SERS to detect presence of target biomolecule. Quantify target biomolecule using label-free SERS.

(v) **Portability**: analyse the captured biomolecule with a handheld Raman spectrometer to test the system for in-field use.

Statement of Contribution of Co-Authors for Thesis by Published Paper

The following is the suggested format for the required declaration provided at the start of any thesis chapter which includes a co-authored publication.

The authors listed below have certified* that:

1. they meet the criteria for authorship in that they have participated in the conception, execution, or interpretation, of at least that part of the publication in their field of expertise;
2. they take public responsibility for their part of the publication, except for the responsible author who accepts overall responsibility for the publication;
3. there are no other authors of the publication according to these criteria;
4. potential conflicts of interest have been disclosed to (a) granting bodies, (b) the editor or publisher of journals or other publications, and (c) the head of the responsible academic unit, and
5. they agree to the use of the publication in the student's thesis and its publication on the Australasian Research Online database consistent with any limitations set by publisher requirements.

In the case of this chapter: A. Sivanesan, E. Izake, R. Agoston, G. Ayoko and M. Sillence. Reproducible and label-free biosensor for the selective extraction and rapid detection of proteins in biological fluids. *Journal of Nanobiotechnology* **2015**, 13, 43.

Publication title and date of publication or status:

Contributor	Statement of Contribution*
Sivanesan Arumugam QUT Verified Signature Date: 15/03/2016	Conducted experiments, data analysis, and primary manuscript authorship and editing.
Roland Agoston QUT Verified Signature Date: 15/03/2016	Contributed to experimental design and major editing.
Emad L. Izake	Supervision and major editing.
Godwin A. Ayoko	Contributed research discussions and editing.
Martin Sillence	Contributed research discussions and editing.

Principal Supervisor Confirmation

I have sighted email or other correspondence from all Co-authors confirming their certifying authorship.

Emad Kiriakous	QUT Verified Signature	15/03/2016
Name	Signature	Date

Reproducible and label-free biosensor for the selective extraction and rapid detection of proteins in biological fluids

Arumugam Sivanesan[a]*, Emad L. Izake[a]*, Roland Agoston[a], Godwin A. Ayoko[a], Martin Sillence[b]

[a] Nanotechnology and Molecular Sciences Discipline, Faculty of Science and Engineering, Queensland University of Technology, 2 George St., Brisbane, QLD 4001, Australia

[b] Discipline of Biosciences, Faculty of Science and Engineering, Queensland University of Technology, 2 George St., Brisbane 4001, QLD, Australia

E-mail address: sivanesan.arumugam@qut.edu.au; asnesan@gmail.com (A. Sivanesan) e.kiriakous@qut.edu.au (E. L. Izake)

[3.1] Abstract

Erythropoietin (EPO), a glycoprotein hormone of ~34 kDa, is an important hematopoietic growth factor, mainly produced in the kidney and controls the number of red blood cells circulating in the blood stream. Sensitive and rapid recombinant human EPO (rHuEPO) detection tools that improve on the current laborious EPO detection techniques are in high demand for both clinical and sports industry. A sensitive aptamer-functionalized biosensor (aptasensor) has been developed by controlled growth of gold nanostructures (AuNS) over a gold substrate (pAu/AuNS). The aptasensor selectively binds to recombinant human erythropoietin (rHuEPO) and, therefore, was used to extract and detect the drug from horse plasma by surface enhanced Raman spectroscopy (SERS). Due to the nanogap separation between the nanostructures, the high population and distribution of hot spots on the pAu/AuNS substrate surface, strong signal enhancement was acquired. By using wide area illumination (WAI) setting for the Raman detection, a low RSD of 4.92% over 150 SERS measurements was achieved. The significant reproducibility of the new biosensor addresses the serious problem of SERS signal inconsistency that hampers the use of the technique in the field. The wide area illumination setting is compatible with handheld Raman devices. Therefore, the new aptasensor can be used for the selective extraction of rHuEPO from biological fluids and subsequently screened with handheld Raman spectrometer for SERS based in-field protein detection.

[3.2] Keywords

Aptamer-functionalized biosensor (aptasensor), nanosensor, homogenous SERS, wide area illumination, erythropoietin (EPO), horse plasma

[3.3] Background

Erythropoietin (EPO), a glycoprotein hormone of ~34 kDa, is an important hematopoietic growth factor, mainly produced in the kidney and controls the number of red blood cells circulating in the blood stream.[165] After the establishment of human EPO gene sequence,[166] recombinant human EPO (rHuEPO), a structural and bio-active analogue of human EPO, has been produced as a pharmaceutical to treat patients suffering from anaemia symptoms associated with various disorders such as cancer.[167] rHuEPO has also been used by athletes as a doping agent in endurance sports to enhance their performance.[168] This prompted World Anti-Doping Agency (WADA) to ban the use of the drug in sports activities.[165] In addition to its chief function in promoting erythropoiesis, it was recently indicated that EPO levels in cancer patients, especially when receiving chemotherapy, may significantly affect the growth and progression of malignant tumours.[169, 170] Thus, sensitive and rapid rHuEPO detection tools are in high demand for both clinical and sports industry.[112]

In recent years, SERS has emerged as an ultra-sensitive analytical tool.[66, 171, 172] The two important features for real world applications of SERS are the homogeneity of the SERS substrate and selectivity towards target.[173] Vast numbers of SERS active surfaces comprising various roughened metallic surfaces and noble metal nanostructures have been produced. However, the majority of surfaces failed to produce a homogeneous SERS signal. Conversely, very few substrates which are promising to deliver homogeneous and reproducible signal are expensive.[174] Therefore, there is a high demand for cheap, homogeneous and reproducible SERS substrates. In principle, the basic requirement for a homogeneous and sensitive SERS substrate is defect-free arrangement of metal nanoparticles or nanostructures within nanometer scale inter-particle distance.[175]

Electrodeposition of metal nanostructures is one of the simple, cost effective and efficient approaches that realize the defect-free packing of nanostructures over a wide area.[176] To enhance the selectivity within SERS, recognition molecules that specifically bind to targets can be immobilized on the SERS substrate. However, the size and length of the recognition molecule should not be very large otherwise the SERS effect may completely diminish due to the long distance between the captured protein and the plasmonic surface. In other words, the binding receptor should not be far away from the surface as SERS signal

exponentially decreases with respect to the increase in distance between the surface and analyte.

Antibodies are frequently used as recognition molecules for detecting proteins. However, antibodies usually have large size that constitutes a serious hurdle to the label-free SERS detection of proteins.[112] Aptamers are now widely emerging as better choice over antibodies.[177] Aptamers are of much smaller size than antibodies and also well-known for their high selectivity, binding affinity, easy and quick production, stability and cost-effectiveness.[178] Moreover, aptamers can bend and orient themselves close to the surface of the SERS substrate after binding with the target protein.[179] This orientation would lead to high intensity SERS signal due to short distance between the captured target and SERS surface. Thus, this article presents a homogeneous and sensitive aptamer-functionalized nanosensor for the rapid reproducible and label-free SERS detection of rHuEPO in biological fluids.

[3.4] Experimental details

[3.4.1] Chemicals and materials

Hydrogen tetrachloroaurate ($HAuCl_4.4H_2O$) and 6-mercaptohexanol were purchased from Sigma Aldrich (USA). The recombinant human erythropoietin (rHuEPO) specific aptamer sequence (5′-HO-S-S-(CH2)6-TTGAAAGGTCTGTTTTTGGGGTTGGTTTGGGTCAA-3')[180, 181] was synthesized by FRIZ Biochem (Neuried, Germany). Tris(2-carboxyethyl)phosphine (TCEP) was purchased from Pierce. All other chemicals were of Analytical grade. All dilutions were made using deionised water (18.2 MΩ.cm) from a Millipore water purification system. Commercial SERS substrates (Au/Si SERStrate) were purchased from Silmeco, Denmark. Polycrystalline gold discs (Au) having a geometric area of 0.502 cm^2 and platinum wire (A & E Metals, Australia) were respectively, used as working and counter electrode. Dry leakless electrode (DRIREF-2, World Precision Instruments, USA) was used as a reference electrode. Polishing slurries and pads (Microcloth®) were purchased from Buehler, Germany.

[3.4.2] Instrumentation

All electrochemical experiments were carried out in Autolab PGSTAT204 potentiostat with a custom-made three-electrode cell setup. All Raman measurements were performed using the Renishaw InVia Raman microscope equipped with 785 nm laser line as excitation source. Spectra were collected using a 50× and 5× objective lens over a wavelength range from 500 cm^{-1} to 2000 cm^{-1} using a laser power of 1 mW for 10s (3 accumulations). For each Aptamer and rHuEPO spectrum, 10 spectra were randomly recorded over the entire surface and averaged. SEM measurements were performed using Zeiss Sigma VP Field Emission Scanning Electron Microscope with an accelerating voltage of 5 kV under high vacuum.

[3.4.3] SERS substrate preparation

Au disc electrodes were manually mirror-polished with alumina slurries of sequentially decreasing particle sizes (0.5 µm, 0.05 µm and 0.02 µm). After each step of polishing, the electrodes were immersed in Millipore water and subsequently sonicated in an aqueous ultrasonic bath for 15 minutes in order to remove the physically adsorbed alumina particles from the electrode surface. Prior to the deposition of gold nanostructures, the Au discs were cleaned by immersing into piranha solution for 10 min (3:1, 98% H_2SO_4 /

30% H_2O_2) and subsequent thorough washing with copious amount of Millipore water. Warning: piranha solution is very corrosive and must be handled with extreme caution; it reacts violently with organic materials and should not be stored in tightly closed vessels.

Nanostructured SERS substrate was prepared by potentiostatic deposition of AuNS over flat Au surface (pAu/AuNS). The three-electrode electrochemical cell was filled with the solution of 4 mM $HAuCl_4$ in 0.1 M HClO4 and subsequently purged with high pure argon gas for 30 min to remove oxygen from solution. A potential of -80 mV was applied for 400 s and then the electrode was removed from the solution and subsequently washed with Millipore water to remove other ions from the surface. The electrode was then dried under a stream of nitrogen gas and used as a SERS substrate.

[3.4.4] Fabrication of aptasensor and rHuEPO capture

The aptamers were received in lyophilized form and dissolved in selection buffer (20 mM Tris-HCl, 140 mM NaCl, 5 mM $MgCl_2$ and 5 mM KCl at pH 7.5) to have a stock concentration of 100 µM. Prior to fabricate the aptamer over pAu/AuNS surface, 100 µL of 0.2 µM aptamer was pre-treated with 100 fold excess of tris(2-carboxyethyl)phosphine (TCEP) for 1 h at room temperature to reduce the disulfide bond of the aptamer. The pAu/AuNS substrate was then incubated in Aptamer-TCEP mixture for overnight at room temperature. Followed by the substrate was washed with selection buffer and copious amount of Millipore water to remove the unbounded aptamer from the surface. The surface was then dried in a gentle stream of argon and immediately transferred into 2 mM 6-mercaptohexanol (6-MH) in selection buffer and allowed to stand for 3 h. Subsequently, the substrate was washed with selection buffer and Millipore water to remove all the unbounded 6-MH from the pAu/AuNS surface. Now the aptasensor (pAu/AuNS/Apt) is ready to capture rHuEPO. The sensor is then incubated into 1 nM rHuEPO in Tris buffer (pH 7.5) for 1 h and subsequently washed in Millipore water to remove the free rHuEPO from the sensor surface. The aptasensor binding to rHuEPO ((pAu/AuNS/Apt/rHuEPO) was then dried in gentle flow of argon prior to SERS measurements.

[3.4.5] Horse Serum Experiment

Blank horse plasma samples were donated by Dr. Rohan Steel, Project Leader, Biological Research Unit, Racing Analytical Services Ltd, Melbourne. The samples were

collected under the Melbourne lab protocols and ethical clearances, arrangements and protocols are all maintained by this lab. The samples were also shipped under their lab protocols for shipping biological specimens. The samples were received at QUT and used as matrix for Raman testing. This did not require PC2 lab at QUT.

rHuEPO was spiked into the horse serum to obtain a final concentration of 1 nM rHuEPO. The aptasensor was then incubated in the rHuEPO spiked horse serum for 1 h and subsequently washed to copious amount of water to remove the biological matrix and unbounded rHuEPO from the sensor surface. Finally, the substrate was dried in gently flow of argon and used for SERS measurements.

[3.5] Results and discussion

[3.5.1] Characterization of SERS substrate

We optimized gold chloride concentration, electrolyte, applied potential and time to have a closely packed single layer of AuNS within nanometer scale inter-particle distance. Figure 19 shows the SEM pictures of pAu/AuNS surface. The SEM image under wider magnification (Figure 19A) illustrates that the deposition of AuNS is virtually uniform over the entire surface.

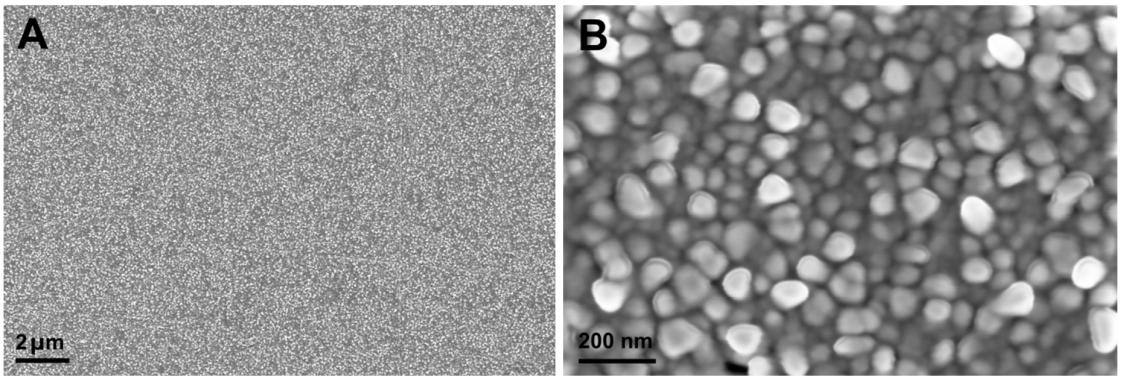

Figure 19 - SEM images of pAu/AuNS surface under different magnifications.

Even at a 100 micron field of view, the particle coverage was uniform and defect free (Figure 20). Similar SEM images were obtained over the entire 8 mm diameter pAu/AuNS disc surface which clearly reveals that the electrodeposition method produced homogeneous AuNS over the entire surface. Although the sizes of AuNS ranged between 10-100 nm (Figure 19B), the uniform close packing of AuNS in single layer lead to homogeneous SERS signal for a focused micron-scale laser spot[173] (vide infra). Polished Au was chosen as the underlying support since it produces more AuNS particle initiation spots during electrodeposition in contrast to glassy carbon or indium tin oxide surfaces.[176] As a result, high density of small-sized and closely packed AuNS was produced and led to enormous SERS enhancement. Furthermore, a possible coupling between the propagating surface plasmon polariton (SPP) of the underlying polished Au surface and surface plasmon resonance (SPR) of the AuNS[176, 182] may lead to additional SERS enhancement.

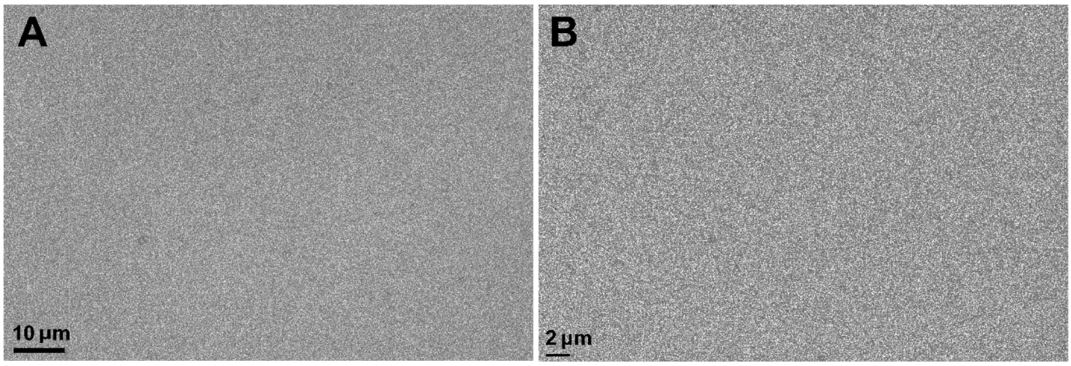

Figure 20 - SEM images of pAu/AuNS surface under wider magnification.

[3.5.2] Reproducibility of SERS spectra

In order to test the homogeneity of the substrate and the reproducibility of the SERS signal from various locations on the sensor, we used 2-quinolinethiol (2-QT) as a probe molecule due to its large Raman scattering cross-section. Figure 21 depicts the SERS spectrum of the self-assembled monolayer of 2-QT over pAu/AuNS substrate.

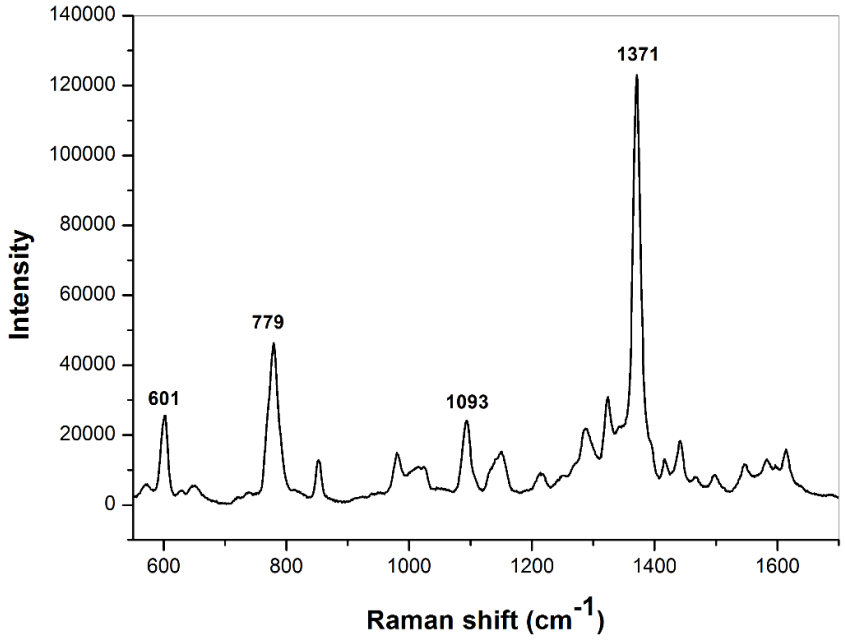

Figure 21 - SERS spectrum 2-QT monolayer on pAu/AuNS surface.

The intense band @ 1371 cm^{-1}, corresponding to the aromatic ring stretching, was used to calculate the relative standard deviation (RSD) of the SERS signal intensity from various surface locations. For comparison purposes, we carried out the SERS measurements using used 5× (spot diameter = 3.99 µm; illuminated area = 12.56 μ^2 and working distance = 14 mm) and 50x (spot diameter = 0.64 µm; illuminated area = 0.32 μ^2 and working distance = 0.37 mm) objectives respectively. When the laser beam is focused using the 50× objective, the RSD of the SERS signal @ 1371 cm^{-1} (150 measurements from various surface spots, Figure 22A) was found to be 8.74%. However, the RSD reduces to 4.92% when using the 5× objective (Figure 22B). This decrease in RSD with increase in laser focusing area (5× objective has 39.25 times higher illumination area than 50× objective) is rational as the acquired SERS signal is highly averaged when increasing the focusing area.

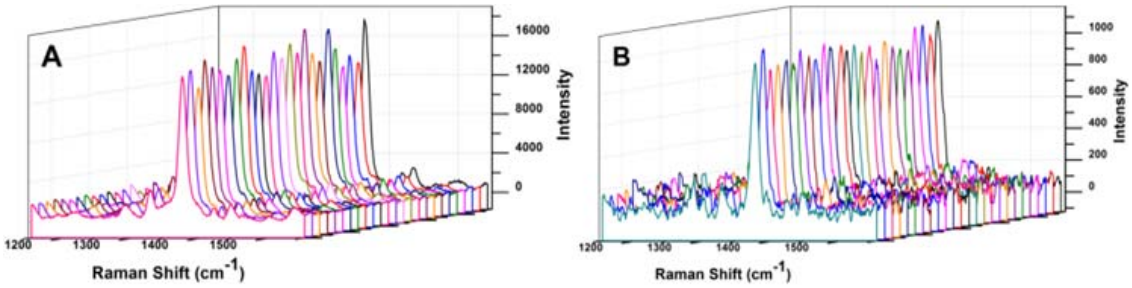

Figure 22 - A series of SERS spectra of 2-QT randomly collected over the entire 8 mm diameter pAu/AuNS disc using (A) 50x objective with a laser focusing area of 0.32 μ^2 and (B) 5x objective with a laser focusing area of 12.56 μ^2.

Using a 5× objective to focus the laser beam onto the pAu/AuNS substrate creates a wide area illumination (WAI) setting which allows for an increased area of the pAu/AuNS surface to be probed when compared to the area probed by the 50x objective. The increase in the area probed by the laser excitation beam contributes to the reproducibility of the SERS signal.[183, 184] This is confirmed by the low RSD of 4.92% obtained when using the 5x objective. In other words, the wide area illumination setting allows for averaging the SERS signal from a large surface area of the aptasensor and hence the low RSD of the SERS measurements. Also the homogeneity of the particle coverage and packing leads to homogeneous distribution of the hot spots to give reproducible SERS signals despite the polydispersity (10-100 nm) of AuNS.

[3.5.3] Selective extraction and SERS investigation of rHuEPO in aqueous medium

The developed pAu/AuNS substrate was then functionalized with EPO-specific aptamer and the remaining bare sites on the surface backfilled with 6-mercapto hexanol (see supplementary materials) to create the aptasensor. The aptamers-functionalized nanosensor was then used for the selective capturing of rHuEPO from aqueous medium followed by the direct SERS detection of the captured protein. To acquire the native Raman fingerprint of rHu-EPO, we dropped 10 nM rHuEPO over a pristine pAu/AuNS surface and allowed it to dry in inert atmosphere. The subsequent SERS spectrum rHuEPO over non-functionalized surface is depicted in Figure 23A(I). It is well known that the amide and aromatic (phenylalanine, tyrosine, tryptophan and histidine) vibrational bands dominate the Raman spectrum of proteins and polypeptides.[154, 185-190] Similarly, the SERS spectrum of pAu/AuNS/rHuEPO (Figure 23A(I)) showed intense bands at 1636 cm^{-1} and 1228 cm^{-1} corresponding to amide I and amide III vibrational modes, respectively.[154, 185-190] The amide I @ 1636 cm^{-1} band represents a unique fingerprint of proteins, as it does not overlap with other vibrational modes from other functional groups. Therefore it can be used as a marker band for the identification of proteins without any external Raman labelling.[189, 191]

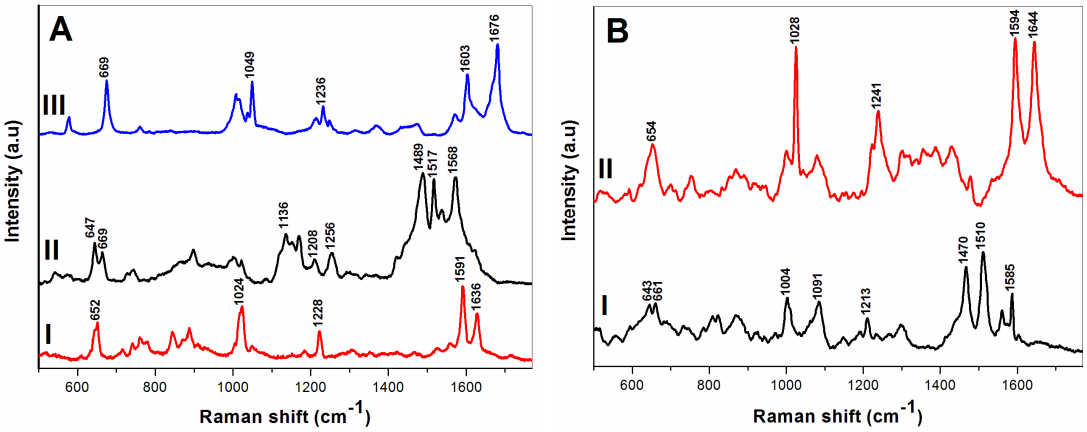

Figure 23 - SERS spectra of A) (I) pAu/AuNS/rHuEPO (drop dry), (II) pAu/AuNS/Apt (self-assembled monolayer), and (III) pAu/AuNS/Apt/rHuEPO (selectively captured). B) SERS spectra of pAu/AuNS/Apt incubated in (I) blank horse plasma and (II) rHuEPO spiked horse plasma. Each spectrum is the average of 10 spectra.

The bands @ 1591 cm^{-1} and 1024 cm^{-1} correspond to the aromatic amino acid vibrational modes. Figure 23A(II) depicts the SERS spectrum of EPO aptamer on nanostructured surface.

The SERS spectrum of an aptamer is usually dominated by adenine and guanine as the order of SERS cross-section is adenine>guanine>cytosine>thymine.[192, 193] Figure 23A(II) clearly indicated that the SERS spectrum of aptasensor is heavily dominated by the guanine vibrational modes @ 647 cm^{-1}, 1489 cm^{-1} and 1568 cm^{-1}. This is because the EPO aptamer has higher contribution from guanine nucleobase than adenine (13:5). Also, the C-S stretching mode for the thiolated aptamer is depicted @ 669 cm^{-1}. Figure 23A(III) shows the SERS spectrum of the apatsensor after capturing the rHuEPO protein (pAu/AuNS/Apt/rHuEPO) on its surface by the EPO aptamers. Scheme 2 depicts the graphical representation of rHuEPO captured aptasensor and subsequent SERS investigation. SERS The strong band @ 1676 cm^{-1} is attributed to the amide I vibrational mode.[154, 185-190] The amide I band @ 1676 cm^{-1} is red shifted by 40 cm^{-1} when compared to that of native rHuEPO @ 1636 cm^{-1} (Figure 23A(I)). Similarly, the vibrational modes of the aromatic amino acids @ 1603 cm^{-1}, 1236 cm^{-1} and 1049 cm^{-1} are also red shifted. The shift in vibrational energy of the rHuEPO over the aptasensor surface is attributed to the aptamer

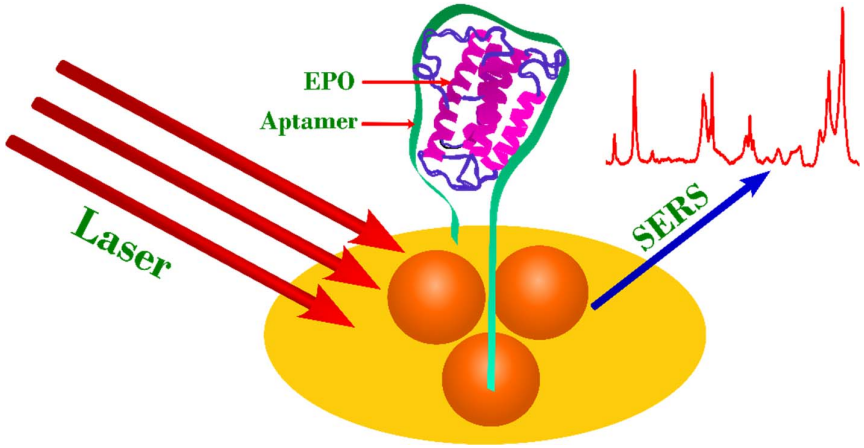

Scheme 2 - Graphical representation of rHuEPO captured aptasensor and subsequent SERS investigation.

conformational rearrangements upon binding rHuEPO to the aptamer fragment antigen binding (Fab) regions in the aqueous medium.[112, 194]

In order to reveal the suitability of the present aptamer modified pAu/AuNS surface towards SERS quantification of rHuEPO, various concentrations of rHuEPO in aqueous medium were employed. To each concentration of rHuEPO, a freshly prepared pAu/AuNS/Apt surface was used to selectively capture rHuEPO onto the aptasensor surface

and subsequently screened under the Raman microscope. Figure 24A shows the SERS spectra (amide 1 vibrational mode) of the pAu/AuNS/Apt/rHuEPO surface within a rHuEPO concentration range of 10 nM to 10 pM (the spectra were normalized and background subtracted). The band centered at 1676 cm^{-1} corresponding to amide I vibrational mode of rHuEPO was used a reference band for rHuEPO quantification. The SERS signals were found to monotonically decrease with decreasing concentration (Figure 24A). A linear relationship was obtained between the SERS signal intensity at 1676 cm^{-1} and the corresponding rHuEPO log concentration plot as depicted in Figure 24B. Similar linear relationship between

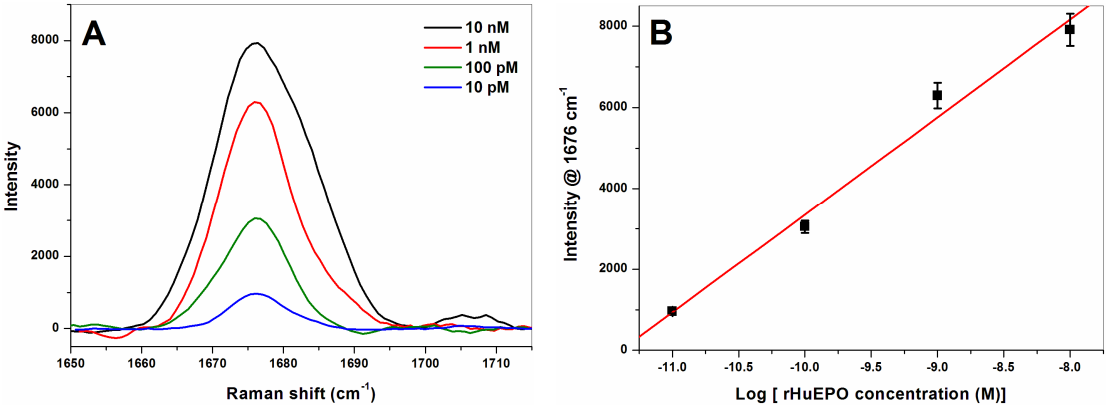

Figure 24 - (A) SERS spectra of pAu/AuNS/Apt/rHuEPO with decreasing concentration of rHuEPO: 10 nM (black), 1 nM (red), 100 pM (green), and 10 pM (blue). (B) Plot demonstrating the linear relationship between log concentration of rHuEPO and SERS intensity at 1676cm^{-1}.

log(concentration) and SERS intensity was formerly demonstrated in the literature.[66, 195] As indicated by Figure 24B, good correlation (R^2 = 0.993) was found over a wide concentration range of rHuEPO (10^{-8} to 10^{-11} M).

[3.5.4] Selective extraction and detection of rHuEPO in biological fluids

As a proof of concept for the SERS detection of EPO doping in biological fluids, we extended our methodology towards the label-free identification of rHuEPO in horse plasma. 1 nM rHuEPO was spiked into neat horse plasma and subsequently dropped over the pAu/AuNS/Apt. After 30 min, the substrate was washed with Millipore water to remove the biological matrix and dried in gentle flow of argon gas. A similar blank experiment was also carried out using un-spiked serum. Figure 23B(I) and Figure 23B(II) show the SERS spectra of blank and rHuEPO spiked (Figure 23B(II)), on aptasensor respectively. Figure 23B(I) shows strong correlation to Figure 23A(II) of the pAu/AuNS/Apt before interaction with EPO

protein. The resemblance between Figure 23A(II) and Figure 23B(I) indicates that the aptasensor when interacted with blank plasma matrix (no EPO spiked in matrix) did not bind with any of the non EPO proteins that exist in horse plasma. This result confirms the selectivity of the aptasensor towards its target protein over other proteins that may co-exist in a biological matrix. This Figure 23B(II) clearly depicted the amide I band @ 1644 cm^{-1} and aromatic amino acid vibrations @ 1594 cm^{-1} and 1028 cm^{-1}. A close comparison between figures Figure 23A(I) and Figure 23B(II) confirms unambiguous resemblance between the spectrum of rHuEPO standard and that of the aptasensor after interacting with the plasma sample spiked with rHuEPO. The shifts in band positions between figures Figure 23A(III) and Figure 23B(II) may be attributed in part to the higher dielectric constant and solvent polarity of aqueous matrix in comparison to those of the protein rich plasma matrix.[176] In Figure 23A(III), the higher dielectric constant and polarity of the aqueous matrix may have caused the red shift of the amide I band to the higher wave number of 1676 cm^{-1} from its position at 1636 cm^{-1} in figures Figure 23A(I) and Figure 23B(II). Therefore, we have successfully demonstrated the selective extraction and SERS identification of rHuEPO in horse plasma. This outcome clearly indicates the significance of using aptamers-functionalized homogeneous SERS substrate for facile and rapid screening of proteins in biological fluids. The full potential of the aptasensor is realized when it is combined with handheld Raman device for the in-field detection of rHuEPO from biological matrices.

[3.6] Conclusion

We demonstrated a sensitive and homogenous aptasensor for the reproducible detection of EPO in biological fluids. Due to the close packing and homogenous distribution of the nanoparticles coverage over the surface, strong and reproducible signal enhancement is acquired especially under wide area illumination conditions where the RSD of the SERS measurements can be as low as 4.92%. By adapting to wide area, handheld Raman devices can used in combination with the new aptasensor for the label-free in-field screening of rHuEPO in horse plasma.

Summary

Restatement of Aims:

1. Develop a system able to (a) selectively capture, (b) detect, and (c) quantify biomolecules from complex biological matrices using SERS.
2. Complement current methods for biomolecule detection by considering: (a) cost-effectiveness; (b) analysis time; (c) ease of use; (d) detection limits and; (e) portability.

Gold-coated iron oxide nanoparticles functionalised with anti-rHuEPO antibody and successfully used to selectively extract rHuEPO from a horse blood plasma matrix (Aim 1a). The presence of rHuEPO was detected indirectly through changes in the SERS spectrum of the functionalised nanoparticles after the antibody-antigen binding event (Aim 1b). The direct SERS spectrum of rHuEPO extracted from a biological matrix was demonstrated for the first time (Aim 1b). The identity of the extracted rHuEPO was confirmed and quantitated by ELISA (Aim 1a). Direct, label-free SERS quantitation was carried out on extracted rHuEPO protein after release from the antibody, with the Raman shift at 1551 cm^{-1} showing a linear relationship between signal intensity and log concentration (Aim 1c). The detection limit for this technique was found to be 10^{-12} M (Aim 2d). The iron oxide core was utilised to expedite the extraction process via magnetic separation (Aim 2b) and reduce the quantity of gold required (Aim 2a). The analysis protocol, starting from mixture through to direct SERS protein spectrum, can take as little as 30 minutes (Aim 2b), and can be carried out without prior training (Aim 2c). The extraction protocol was successfully tested for in-field screening of rHuEPO using a commercially available SERS substrate and handheld Raman spectrometer (Aim 2e).

Aptamer-functionalised nanostructured surfaces were developed for the selective and reproducible detection of EPO in biological fluids (Aim 1a, 1b). These aptasensors consisted of gold nanostructures potentiostatically deposited over a polished gold surface, followed by functionalisation using rHuEPO-specific aptamers. The strong and reproducible SERS signal enhancement was attributed to the close packing and homogeneous distribution of nanoparticles over the surface. These factors led to RSD values of the SERS

measurements as low as 4.92% under wide area illumination, ideal for use with handheld Raman devices that utilise wide area or raster scanning technologies (Aim 2e). When compared to the antibody-nanoparticle methodology, the aptamer-surface approach trades loading capacity for improved screening signal homogeneity and one-step extraction (Aim 2b, 2c), and reduces production costs associated with the selective capture by replacing the costly antibodies with aptamers (Aim 2a).

These works demonstrate the viability of label-free SERS screening of rHuEPO for both clinical and in-field testing, however, they are applicable to any analyte with a specific antibody or aptamer available. Once refined, the ability to directly detect a target protein in-field and obtain the SERS fingerprint, which can then be confirmed against reference spectra, can provide rapid and incontrovertible evidence for fields such as medicine and law enforcement.

Future work

The continued development of reproducible direct SERS for qualitative and quantitative identification of biomolecules in biological matrices remains a focal point in future endeavours. Exploration into antibody fragments and aptamer-based technologies is especially attractive, as they may provide cheaper and more longevous materials for use in the separation process. These experiments are currently prioritised in order to determine optimal separation parameters in terms of specificity, cost, and reliability. Future exploration into electrochemical over chemical means of sample processing are fascinating, and we envision, may enable streamlining and miniaturisation of the process. Cost-effectiveness, user-friendliness, and portability remain key foci moving forward in order to adapt these technologies for use with a wider audience.

References

[1] M. J. Swortwood, W. L. Hearn and A. P. DeCaprio. Cross-reactivity of designer drugs, including cathinone derivatives, in commercial enzyme-linked immunosorbent assays. *Drug Testing and Analysis* **2014**, *6*, 716-727.

[2] T. G. Hall, I. Smukste, K. R. Bresciano, Y. Wang, D. McKearn and R. E. Savage in *Identifying and Overcoming Matrix Effects in Drug Discovery and Development*, (Ed. D. J. Prasain), InTech, **2012**.

[3] M. Thevis, A. Thomas and W. Schänzer. Detecting peptidic drugs, drug candidates and analogs in sports doping: current status and future directions. *Expert Review of Proteomics* **2014**, *11*, 663-673.

[4] A. Kaviraj, E. Unlu, A. Gupta and A. El Nemr. Biomarkers of Environmental Pollutants. *BioMed Research International* **2014**, *2014*, 2.

[5] R. Ravichandran. Nanotechnology Applications in Food and Food Processing: Innovative Green Approaches, Opportunities and Uncertainties for Global Market. *International Journal of Green Nanotechnology: Physics and Chemistry* **2010**, *1*, P72-P96.

[6] N. C. Tansil and Z. Gao. Nanoparticles in biomolecular detection. *Nano Today* **2006**, *1*, 28-37.

[7] K. Hyonchol, T. Hideyuki, H. Masahito, T. Hiroyuki and Y. Kenji. Highly Sensitive Detection of Target Biomolecules on Cell Surface Using Gold Nanoparticle Conjugated with Aptamer Probe. *Japanese Journal of Applied Physics* **2012**, *51*, 06FH01.

[8] S. Jin and K. Ye. Nanoparticle-Mediated Drug Delivery and Gene Therapy. *Biotechnology Progress* **2007**, *23*, 32-41.

[9] E.-K. Lim, T. Kim, S. Paik, S. Haam, Y.-M. Huh and K. Lee. Nanomaterials for Theranostics: Recent Advances and Future Challenges. *Chemical Reviews* **2015**, *115*, 327-394.

[10] S.-H. Tseng, M.-Y. Chou and I. M. Chu. Cetuximab-conjugated iron oxide nanoparticles for cancer imaging and therapy. *International Journal of Nanomedicine* **2015**, *10*, 3663-3685.

[11] D. R. Shankaran, K. V. Gobi and N. Miura. Recent advancements in surface plasmon resonance immunosensors for detection of small molecules of biomedical, food and environmental interest. *Sensors and Actuators B: Chemical* **2007**, *121*, 158-177.

[12] T. J. Crisman, C. N. Parker, J. L. Jenkins, J. Scheiber, M. Thoma, Z. B. Kang, R. Kim, A. Bender, J. H. Nettles, J. W. Davies and M. Glick. Understanding false positives in reporter gene assays: in silico chemogenomics approaches to prioritize cell-based HTS data. *J Chem Inf Model* **2007**, *47*, 1319-1327.

[13] J. Wang and X. Qu. Recent progress in nanosensors for sensitive detection of biomolecules. *Nanoscale* **2013**, *5*, 3589-3600.

[14] R. van der Oost, J. Beyer and N. P. E. Vermeulen. Fish bioaccumulation and biomarkers in environmental risk assessment: a review. *Environmental Toxicology and Pharmacology* **2003**, *13*, 57-149.

[15] J. E. Anderson, L. L. Hansen, F. C. Mooren, M. Post, H. Hug, A. Zuse and M. Los. Methods and biomarkers for the diagnosis and prognosis of cancer and other diseases: towards personalized medicine. *Drug Resist Updat* **2006**, *9*, 198-210.

[16] X. Lin, L. Cui, Y. Huang, Y. Lin, Y. Xie, Z. Zhu, B. Yin, X. Chen and C. J. Yang. Carbon nanoparticle-protected aptamers for highly sensitive and selective detection of biomolecules based on nuclease-assisted target recycling signal amplification. *Chemical Communications* **2014**, *50*, 7646-7648.

[17] R. Mayeux. Biomarkers: Potential Uses and Limitations. *NeuroRx* **2004**, *1*, 182-188.

[18] J. R. Kesting, J. Huang and D. Sørensen. Identification of adulterants in a Chinese herbal medicine by LC–HRMS and LC–MS–SPE/NMR and comparative in vivo study with standards in a hypertensive rat model. *Journal of Pharmaceutical and Biomedical Analysis* **2010**, *51*, 705-711.
[19] M. J. Sheetz and G. L. King. Molecular understanding of hyperglycemia's adverse effects for diabetic complications. *JAMA* **2002**, *288*, 2579-2588.
[20] National Institute on Drug Abuse (NIDA). *Commonly Abused Drug Charts.* **2016**, https://www.drugabuse.gov/drugs-abuse/commonly-abused-drugs-charts
[21] U.S. Department of Justice in *Drugs of Abuse*, *Vol.* (Ed. Drug Enforcement Administration), https://www.dea.gov/pr/multimedia-library/publications/drug_of_abuse.pdf, **2015**.
[22] R. I. G. Holt and P. H. Sönksen. Growth hormone, IGF-I and insulin and their abuse in sport. *British Journal of Pharmacology* **2008**, *154*, 542-556.
[23] B. Alberts, A. Johnson, J. Lewis, M. Raff, K. Roberts and P. Walter. *Molecular Biology of the Cell*, Gardland Science, New York, **2002**, p.
[24] B. Maity, D. Sheff and R. A. Fisher. Immunostaining: detection of signaling protein location in tissues, cells and subcellular compartments. *Methods Cell Biol* **2013**, *113*, 81-105.
[25] Abcam. *Troubleshooting tips and tricks for IHC and ICC, as well as a detailed description of suitable positive and negative controls for both techniques.* **2016**, http://www.abcam.com/protocols/troubleshooting-and-using-controls-in-ihc-and-icc
[26] A. Adan, G. Alizada, Y. Kiraz, Y. Baran and A. Nalbant. Flow cytometry: basic principles and applications. *Critical Reviews in Biotechnology* **2016**, 1-14.
[27] H. Lodish, A. Berk and S. L. Zipursky in *Molecular Cell Biology. 4th Edition.* , W. H. Freeman, New York, **2000**.
[28] E. Uliyanchenko. Size-exclusion chromatography—from high-performance to ultra-performance. *Analytical and Bioanalytical Chemistry* **2014**, *406*, 6087-6094.
[29] GE Healthcare. *Ion Exchange Chromatography.* **2016**, http://www.gelifesciences.com/file_source/GELS/Service%20and%20Support/Documents%20and%20Downloads/Handbooks/pdfs/Ion%20Exchange%20Chromatography.pdf
[30] J. A. Queiroz, C. T. Tomaz and J. M. S. Cabral. Hydrophobic interaction chromatography of proteins. *Journal of Biotechnology* **2001**, *87*, 143-159.
[31] C. C. Chery, L. Moens, R. Cornelis and F. Vanhaecke. Capabilities and limitations of gel electrophoresis for elemental speciation: A laboratory's experience. *Pure Applied Chemistry* **2006**, *78*, 91-103.
[32] T. Rabilloud, A. R. Vaezzadeh, N. Potier, C. Lelong, E. Leize-Wagner and M. Chevallet. Power and limitations of electrophoretic separations in proteomics strategies. *Mass Spectrom Rev* **2009**, *28*, 816-843.
[33] B. Byrne, E. Stack, N. Gilmartin and R. O'Kennedy. Antibody-Based Sensors: Principles, Problems and Potential for Detection of Pathogens and Associated Toxins. *Sensors* **2009**, *9*, 4407.
[34] S. Zhang, A. Garcia-D'Angeli, J. P. Brennan and Q. Huo. Predicting detection limits of enzyme-linked immunosorbent assay (ELISA) and bioanalytical techniques in general. *Analyst* **2014**, *139*, 439-445.
[35] B. L. Milman. General principles of identification by mass spectrometry. *TrAC Trends in Analytical Chemistry* **2015**, *69*, 24-33.
[36] R. Knochenmuss. Ion formation mechanisms in UV-MALDI. *Analyst* **2006**, *131*, 966-986.

[37] M. S. Hanay, S. Kelber, A. K. Naik, D. Chi, S. Hentz, E. C. Bullard, E. Colinet, L. Duraffourg and M. L. Roukes. Single-protein nanomechanical mass spectrometry in real time. *Nat Nano* **2012**, *7*, 602-608.
[38] U. Gala and H. Chauhan. Principles and applications of Raman spectroscopy in pharmaceutical drug discovery and development. *Expert Opin Drug Discov* **2015**, *10*, 187-206.
[39] M. B. Fenn, P. Xanthopoulos, G. Pyrgiotakis, S. R. Grobmyer, P. M. Pardalos and L. L. Hench. Raman Spectroscopy for Clinical Oncology. *Advances in Optical Technologies* **2011**, *2011*.
[40] E. C. Le Ru and P. G. Etchegoin in *Chapter 4 - SERS enhancement factors and related topics*, Eds.: E. C. L. Ru and P. G. Etchegoin), Elsevier, Amsterdam, **2009**, pp. 185-264.
[41] E. C. Le Ru, E. Blackie, M. Meyer and P. G. Etchegoin. Surface Enhanced Raman Scattering Enhancement Factors: A Comprehensive Study. *The Journal of Physical Chemistry C* **2007**, *111*, 13794-13803.
[42] S. Nie and S. R. Emory. Probing Single Molecules and Single Nanoparticles by Surface-Enhanced Raman Scattering. *Science* **1997**, *275*, 1102-1106.
[43] V. I. Kukushkin, A. B. Van'kov and I. V. Kukushkin. Long-range manifestation of surface-enhanced Raman scattering. *JETP Letters* **2013**, *98*, 5.
[44] S. Y. Huang, B.-I. Wu, B. Zhang, Y. H. Lee, V. Liberman and M. Rothschild. An analytical method to study the effects of a substrate in surface-enhanced Raman scattering. *Journal of Applied Physics* **2009**, *106*, 114306-114312.
[45] A. Sivanesan, J. Kozuch, H. K. Ly, G. Kalaivani, A. Fischer and I. M. Weidinger. Tailored silica coated Ag nanoparticles for non-invasive surface enhanced Raman spectroscopy of biomolecular targets. *RSC Advances* **2012**, *2*, 805-808.
[46] J. A. Creighton and D. G. Eadon. Ultraviolet-visible absorption spectra of the colloidal metallic elements. *Journal of the Chemical Society, Faraday Transactions* **1991**, *87*, 3881-3891.
[47] E. Petryayeva and U. J. Krull. Localized surface plasmon resonance: Nanostructures, bioassays and biosensing—A review. *Analytica Chimica Acta* **2011**, *706*, 8-24.
[48] K. A. Willets and R. P. Van Duyne. Localized surface plasmon resonance spectroscopy and sensing. *Annu Rev Phys Chem* **2007**, *58*, 267-297.
[49] M. M. Kathryn, H. Feng, L. Seunghyun, N. Peter and H. H. Jason. A single molecule immunoassay by localized surface plasmon resonance. *Nanotechnology* **2010**, *21*, 255503.
[50] Y. Kitahama and Y. Ozaki in *Analysis of Blinking SERS by a Power Law with an Exponential Function*, John Wiley & Sons, Ltd, **2014**, pp. 107-137.
[51] J. R. Lombardi, R. L. Birke and G. Haran. Single Molecule SERS Spectral Blinking and Vibronic Coupling. *The Journal of Physical Chemistry C* **2011**, *115*, 4540-4545.
[52] N. D. Israelsen, C. Hanson and E. Vargis. Nanoparticle Properties and Synthesis Effects on Surface-Enhanced Raman Scattering Enhancement Factor: An Introduction. *The Scientific World Journal* **2015**, *2015*, 12.
[53] E. D. Getzoff, H. M. Geysen, S. J. Rodda, H. Alexander, J. A. Tainer and R. A. Lerner. Mechanisms of antibody binding to a protein. *Science* **1987**, *235*, 1191-1196.
[54] C. A. Janeway Jr, P. Travers and M. Walport in *The generation of diversity in immunoglobulins*, Garland Science, New York, **2001**.
[55] M. Oda. Review Antibody flexibility observed in antigen binding and its subsequent signaling. *Journal of Biological Macromolecules* **2004**, *4*, 45-56.

[56] T. Sagawa, M. Oda, H. Morii, H. Takizawa, H. Kozono and T. Azuma. Conformational changes in the antibody constant domains upon hapten-binding. *Mol Immunol* **2005**, *42*, 9-18.
[57] C. A. Janeway Jr, P. Travers and M. Walport in *The interaction of the antibody molecule with specific antigen*, Garland Science, New York, **2001**.
[58] A. L. Nelson. Antibody fragments: Hope and hype. *mAbs* **2010**, *2*, 77-83.
[59] F. Li, H. Zhang, Z. Wang, A. M. Newbigging, M. S. Reid, X.-F. Li and X. C. Le. Aptamers Facilitating Amplified Detection of Biomolecules. *Analytical Chemistry* **2015**, *87*, 274-292.
[60] P.-H. Lin, R.-H. Chen, C.-H. Lee, Y. Chang, C.-S. Chen and W.-Y. Chen. Studies of the binding mechanism between aptamers and thrombin by circular dichroism, surface plasmon resonance and isothermal titration calorimetry. *Colloids and Surfaces B: Biointerfaces* **2011**, *88*, 552-558.
[61] G. Mayer. The Chemical Biology of Aptamers. *Angewandte Chemie International Edition* **2009**, *48*, 2672-2689.
[62] S. Kedzierski, M. Khoshnejad and G. T. Caltagirone. Synthetic Antibodies: The Emerging Field of Aptamers. *BioProcessing Journal* **2012**, *11*, 46-49.
[63] P. H. C. Carmago, K. G. Satyanarayana and F. Wypych. Nanocomposites: Synthesis, Structure, Properties and New Application Opportunities. *Materials Research* **2009**, *12*, 39.
[64] T. L. Vasconcelos, B. S. Archanjo, B. Fragneaud, B. S. Oliveira, J. Riikonen, C. Li, D. S. Ribeiro, C. Rabelo, W. N. Rodrigues, A. Jorio, C. A. Achete and L. G. Cançado. Tuning Localized Surface Plasmon Resonance in Scanning Near-Field Optical Microscopy Probes. *ACS Nano* **2015**, *9*, 6297-6304.
[65] M. Nicklaus. *Tip-Enhanced Raman Spectroscopy for Nanoelectronics*, Books on Demand, **2014**, p. 26.
[66] A. K. M. Jamil, E. L. Izake, A. Sivanesan, R. Agoston and G. A. Ayoko. A homogeneous surface-enhanced Raman scattering platform for ultra-trace detection of trinitrotoluene in the environment. *Analytical Methods* **2015**, *7*, 3863-3868.
[67] K. Das, P. Hubert and S. Vengallatore. Patterning Nanomaterials on Fragile Micromachined Structures using Electron Beam Lithography. *MRS Online Proceedings Library* **2011**, *1299*, null-null.
[68] H. Yin, C. Wang, H. Zhu, S. H. Overbury, S. Sun and S. Dai. Colloidal deposition synthesis of supported gold nanocatalysts based on Au-Fe3O4 dumbbell nanoparticles. *Chemical Communications* **2008**, 4357-4359.
[69] M. Bardosova and T. Wagner. *Nanomaterials and Nanoarchitectures: A Complex Review of Current Hot Topics and their Applications*, Springer Netherlands, **2015**, p.
[70] A. K. M. Jamil, E. L. Izake, A. Sivanesan and P. M. Fredericks. Rapid detection of TNT in aqueous media by selective label free surface enhanced Raman spectroscopy. *Talanta* **2015**, *134*, 732-738.
[71] R. Hanna, R. Jerzy, G. Iwona and K. t. Katarzyna in *Electrochemical Sensors and Biosensors Based on Self-Assembled Monolayers: Application of Nanoparticles for Analytical Signals Amplification*, *Vol. 1112* American Chemical Society, **2012**, pp. 293-312.
[72] L. Haeussling, H. Ringsdorf, F. J. Schmitt and W. Knoll. Biotin-functionalized self-assembled monolayers on gold: surface plasmon optical studies of specific recognition reactions. *Langmuir* **1991**, *7*, 1837-1840.
[73] I. Fratoddi, I. Venditti, C. Cametti and M. V. Russo. The puzzle of toxicity of gold nanoparticles. The case-study of HeLa cells. *Toxicology Research* **2015**, *4*, 796-800.

[74] R. Coradeghini, S. Gioria, C. P. García, P. Nativo, F. Franchini, D. Gilliland, J. Ponti and F. Rossi. Size-dependent toxicity and cell interaction mechanisms of gold nanoparticles on mouse fibroblasts. *Toxicology Letters* **2013**, *217*, 205-216.
[75] R. Shukla, V. Bansal, M. Chaudhary, A. Basu, R. R. Bhonde and M. Sastry. Biocompatibility of Gold Nanoparticles and Their Endocytotic Fate Inside the Cellular Compartment: A Microscopic Overview. *Langmuir* **2005**, *21*, 10644-10654.
[76] Z. Fan, M. Shelton, A. K. Singh, D. Senapati, S. A. Khan and P. C. Ray. Multifunctional Plasmonic Shell–Magnetic Core Nanoparticles for Targeted Diagnostics, Isolation, and Photothermal Destruction of Tumor Cells. *ACS Nano* **2012**, *6*, 1065-1073.
[77] M. Hu, J. Chen, Z.-Y. Li, L. Au, G. V. Hartland, X. Li, M. Marquez and Y. Xia. Gold nanostructures: engineering their plasmonic properties for biomedical applications. *Chemical Society Reviews* **2006**, *35*, 1084-1094.
[78] P. Tiwari, K. Vig, V. Dennis and S. Singh. Functionalized Gold Nanoparticles and Their Biomedical Applications. *Nanomaterials* **2011**, *1*, 31.
[79] F. Chen, X. Li, J. Hihath, Z. Huang and N. Tao. Effect of Anchoring Groups on Single-Molecule Conductance: Comparative Study of Thiol-, Amine-, and Carboxylic-Acid-Terminated Molecules. *Journal of the American Chemical Society* **2006**, *128*, 15874-15881.
[80] M. Mahmoudi, A. Simchi, A. S. Milani and P. Stroeve. Cell toxicity of superparamagnetic iron oxide nanoparticles. *Journal of Colloid and Interface Science* **2009**, *336*, 510-518.
[81] Z. Xu, Y. Hou and S. Sun. Magnetic Core/Shell Fe3O4/Au and Fe3O4/Au/Ag Nanoparticles with Tunable Plasmonic Properties. *Journal of the American Chemical Society* **2007**, *129*, 8698-8699.
[82] S. Zong, Z. Wang, H. Chen, G. Hu, M. Liu, P. Chen and Y. Cui. Colorimetry and SERS dual-mode detection of telomerase activity: combining rapid screening with high sensitivity. *Nanoscale* **2014**, *6*, 1808-1816.
[83] V. Amendola, S. Scaramuzza, L. Litti, M. Meneghetti, G. Zuccolotto, A. Rosato, E. Nicolato, P. Marzola, G. Fracasso, C. Anselmi, M. Pinto and M. Colombatti. Magneto-Plasmonic Au-Fe Alloy Nanoparticles Designed for Multimodal SERS-MRI-CT Imaging. *Small* **2014**, *10*, 2476-2486.
[84] E. Çelik, P. Çalık, S. M. Halloran and S. G. Oliver. Production of recombinant human erythropoietin from Pichia pastoris and its structural analysis. *Journal of Applied Microbiology* **2007**, *103*, 2084-2094.
[85] N. Robinson, S. Giraud, C. Saudan, N. Baume, L. Avois, P. Mangin and M. Saugy. Erythropoietin and blood doping. *British Journal of Sports Medicine* **2006**, *40*, i30-i34.
[86] R. J. Woods in *Image of the predicted structure of glycosylated human Erythropoietin*, *Vol. 359 x 335 px* (Ed. glycosylated_EPO_new_r70.png), glycam.org, **2014**.
[87] T. Lappin. The Cellular Biology of Erythropoietin Receptors. *The Oncologist* **2003**, *8*, 15-18.
[88] World Anti-Doping Agency. *A brief History of Anti-Doping.* **2015**, https://www.wada-ama.org/en/who-we-are/a-brief-history-of-anti-doping
[89] L.-J. Xu, C. Zong, X.-S. Zheng, P. Hu, J.-M. Feng and B. Ren. Label-Free Detection of Native Proteins by Surface-Enhanced Raman Spectroscopy Using Iodide-Modified Nanoparticles. *Analytical Chemistry* **2014**, *86*, 2238-2245.
[90] A. M. Schwartzberg, C. D. Grant, A. Wolcott, C. E. Talley, T. R. Huser, R. Bogomolni and J. Z. Zhang. Unique Gold Nanoparticle Aggregates as a Highly Active Surface-Enhanced Raman Scattering Substrate. *The Journal of Physical Chemistry B* **2004**, *108*, 19191-19197.

[91] J. Zhou, K. Ren, Y. Zhao, W. Dai and H. Wu. Convenient formation of nanoparticle aggregates on microfluidic chips for highly sensitive SERS detection of biomolecules. *Analytical and Bioanalytical Chemistry* **2012**, *402*, 1601-1609.
[92] D. Tang, J. C. Sauceda, Z. Lin, S. Ott, E. Basova, I. Goryacheva, S. Biselli, J. Lin, R. Niessner and D. Knopp. Magnetic nanogold microspheres-based lateral-flow immunodipstick for rapid detection of aflatoxin B2 in food. *Biosensors and Bioelectronics* **2009**, *25*, 514-518.
[93] A. C. Manikas, F. Causa, R. Della Moglie and P. A. Netti. Tuning Gold Nanoparticles Interfaces by Specific Peptide Interaction for Surface Enhanced Raman Spectroscopy (SERS) and Separation Applications. *ACS Applied Materials & Interfaces* **2013**, *5*, 7915-7922.
[94] G. G. Huang, M. K. Hossain, X. X. Han and Y. Ozaki. A novel reversed reporting agent method for surface-enhanced Raman scattering; highly sensitive detection of glutathione in aqueous solutions. *Analyst* **2009**, *134*, 2468-2474.
[95] U. Tamer, D. Cetin, Z. Suludere, I. H. Boyaci, H. T. Temiz, H. Yegenoglu, P. Daniel, İ. Dinçer and Y. Elerman. Gold-Coated Iron Composite Nanospheres Targeted the Detection of Escherichia coli. *International Journal of Molecular Sciences* **2013**, *14*, 6223-6240.
[96] M. Kumagai, T. K. Sarma, H. Cabral, S. Kaida, M. Sekino, N. Herlambang, K. Osada, M. R. Kano, N. Nishiyama and K. Kataoka. Enhanced in vivo Magnetic Resonance Imaging of Tumors by PEGylated Iron-Oxide–Gold Core–Shell Nanoparticles with Prolonged Blood Circulation Properties. *Macromolecular Rapid Communications* **2010**, *31*, 1521-1528.
[97] L. Zhang, J. Xu, L. Mi, H. Gong, S. Jiang and Q. Yu. Multifunctional magnetic–plasmonic nanoparticles for fast concentration and sensitive detection of bacteria using SERS. *Biosensors and Bioelectronics* **2012**, *31*, 130-136.
[98] Y. Hu and Y. Sun. Stable Magnetic Hot Spots for Simultaneous Concentration and Ultrasensitive Surface-Enhanced Raman Scattering Detection of Solution Analytes. *The Journal of Physical Chemistry C* **2012**, *116*, 13329-13335.
[99] L. Lou, K. Yu, Z. Zhang, R. Huang, J. Zhu, Y. Wang and Z. Zhu. Dual-mode protein detection based on Fe3O4-Au hybrid nanoparticles. *Nano Research* **2012**, *5*, 272-282.
[100] A. Zengin, U. Tamer and T. Caykara. A SERS-Based Sandwich Assay for Ultrasensitive and Selective Detection of Alzheimer's Tau Protein. *Biomacromolecules* **2013**, *14*, 3001-3009.
[101] P. Quaresma, I. Osorio, G. Doria, P. A. Carvalho, A. Pereira, J. Langer, J. P. Araujo, I. Pastoriza-Santos, L. M. Liz-Marzan, R. Franco, P. V. Baptista and E. Pereira. Star-shaped magnetite@gold nanoparticles for protein magnetic separation and SERS detection. *RSC Advances* **2014**, *4*, 3659-3667.
[102] L. Lin, E. Crew, H. Yan, S. Shan, Z. Skeete, D. Mott, T. Krentsel, J. Yin, N. A. Chernova, J. Luo, M. H. Engelhard, C. Wang, Q. Li and C.-J. Zhong. Bifunctional nanoparticles for SERS monitoring and magnetic intervention of assembly and enzyme cutting of DNAs. *Journal of Materials Chemistry B* **2013**, *1*, 4320-4330.
[103] J. Baniukevic, I. Hakki Boyaci, A. Goktug Bozkurt, U. Tamer, A. Ramanavicius and A. Ramanaviciene. Magnetic gold nanoparticles in SERS-based sandwich immunoassay for antigen detection by well oriented antibodies. *Biosensors and Bioelectronics* **2013**, *43*, 281-288.
[104] B. Guven, N. Basaran-Akgul, E. Temur, U. Tamer and I. H. Boyac. SERS-based sandwich immunoassay using antibody coated magnetic nanoparticles for Escherichia coli enumeration. *Analyst* **2011**, *136*, 740-748.

[105] E. Temur, A. Zengin, İ. H. Boyacı, F. C. Dudak, H. Torul and U. Tamer. Attomole Sensitivity of Staphylococcal Enterotoxin B Detection Using an Aptamer-Modified Surface-Enhanced Raman Scattering Probe. *Analytical Chemistry* **2012**, *84*, 10600-10606.
[106] H. Zhang, X. Ma, Y. Liu, N. Duan, S. Wu, Z. Wang and B. Xu. Gold nanoparticles enhanced SERS aptasensor for the simultaneous detection of Salmonella typhimurium and Staphylococcus aureus. *Biosensors and Bioelectronics* **2015**, *74*, 872-877.
[107] F. Bao, J.-L. Yao and R.-A. Gu. Synthesis of Magnetic Fe2O3/Au Core/Shell Nanoparticles for Bioseparation and Immunoassay Based on Surface-Enhanced Raman Spectroscopy. *Langmuir* **2009**, *25*, 10782-10787.
[108] Y. Wang, S. Ravindranath and J. Irudayaraj. Separation and detection of multiple pathogens in a food matrix by magnetic SERS nanoprobes. *Analytical and Bioanalytical Chemistry* **2011**, *399*, 1271-1278.
[109] J. Yoon, N. Choi, J. Ko, K. Kim, S. Lee and J. Choo. Highly sensitive detection of thrombin using SERS-based magnetic aptasensors. *Biosensors and Bioelectronics* **2013**, *47*, 62-67.
[110] T. Demeritte, B. P. Viraka Nellore, R. Kanchanapally, S. S. Sinha, A. Pramanik, S. R. Chavva and P. C. Ray. Hybrid Graphene Oxide Based Plasmonic-Magnetic Multifunctional Nanoplatform for Selective Separation and Label-Free Identification of Alzheimer's Disease Biomarkers. *ACS Applied Materials & Interfaces* **2015**, *7*, 13693-13700.
[111] Z. Fan, D. Senapati, S. A. Khan, A. K. Singh, A. Hamme, B. Yust, D. Sardar and P. C. Ray. Popcorn-Shaped Magnetic Core–Plasmonic Shell Multifunctional Nanoparticles for the Targeted Magnetic Separation and Enrichment, Label-Free SERS Imaging, and Photothermal Destruction of Multidrug-Resistant Bacteria. *Chemistry – A European Journal* **2013**, *19*, 2839-2847.
[112] J. Hughes, E. L. Izake, W. B. Lott, G. A. Ayoko and M. Sillence. Ultra sensitive label free surface enhanced Raman spectroscopy method for the detection of biomolecules. *Talanta* **2014**, *130*, 20-25.
[113] I. Finoulst, M. Pinkse, W. Van Dongen and P. Verhaert. Sample Preparation Techniques for the Untargeted LC-MS-Based Discovery of Peptides in Complex Biological Matrices. *Journal of Biomedicine and Biotechnology* **2011**, *2011*.
[114] N. Miekus, I. Oledzka, A. Plenis, Z. Wozniak, A. Lewczuk, P. Koszalka, B. Seroczynska and T. Baczek. Gel electrophoretic separation of proteins from cultured neuroendocrine tumor cell lines. *Molecular Medicine Reports* **2015**, *11*, 1407+.
[115] H. Mirzaei and F. Regnier. Structure specific chromatographic selection in targeted proteomics. *Journal of Chromatography B* **2005**, *817*, 23-34.
[116] A. Poliwoda and P. Wieczorek. Sample pretreatment techniques for oligopeptide analysis from natural sources. *Analytical and Bioanalytical Chemistry* **2009**, *393*, 885-897.
[117] C. Seger. Usage and limitations of liquid chromatography-tandem mass spectrometry (LC–MS/MS) in clinical routine laboratories. *Wiener Medizinische Wochenschrift* **2012**, *162*, 499-504.
[118] P. J. Tighe, R. R. Ryder, I. Todd and L. C. Fairclough. ELISA in the multiplex era: Potentials and pitfalls. *PROTEOMICS – Clinical Applications* **2015**, *9*, 406-422.
[119] P. E. Groleau, P. Desharnais, L. Coté and C. Ayotte. Low LC-MS/MS detection of glycopeptides released from pmol levels of recombinant erythropoietin using nanoflow HPLC-chip electrospray ionization. *Journal of Mass Spectrometry* **2008**, *43*, 924-935.
[120] F. Guan, C. E. Uboh, L. R. Soma, E. Birks, J. Chen, Y. You, J. Rudy and X. Li. Differentiation and Identification of Recombinant Human Erythropoietin and Darbepoetin

Alfa in Equine Plasma by LC–MS/MS for Doping Control. *Analytical Chemistry* **2008**, *80*, 3811-3817.
[121] Thermo Scientific. *1602127-Assay-Development-Handbook.* **2014**, https://tools.thermofisher.com/content/sfs/brochures/1602127-Assay-Development-Handbook.pdf
[122] X. X. Han, B. Zhao and Y. Ozaki. Surface‐enhanced Raman scattering for protein detection. *Anal. Bioanal. Chem.* **2009**, *394*, 1719.
[123] K. Hering, D. Cialla, K. Ackermann, T. Dörfer, R. Möller, H. Schneidewind, R. Mattheis, W. Fritzsche, P. Rösch and J. Popp. SERS: a versatile tool in chemical and biochemical diagnostics. *Analytical and Bioanalytical Chemistry* **2008**, *390*, 113-124.
[124] A. Sivanesan, H. K. Ly, J. Kozuch, M. Sezer, U. Kuhlmann, A. Fischer and I. M. Weidinger. Functionalized Ag nanoparticles with tunable optical properties for selective protein analysis. *Chemical Communications* **2011**, *47*, 3553-3555.
[125] A. Campion and P. Kambhampati. Surface-enhanced Raman scattering. *Chemical Society Reviews* **1998**, *27*, 241-250.
[126] C. L. Haynes, A. D. McFarland and R. P. Van Duyne. Surface-Enhanced Raman Spectroscopy. *Analytical Chemistry* **2005**, *77*, 338A-346A.
[127] J. Qi, P. Motwani, M. Gheewala, C. Brennan, J. C. Wolfe and W.-C. Shih. Surface-enhanced Raman spectroscopy with monolithic nanoporous gold disk substrates. *Nanoscale* **2013**, *5*, 4105-4109.
[128] K. C. Bantz, A. F. Meyer, N. J. Wittenberg, H. Im, O. Kurtulus and S. H. Lee. Recent progress in SERS biosensing. *Physical Chemistry Chemical Physics* **2011**, *13*, 11551-11567.
[129] E. Podstawka, Y. Ozaki and L. M. Proniewicz. Part III: surface-enhanced Raman scattering of amino acids and their homo dipeptide monolayers deposited onto colloidal gold surface. *Applied Spectroscopy* **2005**, *59*, 1516-1525.
[130] A. Sivanesan, E. Izake, R. Agoston, G. Ayoko and M. Sillence. Reproducible and label-free biosensor for the selective extraction and rapid detection of proteins in biological fluids. *Journal of Nanobiotechnology* **2015**, *13*, 43.
[131] J. W. Regulation of erythropoietin production. *J Physiology* **2011**, *589*, 1251-1258.
[132] S. Lamon, N. Robinson and M. Saugy. Procedures for monitoring recombinant erythropoietin and analogs in doping. *Endocrinol Metab Clin North Am* **2010**, *39*.
[133] J. Morkeberg, C. Lundby, G. R. O. Nissen-Lie, T. K. Nielsen, P. Hemmersbach and R. Damsgaard. Detection of darbepoetin alfa misuse in urine and blood: a preliminary investigation. *Med Sci Sports Exerc* **2007**, *39*, 1742-1747.
[134] G. R. O. Nissen-Lie, K. Birkeland, P. Hemmersbach and V. Skibeli. Serum sTfR Levels May Indicate Charge Profiling of Urinary r-hEPO in Doping Control. *Med Sci Sports Exerc* **2004**, *36*, 588-593.
[135] M. Ashenden, E. Varlet-Marie, F. Lasne and M. Audran. The effects of microdose recombinant human erythropoietin regimens in athletes. *Haematologica* **2006**, *91*, 1143-1144.
[136] WADA EPO Working Group in *WADA Technical Document – TD2014EPO*, *Vol.* (Ed. World Anti-Doping Agency), https://wada-main-prod.s3.amazonaws.com/resources/files/WADA-TD2014EPO-v1-Harmonization-of-Analysis-and-Reporting-of-ESAs-by-Electrophoretic-Techniques-EN.pdf, **2014**.
[137] Y. O. Schumacher, M. Saugy, T. Pottgiesser and N. Ronbinson. Detection of EPO doping and blood doping: the haematological module of the Athlete Biological Passport. *Drug Testing and Analysis* **2012**, *4*, 846-854.

[138] D. Ciallaa, S. Polloka, C. Steinbrucker, K. Weber and J. Popp. SERS-based detection of biomolecules. *Nanophotonics* **2014**, *3*, 383-411.
[139] Ocean Optics. *High Quality Raman Data for Non-Homogeneous Samples Using Raster Orbital Scanning.* **2014**, http://oceanoptics.com/wp-content/uploads/App-Note-High-Quality-Raman-Data-for-Non-Homogeneous-Samples-Using-Raster-Orbital-Scanning.pdf
[140] P. K. Jain, Y. Xiao, R. Walsworth and A. E. Cohen. Surface plasmon resonance enhanced magneto (SuPREMO): Faraday rotation enhancement in gold-coated iron oxide nanocrystals. *Nano Letters* **2009**, *4*, 1644-1650.
[141] U. Tamer, Y. Gündoğdu, İ. Boyacı and K. Pekmez. Synthesis of magnetic core–shell Fe3O4–Au nanoparticle for biomolecule immobilization and detection. *Journal of Nanoparticle Research* **2010**, *12*, 1187-1196.
[142] A. Sharma, Z. Matharu, G. Sumana, P. R. Solanki, C. G. Kim and B. D. Malhotra. Antibody immobilized cysteamine functionalized-gold nanoparticles for aflatoxin detection. *Thin Solid Films* **2010**, *519*, 1213-1218.
[143] T. Yannick, A. Brioude, A. W. Coleman, M. Rhimi and B. Kim. Molecular recognition by gold, silver and copper nanoparticles. *World Journal of Biological Chemistry* **2013**, *4*, 35-63.
[144] W. Wang, Q. Wei, J. Wang, B. Wang, S. Zhang and Z. Yuan. Role of thiol-containing polyethylene glycol (thiol-PEG) in the modification process of gold nanoparticles (AuNPs): Stabilizer or coagulant. *J Colloid Interface Sci* **2013**, *404*, 223-229.
[145] M. Lönnberg, Y. Dehnes, M. Drevin, M. Garle, S. Lamon and N. Leuenberger. Rapid affinity purification of erythropoietin from biological samples using disposable monoliths. *J Chromatogr* **2010**, *1217*, 7031-7037.
[146] M. S. Schmidt, J. Hübner and A. Boisen. Large Area Fabrication of Leaning Silicon Nanopillars for Surface Enhanced Raman Spectroscopy. *Adv Mater* **2012**, *2012*, OP11-OP18.
[147] J. Yang, M. Palla, F. G. Bosco, T. Rindzevicius, T. S. Alstrøm and M. S. Schmidt. Surface-enhanced Raman spectroscopy based quantitative bioassay on aptamer-functionalized nanopillars using large-area Raman mapping. *ACS Nano* **2013**, *2013*.
[148] R&D Systems. *Human Erythropoietin Quantikine IVD ELISA Kit: R&D Systems.* **2016**, https://www.rndsystems.com/products/human-erythropoietin-quantikine-ivd-elisa-kit_dep00
[149] C. Hoskins, Y. Min, M. Gueorguieva, C. McDougall, A. Volovick, P. Prentice, Z. Wang, A. Melzer, A. Cuschieri and L. Wang. Hybrid gold-iron oxide nanoparticles as a multifunctional platform for biomedical application. *J Nanobiotechnol* **2012**, *10*.
[150] Z. Li, L. Wei, M. Y. Gao and H. Lei. One pot reaction to synthesize biocompatible magnetite nanoparticles. *Adv Mater* **2005**, *17*, 1001-1005.
[151] A. K. Gupta and M. Gupta. Synthesis and surface engineering of iron oxide nanoparticles for biomedical applications. *Biomaterials* **2005**, *26*, 3995-4021.
[152] J. Drbohlavova, R. Hrdy, V. Adam, R. Kizek, O. Schneeweiss and J. Hubalek. Preparation and Properties of Various Magnetic Nanoparticles. *Sensors* **2009**, *9*, 2352.
[153] D. C. Rodrigues, M. L. de Souza, K. S. Souza, D. P. dos Santos, G. F. S. Andrade and M. L. A. Temperini. Critical assessment of enhancement factor measurements in surface-enhanced Raman scattering on different substrates. *Physical Chemistry Chemical Physics* **2015**.
[154] E. Podstawka, Y. Ozaki and L. M. Proniewicz. Adsorption of S-S containing proteins on a colloidal silver surface studied by surface-enhanced Raman spectroscopy. *Applied Spectroscopy* **2004**, *58*, 1147-1156.

[155] M. Kahraman and S. Wachsmann-Hogiu. Label-free and direct protein detection on 3D plasmonic nanovoid structures using surface-enhanced Raman scattering. *Analytica Chimica Acta* **2015**, *856*, 74-81.
[156] A. K. M. Jamil, E. L. Izake, A. Sivanesan and P. M. Fredericks. Rapid detection of TNT in aqueous media by selective label free surface enhanced Raman spectroscopy. *Talanta* **2015**, *134*, 732-738.
[157] G. V. P. Kumar, R. Selvi, A. H. Kishore, T. K. Kundu and C. Narayana. Surface-Enhanced Raman Spectroscopic Studies of Coactivator-Associated Arginine Methyltransferase 1. *The Journal of Physical Chemistry B* **2008**, *112*, 6703-6707.
[158] J. Wang, D. Lin, J. Lin, Y. Yu, Z. Huang, Y. Chen, J. Lin, S. Feng, B. Li, N. Liu and R. Chen. Label-free detection of serum proteins using surface-enhanced Raman spectroscopy for colorectal cancer screening. *Journal of Biomedical Optics* **2014**, *19*, 087003-087003.
[159] X. Yang, C. Gu, F. Qian, Y. Li and J. Z. Zhang. Highly Sensitive Detection of Proteins and Bacteria in Aqueous Solution Using Surface-Enhanced Raman Scattering and Optical Fibers. *Analytical Chemistry* **2011**, *83*, 5888-5894.
[160] M. Wang, M. Benford, N. Jing, G. Coté and J. Kameoka. Optofluidic device for ultra-sensitive detection of proteins using surface-enhanced Raman spectroscopy. *Microfluidics and Nanofluidics* **2009**, *6*, 411-417.
[161] C. V. Pagba, S. M. Lane, H. Cho and S. Wachsmann-Hogiu. Direct detection of aptamer-thrombin binding via surface-enhanced Raman spectroscopy. *Journal of Biomedical Optics* **2010**, *15*, 047006-047008.
[162] P. P. Kundu, T. Bhowmick, G. Swapna, G. V. Pavan Kumar, V. Nagaraja and C. Narayana. Allosteric Transition Induced by Mg2+ Ion in a Transactivator Monitored by SERS. *The Journal of Physical Chemistry B* **2014**, *118*, 5322-5330.
[163] N. J. Aachmann-Andersen, S. Just Christensen, K. Lisbjerg, P. Oturai, A. K. Meinild-Lundby and N. H. Holstein-Rathlou. Recombinant Erythropoietin in Humans Has a Prolonged Effect on Circulating Erythropoietin Isoform Distribution. *PLoS ONE* **2014**, *9*.
[164] D. Kurouski and R. P. Van Duyne. In Situ Detection and Identification of Hair Dyes Using Surface-Enhanced Raman Spectroscopy (SERS). *Analytical Chemistry* **2015**, *87*, 2901-2906.
[165] J. W. Fisher. Erythropoietin: Physiology and pharmacology update. *Experimental Biology and Medicine* **2003**, *228*, 1-14.
[166] K. Jacobs, C. Shoemaker, R. Rudersdorf, S. D. Neill, R. J. Kaufman, A. Mufson, J. Seehra, S. S. Jones, R. Hewick, E. F. Fritsch, M. Kawakita, T. Shimizu and T. Miyake. Isolation and characterization of genomic and cDNA clones of human erythropoietin. *Nature* **1985**, *313*, 806-810.
[167] M. Henke, R. Laszig, C. Rübe, U. Schäfer, K. D. Haase, B. Schilcher, S. Mose, K. T. Beer, U. Burger, C. Dougherty and H. Frommhold. Erythropoietin to treat head and neck cancer patients with anaemia undergoing radiotherapy: Randomised, double-blind, placebo-controlled trial. *Lancet* **2003**, *362*, 1255-1260.
[168] R. Parisotto, M. Wu, M. J. Ashenden, K. R. Emslie, C. J. Gore, C. Howe, R. Kazlauskas, K. Sharpe, G. J. Trout, M. Xie and A. G. Hahn. Detection of recombinant human erythropoietin abuse in athletes utilizing markers of altered erythropoiesis. *Haematologica* **2001**, *86*, 128-137.
[169] A. G. Schache, T. Liloglou, J. M. Risk, A. Filia, T. M. Jones, J. Sheard, J. A. Woolgar, T. R. Helliwell, A. Triantafyllou, M. Robinson, P. Sloan, C. Harvey-Woodworth, D. Sisson and R. J. Shaw. Evaluation of human papilloma virus diagnostic testing in oropharyngeal squamous

cell carcinoma: Sensitivity, specificity, and prognostic discrimination. *Clinical Cancer Research* **2011**, *17*, 6262-6271.
[170] Y. Yasuda, Y. Fujita, T. Matsuo, S. Koinuma, S. Hara, A. Tazaki, M. Onozaki, M. Hashimoto, T. Musha, K. Ogawa, H. Fujita, Y. Nakamura, H. Shiozaki and H. Utsumi. Erythropoietin regulates tumour growth of human malignancies. *Carcinogenesis* **2003**, *24*, 1021-1029.
[171] A. Sivanesan, J. Kozuch, H. K. Ly, G. Kalaivani, A. Fischer and I. M. Weidinger. Tailored silica coated Ag nanoparticles for non-invasive surface enhanced Raman spectroscopy of biomolecular targets. *RSC Advances* **2012**, *2*, 805-808.
[172] A. Sivanesan, E. Witkowska, W. Adamkiewicz, Ł. Dziewit, A. Kamińska and J. Waluk. Nanostructured silver-gold bimetallic SERS substrates for selective identification of bacteria in human blood. *Analyst* **2014**, *139*, 1037-1043.
[173] H. Ko, S. Singamaneni and V. V. Tsukruk. Nanostructured surfaces and assemblies as SERS media. *Small* **2008**, *4*, 1576-1599.
[174] A. Kamińska, I. Dzicielewski, J. L. Weyher, J. Waluk, S. Gawinkowski, V. Sashuk, M. Fiałkowski, M. Sawicka, T. Suski, S. Porowski and R. Hołyst. Highly reproducible, stable and multiply regenerated surface-enhanced Raman scattering substrate for biomedical applications. *Journal of Materials Chemistry* **2011**, *21*, 8662-8669.
[175] D. Natelson, Y. Li and J. B. Herzog. Nanogap structures: Combining enhanced Raman spectroscopy and electronic transport. *Physical Chemistry Chemical Physics* **2013**, *15*, 5262-5275.
[176] A. Sivanesan, W. Adamkiewicz, G. Kalaivani, A. Kamińska, J. Waluk, R. Hołyst and E. L. Izake. Towards improved precision in the quantification of surface-enhanced Raman scattering (SERS) enhancement factors: A renewed approach. *Analyst* **2015**, *140*, 489-496.
[177] M. Mascini, I. Palchetti and S. Tombelli. Nucleic acid and peptide aptamers: Fundamentals and bioanalytical aspects. *Angewandte Chemie - International Edition* **2012**, *51*, 1316-1332.
[178] Y. C. Lim, A. Z. Kouzani and W. Duan. Aptasensors: A review. *Journal of Biomedical Nanotechnology* **2010**, *6*, 93-105.
[179] L. Feng, A. Sivanesan, Z. Lyu, A. Offenhäusser and D. Mayer. Electrochemical current rectification-a novel signal amplification strategy for highly sensitive and selective aptamer-based biosensor. *Biosensors and Bioelectronics* **2015**, *66*, 62-68.
[180] J. Sun, A. Guo, Z. Zhang, L. Guo and J. Xie. A Conjugated Aptamer-Gold Nanoparticle Fluorescent Probe for Highly Sensitive Detection of rHuEPO-α. *Sensors* **2011**, *11*, 10490.
[181] Z. Zhang, L. Guo, J. Tang, X. Guo and J. Xie. An aptameric molecular beacon-based "Signal-on" approach for rapid determination of rHuEPO-α. *Talanta* **2009**, *80*, 985-990.
[182] N. Félidj, J. Aubard, G. Lévi, J. R. Krenn, G. Schider, A. Leitner and F. R. Aussenegg. Enhanced substrate-induced coupling in two-dimensional gold nanoparticle arrays. *Physical Review B - Condensed Matter and Materials Physics* **2002**, *66*, 2454071-2454077.
[183] K. Shin and H. Chung. Wide area coverage Raman spectroscopy for reliable quantitative analysis and its applications. *Analyst* **2013**, *138*, 3335-3346.
[184] K. Shin, K. Ryu, H. Lee, K. Kim, H. Chung and D. Sohn. Au nanoparticle-encapsulated hydrogel substrates for robust and reproducible SERS measurement. *Analyst* **2013**, *138*, 932-938.
[185] C. Blum, T. Schmid, L. Opilik, N. Metanis, S. Weidmann and R. Zenobi. Missing amide i mode in gap-mode tip-enhanced raman spectra of proteins. *Journal of Physical Chemistry C* **2012**, *116*, 23061-23066.

[186] T. E. Keyes, D. Leane, R. J. Forster, N. Moran and D. Kenny. New insights into the molecular mechanisms of thrombosis from high resolution surface enhanced Raman microscopy. *Proceedings of SPIE-the international society for optical engineering* **2005**.
[187] G. V. P. Kumar, R. Selvi, A. H. Kishore, T. K. Kundu and C. Narayana. Surface-enhanced Raman spectroscopic studies of coactivator-associated arginine methyltransferase 1. *Journal of Physical Chemistry B* **2008**, *112*, 6703-6707.
[188] P. P. Kundu, T. Bhowmick, G. Swapna, G. V. Pavan Kumar, V. Nagaraja and C. Narayana. Allosteric transition induced by Mg2+ ion in a transactivator monitored by SERS. *Journal of Physical Chemistry B* **2014**, *118*, 5322-5330.
[189] D. Kurouski, T. Postiglione, T. Deckert-Gaudig, V. Deckert and I. K. Lednev. Amide i vibrational mode suppression in surface (SERS) and tip (TERS) enhanced Raman spectra of protein specimens. *Analyst* **2013**, *138*, 1665-1673.
[190] P. Negri, G. Chen, A. Kage, A. Nitsche, D. Naumann, B. Xu and R. A. Dluhy. Direct optical detection of viral nucleoprotein binding to an anti-influenza aptamer. *Analytical Chemistry* **2012**, *84*, 5501-5508.
[191] S. U. Sane, S. M. Cramer and T. M. Przybycien. A Holistic Approach to Protein Secondary Structure Characterization Using Amide I Band Raman Spectroscopy. *Analytical Biochemistry* **1999**, *269*, 255-272.
[192] A. Barhoumi, D. Zhang, F. Tam and N. J. Halas. Surface-Enhanced Raman Spectroscopy of DNA. *Journal of the American Chemical Society* **2008**, *130*, 5523-5529.
[193] Y. Lu, Q. Huang, G. Meng, L. Wu and Z. Jingjing. Label-free selective SERS detection of PCB-77 based on DNA aptamer modified SiO2@Au core/shell nanoparticles. *Analyst* **2014**, *139*, 3083-3087.
[194] K. Mantelingu, A. H. Kishore, K. Balasubramanyam, G. V. P. Kumar, M. Altaf, S. N. Swamy, R. Selvi, C. I. Das, C. Narayana, K. S. Rangappa and T. K. Kundu. Activation of p300 histone acetyltransferase by small molecules altering enzyme structure: Probed by surface-enhanced raman spectroscopy. *Journal of Physical Chemistry B* **2007**, *111*, 4527-4534.
[195] K. K. Sen, S. K. Basu and S. K. Dutta. Binding studies of lamotrigine with sera of different animal species. *Tropical Journal of Pharmaceutical Research* **2009**, *8*, 409-415.